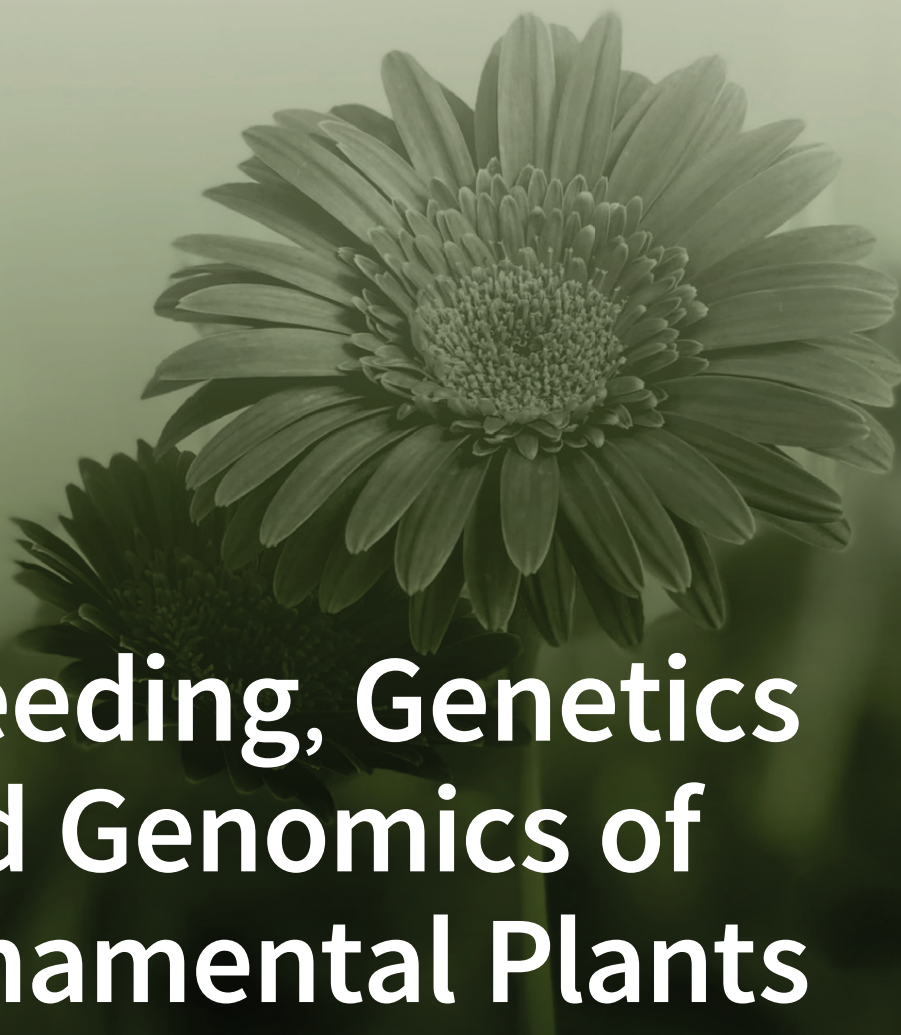




horticulturae



Breeding, Genetics and Genomics of Ornamental Plants

Edited by

Johan Van Huylbroeck, Kenneth W. Leonhardt,
Teresita D. Amore and Krishna Bhattarai

Printed Edition of the Special Issue Published in *Horticulturae*

Breeding, Genetics and Genomics of Ornamental Plants

Breeding, Genetics and Genomics of Ornamental Plants

Editors

Johan Van Huylbroeck

Kenneth W. Leonhardt

Teresita D. Amore

Krishna Bhattarai

MDPI • Basel • Beijing • Wuhan • Barcelona • Belgrade • Manchester • Tokyo • Cluj • Tianjin



Editors

Johan Van Huylbroeck
Flanders Research Institute
for Agriculture, Fisheries and
Food / Plant Sciences Unit
Belgium

Kenneth W. Leonhardt
University of Hawaii at
Manoa
USA

Teresita D. Amore
University of Hawaii at
Manoa
USA

Krishna Bhattarai
University of California Davis
USA

Editorial Office

MDPI
St. Alban-Anlage 66
4052 Basel, Switzerland

This is a reprint of articles from the Special Issue published online in the open access journal *Horticulturae* (ISSN 2311-7524) (available at: https://www.mdpi.com/journal/horticulturae/special_issues/Ornamental_Plants).

For citation purposes, cite each article independently as indicated on the article page online and as indicated below:

LastName, A.A.; LastName, B.B.; LastName, C.C. Article Title. <i>Journal Name</i> Year , <i>Volume Number</i> , Page Range.
--

ISBN 978-3-0365-3793-1 (Hbk)

ISBN 978-3-0365-3794-8 (PDF)

Cover image courtesy of Krishna Bhattarai and Sadikshya Sharma

© 2022 by the authors. Articles in this book are Open Access and distributed under the Creative Commons Attribution (CC BY) license, which allows users to download, copy and build upon published articles, as long as the author and publisher are properly credited, which ensures maximum dissemination and a wider impact of our publications.

The book as a whole is distributed by MDPI under the terms and conditions of the Creative Commons license CC BY-NC-ND.

Contents

Krishna Bhattarai and Johan Van Huylbroeck Breeding, Genetics, and Genomics of Ornamental Plants Reprinted from: <i>Horticulturae</i> 2022 , <i>8</i> , 148, doi:10.3390/horticulturae8020148	1
Emmy Dhooghe, Dirk Reheul and Marie-Christine Van Labeke Overcoming Pre-Fertilization Barriers in Intertribal Crosses between <i>Anemone coronaria</i> L. and <i>Ranunculus asiaticus</i> L. Reprinted from: <i>Horticulturae</i> 2021 , <i>7</i> , 529, doi:10.3390/horticulturae7120529	5
Lin Ouyang, Leen Leus, Ellen De Keyser and Marie-Christine Van Labeke Dehydrins and Soluble Sugars Involved in Cold Acclimation of <i>Rosa wichurana</i> and Rose Cultivar ‘Yesterday’ Reprinted from: <i>Horticulturae</i> 2021 , <i>7</i> , 379, doi:10.3390/horticulturae7100379	19
Shiro Mori, Masaki Yahata, Ayano Kuwahara, Yurina Shirono, Yasufumi Ueno, Misaki Hatanaka, Yoshimi Honda, Keita Sugiyama, Naho Murata, Yoshihiro Okamoto and Takahiro Wagatsuma Morphological Characterization of Tetraploids of <i>Limonium sinuatum</i> (L.) Mill. Produced by Oryzalin Treatment of Seeds Reprinted from: <i>Horticulturae</i> 2021 , <i>7</i> , 248, doi:10.3390/horticulturae7080248	31
Michelle L. Jones, Shuangyi Bai, Yiyun Lin and Laura J. Chapin The Senescence-Associated Endonuclease, <i>PhENDOL1</i> , Is Upregulated by Ethylene and Phosphorus Deficiency in Petunia Reprinted from: <i>Horticulturae</i> 2021 , <i>7</i> , 46, doi:10.3390/horticulturae7030046	41
Xingbo Wu, Amanda M. Hulse-Kemp, Phillip A. Wadl, Zach Smith, Keithanne Mockaitis, Margaret E. Staton, Timothy A. Rinehart and Lisa W. Alexander Genomic Resource Development for Hydrangea (<i>Hydrangea macrophylla</i> (Thunb.) Ser.)—A Transcriptome Assembly and a High-Density Genetic Linkage Map Reprinted from: <i>Horticulturae</i> 2021 , <i>7</i> , 25, doi:10.3390/horticulturae7020025	59
Ryan N. Contreras and Tyler C. Hoskins Developing Triploid Maples Reprinted from: <i>Horticulturae</i> 2020 , <i>6</i> , 70, doi:10.3390/horticulturae6040070	73



Editorial

Breeding, Genetics, and Genomics of Ornamental Plants

Krishna Bhattarai ^{1,*} and Johan Van Huylenbroeck ^{2,*}¹ UF/IFAS Gulf Coast Research and Education Center, 14625 County Road 672, Wimauma, FL 33598, USA² Flanders Research Institute for Agriculture, Fisheries and Food (ILVO), Caritasstraat, 39, 9090 Melle, Belgium

* Correspondence: krishnabhattarai@ufl.edu (K.B.); johan.vanhuylenbroeck@ilvo.vlaanderen.be (J.V.H.)

Ornamental crops include a broad range of plants, including herbaceous seasonal flowers to woody perennial trees. Due to their wide diversity, different breeding methods have been utilized in ornamental crops to develop new cultivars. Cultivar development in ornamental crops is currently performed by making intraspecific and interspecific crosses, ploidy manipulation, mutation breeding, and molecular breeding. Except for a few floral species, limited genetic, genomic, and breeding information is publicly available, owing to the fact that the majority of breeding work is performed by the private sector. Compared to agricultural or vegetable crops, ornamental crops are diverse, which means that each individual species has a relatively low economic turnover, and subsequent lower budgets are attributed to research and developmental activities. However, public research programs are participating in ornamental cultivar development and genetic studies. This has contributed to the identification of important genes, genetic architecture, and the genomic information of some economically important ornamental crops. To date, limited genome-informed breeding strategies have been applied in ornamental crops. However, with the decreasing sequencing costs and availability of reference genomes of flowers, it is likely that genomic-assisted breeding will be applied in cultivar development as observed in other row, vegetable, and fruit crops.

This Special Issue (SI) was developed to present the advancements made in the field of ornamental crops, with a focus on understanding the genetics, genomics, and breeding frontiers leading to cultivar development. More specifically, the objectives of this SI were to report novel genes; their functionality and cross talks with other genes; breeding activities, including the development and characterization of new cultivars; and the development of genomic resources, including high-density linkage map and transcriptome, and their applications in breeding. This SI gathered six research papers [1–6] based on a wide array of herbaceous and perennial ornamental crops in the fields of gene identification and interactions, ploidy manipulation, and genomics research.

Ploidy manipulation has been commonly used in ornamental crops for cultivar development. In many species, it has led to the creation of new cultivars with altered morphology and increased stress resistance. In addition to obtaining valuable morphological or physiological variations, one of the driving factors for using ploidy manipulation is to develop reproductive sterility in plants to check the invasiveness of the species and the extent to which it is endangering native plants in the environment. Currently, three maple species have been listed as noxious weeds in Connecticut and Massachusetts due to their ability to produce an undesirable number of seedlings, posing an extreme threat to encroaching natural vegetation. Although measures to check the spread of these species are implemented in only two states, the naturalization of these species has already occurred in large areas in different regions of the United States [1]. The development of maple plants that do not produce viable seeds can help in controlling the spread of maple in the wild. Using ploidy manipulation, triploid plants can be developed, which are found to be sterile and do not produce viable seeds. Conteras and Hoskins developed triploid maple by ploidy manipulation and backcrossing methods [1]. Oryzalin treatment of seedling meristem is

Citation: Bhattarai, K.; Van Huylenbroeck, J. Breeding, Genetics, and Genomics of Ornamental Plants. *Horticulturae* **2022**, *8*, 148. <https://doi.org/10.3390/horticulturae8020148>

Received: 2 February 2022

Accepted: 6 February 2022

Published: 9 February 2022

Publisher's Note: MDPI stays neutral with regard to jurisdictional claims in published maps and institutional affiliations.



Copyright: © 2022 by the authors. Licensee MDPI, Basel, Switzerland. This article is an open access article distributed under the terms and conditions of the Creative Commons Attribution (CC BY) license (<https://creativecommons.org/licenses/by/4.0/>).

used to develop tetraploid maple, which is then crossed with diploid maple and results in triploid maple [1]. Several years of screening of triploid maple plants have shown that the triploid maple does not produce flowers, or if the flowers are produced, they are sterile [1]. This triploid maple showed the potential to be released as new cultivars for nursery growers and land managers [1].

Polyploids show enhanced desirable traits, such as larger flowers, as compared to their diploid counterparts, which make them more appealing to consumers. Increased organ enlargement due to polyploidy is attributed to the chromosomal doubling and gene dosage effects. Polyploidy has been used in ornamental plants showing narrow genetic diversity and compatibility issues in search of novel or improved traits and make interspecific and intergeneric crosses. *Limonium sinuatum* flowers are desired for their wide range of colors and longer vase life [4]. However, developing new cultivars with novel attractive traits is not easy due to their narrow genetic diversity and the difficulty of crossbreeding with related species, with few exceptions. The development of polyploid plants can potentially result in larger flowers and increased vigor in *L. sinuatum*, making it more desirable for consumers. The *in vivo* treatment of seedling meristem with oryzalin successfully developed polyploid individuals, including tetraploids and mixoploids [4]. Tetraploid plants showed increased leaf width, stomatal size, and flower length; however, a significant improvement in ornamental value was not obtained [4]. Further study is needed to cross tetraploid and diploid *L. sinuatum* individuals to develop triploid plants and assess them for potential cultivar development with enhanced traits [4]. While traits such as larger flower size are highly desirable to the ornamental industry, not all morphological changes caused by polyploidy positively impact the consumer. Tetraploid *L. sinuatum* exhibited thickened stem wings and inflorescence clogging, which are not desirable ornamental traits [4]. These traits can potentially be improved or eliminated with the use of breeding strategies while retaining the desirable novel traits obtained by ploidy manipulation.

Despite high demand and global production, ornamental crops fall behind in the public availability of genomic resources owing to their high level of heterozygosity, varying ploidy level within the same species and wide range of complex genome sizes. Recently, efforts are being made to develop genomic resources in some widely cultivated and economically important ornamental crops, such as hydrangea (*Hydrangea macrophylla*) [2]. Hydrangea, being a woody ornamental, requires a longer conventional breeding time. The development and incorporation of molecular markers can reduce generation interval times and expedite breeding using marker-assisted selection. Wu et al. used genome reduction techniques, such as genotyping by sequencing (GBS) and transcriptome sequencing, to identify simple sequence repeat (SSR) and single nucleotide polymorphism (SNP) markers and construct a linkage map in hydrangea [2]. Genome reduction techniques, such as GBS and transcriptome sequencing, can be used to identify SNPs and develop molecular markers to facilitate marker-assisted selection in ornamental crops with highly heterozygous, complex, and relatively large genome sizes. When reference genomes or physical maps are not available, linkage maps are used in identifying genomic regions conferring phenotypic traits of interest and developing molecular markers. Wu et al. constructed a linkage map consisting of 18 linkage groups incorporating 1621 SNPs and 146 SSRs [2]. These efforts help in realizing the application of marker-assisted and genome-informed selections in ornamental crops in addition to facilitating QTL mapping, association mapping, gene identification and gene cloning. With the decreasing sequencing cost, the availability of genomic resources for more ornamental crops are expected to be available in future.

The identification of gene functions has led to a better understanding of flower development and physiology. Jones et al. cloned *Petunia hybrida* *Endonuclease 1* (*PhENDO1*) gene using two-dimensional gel electrophoresis based on endonuclease enzyme (*PhNUC1*) activity encoded by the gene [3]. The downregulation of *PhENDO1* using virus-induced gene silencing revealed the role of *PhENDO1* in decreased nucleic acid content in the corolla; however, it did not independently play any role in delaying flower senescence [3]. Similarly, gene expression studies have led to a greater understanding of plant acclimatization to

abiotic stresses. During cold acclimation, the higher expression of dehydrins and increased sugar accumulation played an important role in roses [5]. This was verified by the increased transcript levels of *Rosa hybrida sucrose-phosphate synthase (RhSPS)* and *Rosa hybrida invertase 2 (RhINV)* genes in “Yesterday” and *R. wichurana*, respectively, while *R. hybrida sucrose synthase (RhSUS)* expression was downregulated in both cultivars during the cold months [5]. Meanwhile, the expression of *RhSPS* and *RhINV2* was found to be decreased during the warmer months of April, which signifies the involvement of oligosaccharides in cold acclimation [5].

The pursuit of novel traits in ornamental crops has led to the adoption of distant crosses. Crosses between plants with high genetic distance provide the opportunity to inherit a high amount of variation in the offspring. Interspecific and intergeneric crosses are made in ornamental crops in efforts to develop cultivars with new and improved ornamental traits. However, not all distant crosses are successful due to pre- or post-fertilization barriers. In an intertribal cross between *Anemone coronaria* and *Ranunculus asiaticus*, pre-fertilization barriers were observed due to the interstylar growth of pollen tubes, whereas minimal stigmatic incongruity was observed between the two species [6]. This barrier was minimized by increasing the ratio of pollen tube length to the total style length using 2,4-D treatment [6]. A full seed set without the necessity of pollination indicated apomictic seed generation [6]. Overcoming the pre- and post-fertilization barrier due to artificial treatment can assist in distant crosses and viable seed production and harness the wide genetic variation inherited from distant crosses and use in ornamental breeding.

This SI provides an insight into the application of breeding, genetics, and genomic tools to understand the biology of the ornamental plants and develop new cultivars for ornamental nurseries. In the era where sequencing-based tools are being increasingly applied in ornamental crops, it is expected that future research will incorporate these techniques to develop cultivars and discover or understand biological phenomena in ornamental crops. In the future, once the genetic bases of (complex) traits are resolved, the breeding of ornamental plants will become more efficient.

Author Contributions: Writing, review and editing, K.B. and J.V.H. All authors have read and agreed to the published version of the manuscript.

Funding: This research received no external funding.

Institutional Review Board Statement: Not applicable.

Informed Consent Statement: Not applicable.

Data Availability Statement: Not applicable.

Conflicts of Interest: The authors declare no conflict of interest.

References

1. Contreras, R.; Hoskins, T. Developing Triploid Maples. *Horticulturae* **2020**, *6*, 70. [\[CrossRef\]](#)
2. Wu, X.; Hulse-Kemp, A.; Wadl, P.; Smith, Z.; Mockaitis, K.; Staton, M.; Rinehart, T.; Alexander, L. Genomic Resource Development for *Hydrangea macrophylla* (Thunb.) Ser.—A Transcriptome Assembly and a High-Density Genetic Linkage Map. *Horticulturae* **2021**, *7*, 25. [\[CrossRef\]](#)
3. Jones, M.; Bai, S.; Lin, Y.; Chapin, L. The Senescence-Associated Endonuclease, *PhENDO1*, Is Upregulated by Ethylene and Phosphorus Deficiency in *Petunia*. *Horticulturae* **2021**, *7*, 46. [\[CrossRef\]](#)
4. Mori, S.; Yahata, M.; Kuwahara, A.; Shirono, Y.; Ueno, Y.; Hatanaka, M.; Honda, Y.; Sugiyama, K.; Murata, N.; Okamoto, Y.; et al. Morphological Characterization of Tetraploids of *Limonium sinuatum* (L.) Mill. Produced by Oryzalin Treatment of Seeds. *Horticulturae* **2021**, *7*, 248. [\[CrossRef\]](#)
5. Ouyang, L.; Leus, L.; De Keyser, E.; Van Labeke, M. Dehydrins and Soluble Sugars Involved in Cold Acclimation of *Rosa wichurana* and Rose Cultivar ‘Yesterday’. *Horticulturae* **2021**, *7*, 379. [\[CrossRef\]](#)
6. Dhooche, E.; Reheul, D.; Van Labeke, M. Overcoming Pre-Fertilization Barriers in Intertribal Crosses between *Anemone coronaria* L. and *Ranunculus asiaticus* L. *Horticulturae* **2021**, *7*, 529. [\[CrossRef\]](#)



Article

Overcoming Pre-Fertilization Barriers in Intertribal Crosses between *Anemone coronaria* L. and *Ranunculus asiaticus* L.

Emmy Dhooghe ^{1,*}, Dirk Reheul ² and Marie-Christine Van Labeke ²

¹ Plant Sciences Unit, Flanders Research Institute for Agricultural, Fisheries and Food Research (ILVO), Caritasstraat 39, 9090 Melle, Belgium

² Department Plants and Crops, Faculty of Bioscience Engineering, Ghent University, Coupure Links 653, 9000 Ghent, Belgium; dirk.reheul@ugent.be (D.R.); mariechristine.vanlabeke@ugent.be (M.-C.V.L.)

* Correspondence: emmy.dhooghe@ilvo.vlaanderen.be

Citation: Dhooghe, E.; Reheul, D.; Van Labeke, M.-C. Overcoming Pre-Fertilization Barriers in Intertribal Crosses between *Anemone coronaria* L. and *Ranunculus asiaticus* L. *Horticulturae* **2021**, *7*, 529. <https://doi.org/10.3390/horticulturae7120529>

Academic Editors: Douglas D. Archbold and Sergio Ruffo Roberto

Received: 21 September 2021
Accepted: 26 November 2021
Published: 29 November 2021

Publisher's Note: MDPI stays neutral with regard to jurisdictional claims in published maps and institutional affiliations.



Copyright: © 2021 by the authors. Licensee MDPI, Basel, Switzerland. This article is an open access article distributed under the terms and conditions of the Creative Commons Attribution (CC BY) license (<https://creativecommons.org/licenses/by/4.0/>).

Abstract: Hybridization in flowering plants depends, in the first place, on the delivery of pollen to a receptive stigma and the subsequent growth of pollen tubes through the style to the ovary, where the sperm nucleus of the pollen grain can ultimately fertilize the egg cell. However, reproductive failure is often observed in distant crosses and is caused by pre- and/or post-zygotic barriers. In this study, the reproductive pre-fertilization barriers of intertribal crosses between *Anemone coronaria* L. and *Ranunculus asiaticus* L., both belonging to the Ranunculaceae, were investigated. Despite the incongruity of intertribal crosses between *A. coronaria* and *R. asiaticus* having been of low intensity at the stigmatic level, interstylar obstructions of the pollen tube growth occurred, which confirmed the presence of pre-fertilization barriers. We show that these barriers could be partially bypassed by combining pollination with a stigma treatment. More specifically, a significantly higher ratio of the pollen tube length to the total style length and a better seed set were observed when the stigma was treated with the auxin 2,4-dichlorophenoxyacetic acid (2,4-D, 1 mg·mL⁻¹) together with the cytokinin kinetin (KIN, 0.5 mg·mL⁻¹) 24 h after pollination, irrespective of the cross direction. More specifically, the stigma treatments with any form of auxin (combined or not combined with cytokinin) resulted in a full seed set, assuming an apomictic fruit set, because no pollination was needed to obtain these seeds.

Keywords: breeding; geophytes; interspecific cross; plant hormone treatment; pollen-pistil interaction; pre-zygotic barrier; Ranunculaceae

1. Introduction

Plant variation is the driving force in ornamental plant cultivation. Crosses between partners with a high genetic distance are important inducers of variation, provided they produce viable seeds. However often incongruity occurs, which can be defined as a mechanism for the common phenomenon of non-functioning of pollen–pistil relationships in interpopulational matings [1]. This is not the same as incompatibility, which is based on a non-recognition system between a male and female determinant (*S*-locus) [2]. These interpopulational reproductive barriers occur in and can be divided into pre-zygotic (or pre-fertilization) and post-zygotic (or post-fertilization) barriers, depending on the time and place of occurrence [3–7]. Pre-zygotic barriers are observed before fertilization and are mostly situated at the stigmatic surface or in the style, while post-zygotic barriers prevent further embryo development into a plant. The interactions that occur between pollen and stigma/style consist of six key stages: pollen capture and adhesion, pollen hydration, pollen germination, pollen tube penetration, tube growth through the stigma and style, entry of the pollen tube into the ovule, and discharge of the sperm cells [8]. In a successful interaction, all six steps are completed, while, in an incongruous interaction, one or more steps may be hindered preventing fertilization [8]. The stigma type can influence this interaction. Stigmas are divided in dry and wet stigmas depending on the occurrence

of exudation during stigma receptivity [9]. Pollen rejection is more likely to occur in plant species with dry stigmas, as the secretions on a wet stigma do not discriminate pollen and trap and hydrate all of them [10]. Besides the effect of the stigma type, barriers can limit or obstruct the growth of the pollen tube in the style induced by cytotoxins or cell wall modifying enzymes produced by the female transmitting tissue [10].

In this study, we focus on the pre-zygotic barriers. Although these barriers are efficient and successful to prevent distant crosses in nature, they can be artificially overruled [11]. Pre-zygotic barriers can be bypassed by reciprocal crosses, mixed pollinations (pollination with a combination of incongruent and congruent pollen) or pollinations by mentor pollen (pollination with a combination of incongruent and irradiated congruent pollen with nonfunctional sperm nuclei), style manipulations, crosses at an aberrant flower age or by stigma treatments with different chemical compounds [7,12,13]. In the interspecific hybridization of *Banksia hookeriana* and *Banksia prionotes*, hybrids were only observed when *Banksia hookeriana* was used as female parent [14]. Artificial crosses between *Diploaxis siettiana* and *Brassica juncea* are not successful, but when pollen of *Diploaxis siettiana* was irradiated with 1000 Gy gamma radiation and was dusted on the stigma, fertilization could occur [15]. Mixed pollinations produced wide hybridizations in blueberry [16] as has style manipulations in *Lilium* [17]. The flower's age can also have an effect on its receptivity and its pollen reaction. Delayed pollination can overcome self-incompatibility, while a functional incongruity system might be not yet fully established in younger flowers [18]. Compounds that are added at the stigma are based on the composition of exudates that occur at wet stigmas. In wet stigmas, either lipid-rich or carbohydrate-rich compounds occur [8]. In species with dry stigma, such as *Anemone coronaria* L. and *Ranunculus asiaticus* L. [19], the pollen kit takes over the function of the exudates, suggesting that sugars or lipids may also be required for pollen tube penetration in species with dry stigmas [20]. The application of growth regulators, such as auxins, cytokinins and gibberellins, to the stigma at the time of, or soon after pollination may improve seed set in distant crosses [7,21,22].

In this study, pollen-stigma interactions were studied in crosses between *A. coronaria* and *R. asiaticus*. These are both important ornamental species belonging to the Ranunculaceae. The Ranunculaceae are grouped based on chromosome types into Ranunculoideae and Thalictroideae [23]. The subfamily, Ranunculoideae, is ordered in several tribes where the genus *Anemone* is included within the Anemoneae and *Ranunculus* within the Ranunculeae, resulting in intertribal cross combinations when crosses are done between both genera. In the present study, pre-zygotic barriers were extensively investigated and protocols to overcome barriers were tested in these genetic distant crosses between *A. coronaria* and *R. asiaticus*.

2. Materials and Methods

2.1. Plant Material and Growth Conditions

Three cultivars of *Anemone coronaria* L. (i.e., 'Mistral Wine', 'Mistral Fucsia' (both Mistral® Line, Biancheri Creations, Camporosso Mare, Italy) and 'Wicabri Blue' (Wicabri® Line, the Netherlands)) were combined according to the availability of receptive flower stages for mating and pollen availability with three cultivars of *Ranunculus asiaticus* L., ('Alfa' (Vitro Line Success®, Biancheri Creations, Camporosso Mare, Italy), 'Krisma' (Istituto Regionale per la Floricoltura, Sanremo, Italy) and 'Bianco Strié' (Biancheri Creations, Camporosso Mare, Italy)). From each cultivar more than 30 plants were available.

Rhizomes were planted in September as followed: tuberous rhizomes were soaked in water for 24 h at 10 °C and subsequently planted in a peat mixture (pH_{H2O} 6.5–7.5) with 5% perlite, 5% clay and fertilizers (NPK 14-16-18, 1 kg m⁻³). The soil surface was sprayed with prochloraz (Sporgon®, 0.6 g L⁻¹) directly after planting, to prevent root rot by fungi. Standard nursery practices were used for watering, fertilization and pest control [24–26]. Plants were grown in a greenhouse (natural photoperiod regime) with climate condition settings of 18 °C day temperature and 5 °C night temperature. During the day (8 a.m.–4 p.m.) extra assimilation light was given (assimilation light HPI-T Plus

Philips, PAR: 25–30 $\mu\text{mol m}^{-2} \text{s}^{-1}$). All plants spontaneously started to flower in the March–April period.

2.2. Crosses and Observation of Pre-Fertilization Barriers

Flowers that were used as mother plants were emasculated one day before pollination and protected from surrounding pollen by a paper bag. Pollen was freshly harvested from flowering plants and collected with a brush (one specific brush for each cultivar) in a Petri dish. Pollination (done one time per cross) was achieved by dusting pollen with a brush on the receptive carpels. After pollination, which was done before noon, the flower was packed in a paper bag to prevent other pollinations.

To investigate pre-fertilization barriers for the intertribal and reciprocal crosses between *Anemone* and *Ranunculus*, scanning electron microscopy (TM-1000 Tabletop microscope, HITACHI) was combined with aniline blue staining monitored by fluorescence microscopy (Olympus IX81).

Aniline blue staining of the carpels was started 56 h after pollination. The pollinated carpels (10 to 20 per cross combination) were fixed in FAA (formaldehyde:alcohol (ethanol 70%):acetic acid, 1:1:18) for 24 h and subsequently macerated by NaOH (8 M) for 16 h. After being thoroughly washed in water, the carpels were stained in a 0.1 % (*w/v*) aniline blue solution in 0.033 M K_3PO_4 for 3 h in the dark.

2.3. Techniques to Bypass Pre-Fertilization Barriers

Undisturbed carpels were treated with one of the following solutions (acronym):

- pollen germination medium (PM) (100 $\text{mg}\cdot\text{L}^{-1}$ H_3BO_3 , 700 $\text{mg}\cdot\text{L}^{-1}$ $\text{Ca}(\text{NO}_3)_2\cdot 4\text{H}_2\text{O}$, 200 $\text{mg}\cdot\text{L}^{-1}$ $\text{MgSO}_4\cdot 7\text{H}_2\text{O}$, 100 $\text{mg}\cdot\text{L}^{-1}$ KNO_3 , 150 $\text{g}\cdot\text{L}^{-1}$ PEG 6000, 740 $\text{mg}\cdot\text{L}^{-1}$ L-glutamic acid and 100 $\text{g}\cdot\text{L}^{-1}$ sucrose, pH 6.0), just before pollination;
- sucrose solutions (5% (*w/v*), sucrose), just before pollination;
- salt solution (0.5 M NaCl, salt), just before pollination;
- olive oil (oil), just before pollination;
- auxin 2,4-dichlorophenoxyacetic acid (2,4-D, 1 $\text{mg}\cdot\text{mL}^{-1}$), 24 h after pollination;
- auxin 1-naphthaleneacetic acid (NAA, 1 $\text{mg}\cdot\text{mL}^{-1}$), 24 h after pollination;
- gibberellic acid (GA_3 , 1 $\text{mg}\cdot\text{mL}^{-1}$), 24 h after pollination;
- cytokinin kinetin (KIN, 1 $\text{mg}\cdot\text{mL}^{-1}$), 24 h after pollination; or
- the combination of 2,4-D (1 $\text{mg}\cdot\text{mL}^{-1}$) and KIN (0.5 $\text{mg}\cdot\text{mL}^{-1}$) together (Comb), 24 h after pollination.

Furthermore, other applied techniques were:

- cut-style pollination (SC): 3/4 of the stylar tissue was cut where after the wound was pollinated;
- mentor pollination (mentor): plants were pollinated with a mix of intrageneric pollen (congruent, i.e., *R. asiaticus* 'Alfa' pollen for *Ranunculus* \times *Anemone*) and intertribal pollen but the congruent pollen was irradiated with 2000 Gy to prevent the formation of viable sperm nuclei;
- mixed pollination (mix): carpels were pollinated with the pollen of the other genus and one to two days later with compatible pollen (of the same cultivar for *Anemone* or with 'Bianco Strié' for *Ranunculus*);
- use of rehydrated pollen (2 h in a fog tunnel prior to pollination) (RV);
- pollination of old, emasculated flowers (old, carpels 3–6 days after anthesis for *Anemone* and 4–10 days after anthesis for *Ranunculus*); and
- pollination of young, emasculated flowers (young, 5 to 8 days before anthesis).

Aniline blue staining was used in part of the crosses to check if the pre-zygotic barriers had been bypassed (number of crosses per treatment and per cross direction, see Table 2) and part of the crosses was left untouched to determine the seed formation and the success rate of the manipulations (number of crosses per treatment and per cross direction, see Table 3).

2.4. Flow Cytometry of Fruitlets

Leaf tissue (standard), green fully developed fruitlets, obtained after self-pollination (standard); fruitlets, obtained after 2,4-D treatment ($1 \text{ mg} \cdot \text{mL}^{-1}$) without pollination + packed in a paper bag; and fruitlets, obtained after stigma treatment with 2,4-D ($1 \text{ mg} \cdot \text{mL}^{-1}$, 24 h post-pollination with compatible pollen) from *Anemone* 'Wicabri Blue', were used for flow cytometry. These fruitlets were peeled and subsequently chopped with a sharp razor blade in $250 \text{ } \mu\text{L}$ 0.1-M citric acid monohydrate and 0.5 % Tween[®] according to Galbraith et al. [27]. Subsequently, the samples were filtered (pore size $100 \text{ } \mu\text{m}$). The filter was washed by adding $500 \text{ } \mu\text{L}$ staining solution with 0.4 M $\text{Na}_2\text{HPO}_4 \cdot 12\text{H}_2\text{O}$ and $2 \text{ mg} \cdot \text{L}^{-1}$ 4',6-diamidino-2-phenylindole (DAPI) [28]. The relative fluorescence of the total DNA of a single nuclei was analyzed using a flow cytometer equipped with a mercury lamp (Partec PAS III). At least ten fruitlets per case were analyzed. For the analysis of leaf material, at least 3000 nuclei were counted; in the case of fruitlets, the number of nuclei was lower (min. 1000 nuclei) due to the lesser amount of cells in the individual seeds.

2.5. Statistics

The ratio pollen tube length/total style length was evaluated by analysis of variance with the statistical program SPSS Statistics 26.0. A two-tailed Dunnett's test was done as a post-hoc test on a one-way ANOVA in which the stigma treatments and pollination techniques were compared to the control cross.

3. Results

Pollen-stigma interaction in the intertribal crosses between *A. coronaria* and *R. asiaticus* was regular, as pollen adhesion and hydration, followed by germination and pollen tube penetration, could be clearly observed (Figure 1).

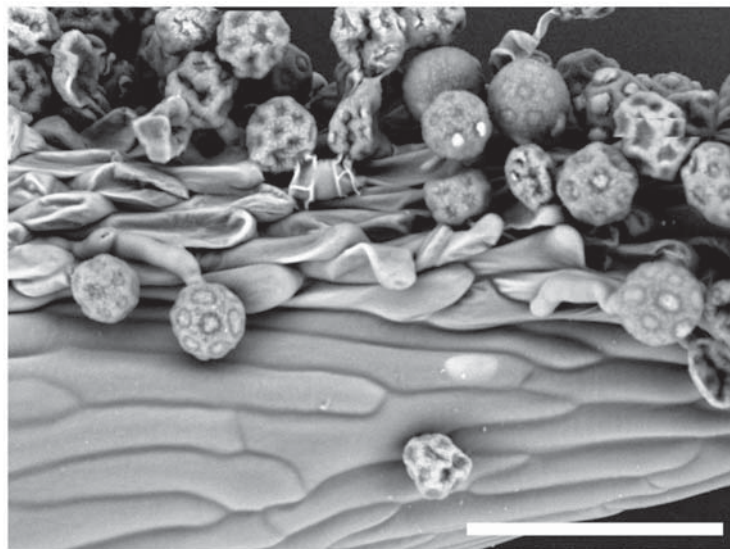


Figure 1. Scanning electron microscopy of stigmatic papillae of *R. asiaticus* 'Alfa' which was pollinated with *A. coronaria* 'Mistral Wine' (bar = $100 \text{ } \mu\text{m}$).

Despite this normal pollen–stigma event, pollen tubes mostly did not reach the ovules. However, using *Anemone* as a mother plant resulted in higher ratios of the pollen tube length to the total style length compared with the reciprocal crosses, except for *R.* 'Alfa' \times *A.* 'Mistral Wine' (Table 1).

Table 1. Ratio of the pollen tube length to the total style length in intertribal crosses between *A. coronaria* and *R. asiaticus*, visualized by aniline blue staining 56 h after pollination (mean \pm SE (n = number of repetitions)).

Mother Plant	Male Plant	Pollen Tube Length/ Total Style Length (n)
A. 'Mistral Fucsia'	R. 'Alfa'	0.229 \pm 0.064 (27)
	R. 'Krisma'	0.649 \pm 0.141 (10)
	R. 'Bianco Strié'	0.175 \pm 0.035 (20)
A. 'Mistral Wine'	R. 'Alfa'	0.194 \pm 0.044 (27)
	R. 'Krisma'	0.385 \pm 0.068 (10)
	R. 'Bianco Strié'	0.391 \pm 0.081 (11)
A. 'Wicabri Blue'	R. 'Alfa'	0.203 \pm 0.040 (19)
	R. 'Krisma'	0.133 \pm 0.021 (20)
	R. 'Bianco Strié'	0.118 \pm 0.017 (20)
R. 'Alfa'	A. 'Mistral Fucsia'	0.168 \pm 0.026 (37)
	A. 'Mistral Wine'	0.261 \pm 0.041 (15)
	A. 'Wicabri Blue'	0.159 \pm 0.029 (35)
R. 'Krisma'	A. 'Mistral Fucsia'	0.182 \pm 0.032 (27)
	A. 'Mistral Wine'	0.068 \pm 0.012 (19)
	A. 'Wicabri Blue'	0.036 \pm 0.005 (19)
R. 'Bianco Strié'	A. 'Mistral Fucsia'	0.042 \pm 0.005 (19)
	A. 'Mistral Wine'	0.057 \pm 0.009 (19)
	A. 'Wicabri Blue'	0.046 \pm 0.006 (19)

Compared to self-pollinations, the intertribal crosses caused an inhibition of the growth in the style, visualized by abnormalities like coiled and spirally twisted pollen tubes, disorientation of pollen tubes and a higher level of deposition of callose plugs (densely illuminated regions) (Figure 2).

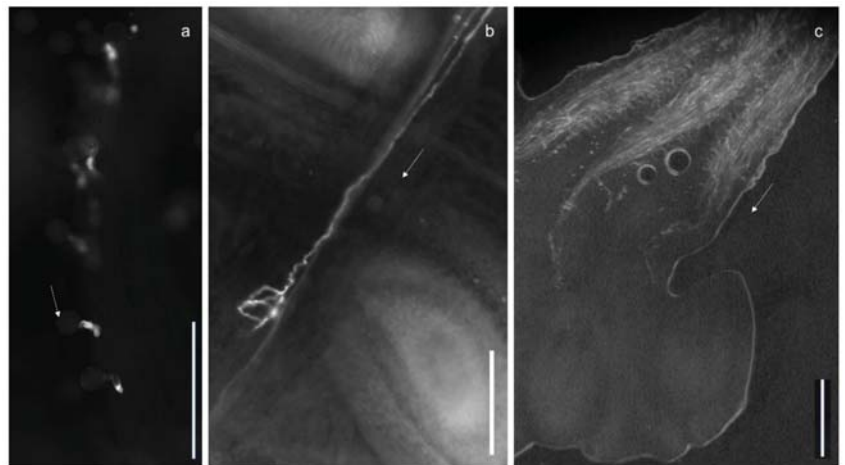


Figure 2. Aniline blue staining of intertribal crosses between (a) *R. asiaticus* 'Bianco Strié' \times *A. coronaria* 'Mistral Fucsia' showing very short pollen tubes and (b) *A. coronaria* 'Mistral Wine' \times *R. asiaticus* 'Krisma' with a pollen tube with abnormal coils. (c) Aniline blue staining of self-pollinated *A. coronaria* 'Wicabri Blue' carpels showing pollen tubes reaching the ovules (bar = 0.2 mm). The arrow shows the direction to the ovules.

Compared to the untreated stigmas, the combined treatment of the stigma with 2,4-D together with KIN (Comb) 24 h after pollination resulted in a significant increase in the ratio of the pollen tube length to the total style length (Table 2), both in the *Ranunculus* × *Anemone* cross and its reciprocal. When treating an *Anemone* stigma 24 h post-pollination with 2,4-D or NAA alone, a longer pollen tube length was noticed in the crosses of *Anemone* × *Ranunculus* compared to the untreated cross. Some ratios of the pollen tube length to total style length were negatively affected by the treatments. This was the case for the use of pollen germination medium (PM), cut style method (SC) and mentor pollination for the cross *Ranunculus* × *Anemone*, while, in the reciprocal cross, only the application of oil had a negative effect, resulting in no pollen tube growth at all (Table 2).

Table 2. Ratio of the pollen tube length to the total style length, visualized by aniline blue staining of the intertribal crosses *Ranunculus* × *Anemone* and the reciprocal cross thereof using different treatments and techniques to overcome pre-fertilization barriers (PM = pollen medium, sucrose = 5 % (*w/v*) sucrose solution, salt = 0.5 M NaCl, oil = olive oil, comb = 2,4-D + KIN 24 h after pollination, SC = cut-style pollination, mentor = mentor pollination, mix = mixed pollination, RV = pollen rehydration, old = an older flower stage than the reference flower stage, young = a younger flower stage than the reference stage) (mean ± SE). (n = number of crosses).

Treatment/ Technique	<i>Ranunculus</i> × <i>Anemone</i>			<i>Anemone</i> × <i>Ranunculus</i>		
	n	Pollen Tube Length/Total Style Length	Test Cross	n	Pollen Tube Length/Total Style Length	Test Cross
PM	11	0.026 ± 0.005 * ^y	'Alfa' × 'Mistral Wine'	9	0.302 ± 0.064	'Wicabri Blue' × 'Alfa'
sucrose	8	0.136 ± 0.029	'Alfa' × 'Mistral Wine'	5	0.559 ± 0.096	'Mistral Fucsia' × 'Alfa'
salt	12	0.159 ± 0.028	'Alfa' × 'Mistral Wine'	5	0.143 ± 0.035	'Mistral Fucsia' × 'Bianco Strié'
oil	20	0.292 ± 0.054	'Alfa' × 'Mistral Wine'	10	0.000 ± 0.000 * ^y	'Mistral Wine' × 'Bianco Strié'
2,4-D	6	0.078 ± 0.008	'Alfa' × 'Mistral Fucsia'	7	0.529 ± 0.164 *	'Wicabri Blue' × 'Alfa'
NAA	4	0.112 ± 0.062	'Alfa' × 'Mistral Fucsia'	5	0.681 ± 0.155 *	'Mistral Fucsia' × 'Alfa'
GA ₃	10	0.200 ± 0.055	'Alfa' × 'Mistral Fucsia'	4	0.490 ± 0.135	'Mistral Fucsia' × 'Alfa'
KIN	7	0.169 ± 0.060	'Alfa' × 'Mistral Fucsia'	6	0.258 ± 0.106	'Mistral Wine' × 'Bianco Strié'
comb	9	0.423 ± 0.121 *	'Alfa' × 'Mistral Fucsia'	4	0.505 ± 0.096 *	'Mistral Fucsia' × 'Bianco Strié'
SC	10	0.000 ± 0.000 *	'Alfa' × 'Mistral Wine'	6	0.199 ± 0.025	'Wicabri Blue' × 'Alfa'
mentor	9	0.038 ± 0.018 *	'Krisma' × 'Mistral Fucsia'	0	-	-
mix	0 ^z	-	-	0 ^z	-	-
RV	16	0.189 ± 0.044	'Alfa' × 'Mistral Wine'	5	0.439 ± 0.212	'Mistral Wine' × 'Alfa'
old	7	0.070 ± 0.012	'Alfa' × 'Mistral Fucsia'	6	0.066 ± 0.018	'Mistral Fucsia' × 'Alfa'
young	7	0.103 ± 0.029	'Alfa' × 'Mistral Fucsia'	5	0.439 ± 0.069	'Mistral Wine' × 'Alfa'

^z Aniline blue staining was not conducted for the mixed pollination, because pollen could not be distinguished. ^y Dunnett's *t* test (two-sided, *p* ≤ 0.05). * means significant different compared to reference control cross done during the same time period (see Table 1), each test cross was analyzed separately.

Although an increased ratio of pollen tube length to total style length of some of these treatments and techniques was observed, sometimes the pollen tubes showed aberrant orientations (Figure 3). Often, highly twisted pollen tubes were observed with callose plugs (Figure 3a,c,d,g).

The positive effect of the application of auxin (2,4-D, NAA), alone or in combination with KIN (Comb) 24 h post-pollination, resulted in a normal seed set, both in *Anemone* × *Ranunculus* crosses and their reciprocals (Table 3). This was also the case when the 2,4-D was applied 24 h before pollination (data not shown) and when mixed pollination was applied. In contrast to auxin, KIN, GA₃ and mentor pollination did not result in a complete seed set, but they slightly enhanced fruitlet formation in the *Ranunculus* × *Anemone* cross but not in the reciprocal cross (Table 3). Application of other components to the carpels or pollination techniques did not improve seed set substantially (Table 3). The treatment of the carpels with pollen germination medium or sugar resulted often in a dehydrated thalamus not able to bear any fruitlets.

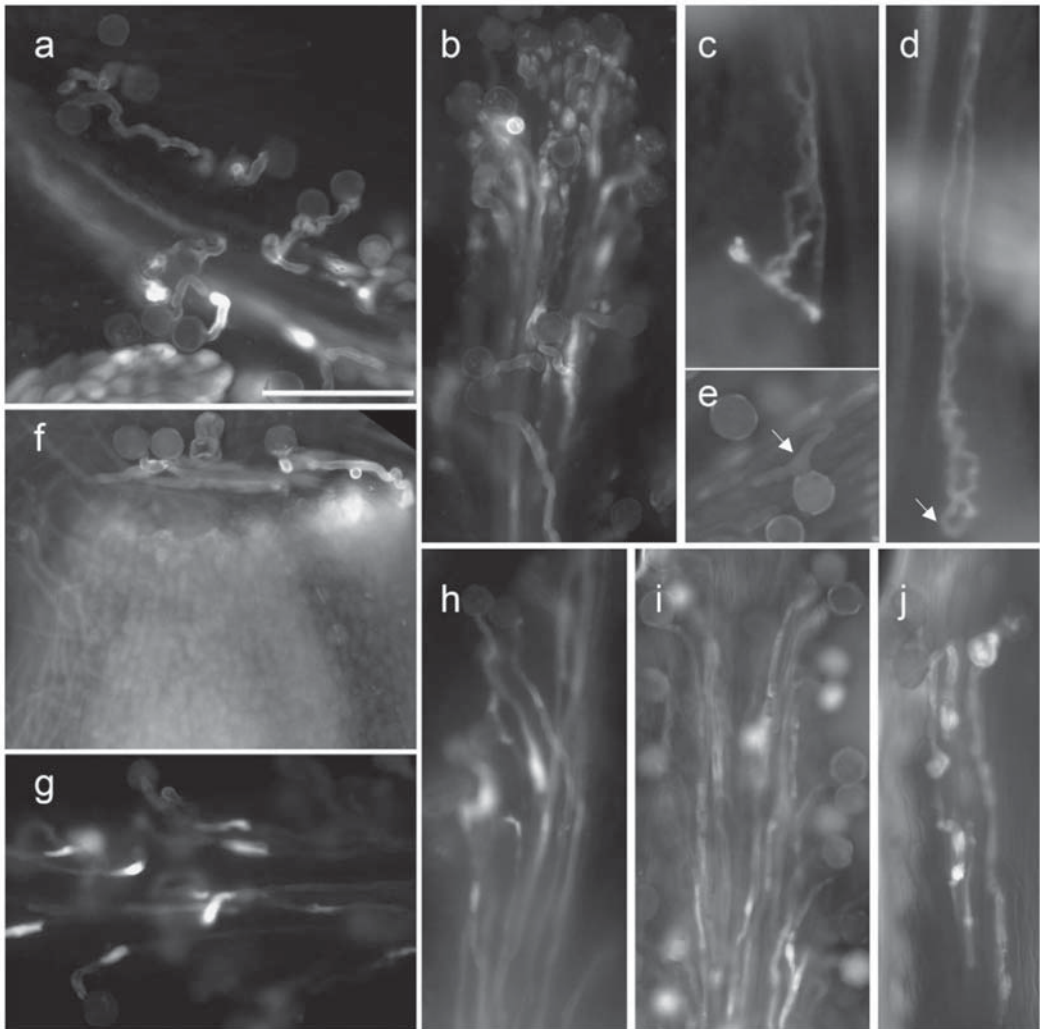


Figure 3. Aniline blue staining of intertribal crosses between *A. coronaria* and *R. asiaticus* using different treatments and techniques to overcome pre-zygotic barriers (bar = 0.125 mm). (a) Spirally growth of pollen tubes with many callose plugs (intense illuminated regions) were observed when the pollen germination medium (PM) was sprayed on the stigma before pollination (*A. 'Wicabri Blue'* × *R. 'Alfa'*). (b) Pollen tube growth in a cross of *A. 'Wicabri Blue'* × *R. 'Alfa'* after a 2,4-D treatment. (c,d) A relative long pollen tube of *R. 'Alfa'* in the style of *A. 'Mistral Fucsia'* after a NAA treatment, but when the pollen tube came near to the ovule a loop (see arrow) was formed and the pollen tube was totally disoriented. (e) In the cross of *'Mistral Fucsia'* × *'Alfa'* a branched pollen tube (see arrow) was observed when older carpels were pollinated. (f) Cut-style pollination resulted in pollen tube growth but with only slight penetration in the style (*'Wicabri Blue'* × *'Alfa'*). (g) Young, pollinated carpels showed many callose plugs (*'Mistral Wine'* × *'Alfa'*). (h) GA_3 treatment gave a relative normal pollen tube growth in *'Mistral Fucsia'* × *'Alfa'*. (i) Pollen tube growth of *'Bianco Strié'* in the style, after a 2,4-D and KIN treatment (comb) of carpels, of *'Mistral Fucsia'*. (j) Pollen tube growth of *'Mistral Fucsia'* in the style, after a 2,4-D and KIN treatment (comb), of *'Alfa'* carpels.

Table 3. Number (#) of intertribal crosses, total number (#) of fruitlets and the ratio of the total number (#) of fruitlets on the total number (#) of crosses between *Ranunculus* × *Anemone* and their reciprocal crosses, using different treatments and techniques to overcome pre-zygotic barriers (PM = pollen medium, sucrose = 5 % (*w/v*) sucrose solution, salt = 0.5 M NaCl, oil = olive oil, comb = 2,4-D + KIN 24 h after pollination, SC = cut-style pollination, mentor = mentor pollination, mix = mixed pollination, RV = pollen rehydration, old = an older flower stage than the reference flower stage, Young = a younger flower stage than the reference stage).

Treatment/ Technique	<i>Ranunculus</i> × <i>Anemone</i>			<i>Anemone</i> × <i>Ranunculus</i>		
	# Crosses	# Fruitlets	# Fruitlets/# Cross	# Crosses	# Fruitlets	# Fruitlets/# Cross
control	149	96	0.6	44	136	3.1
PM	58	9	0.2	1	0	0.0
sugar	43	10	0.2	0	-	-
salt	43	9	0.2	0	-	-
oil	60	19	0.3	4	1	0.3
2,4-D	75	3760	50.1	8	630	78.8
NAA	43	2657	61.8	6	210	35.0
GA ₃	45	57	1.3	7	4	0.6
KIN	48	118	2.5	3	1	0.3
comb	42	2697	64.2	12	588	49.0
SC	20	4	0.2	3	3	1.0
mentor	5	8	1.6	0	-	-
mix	20	858	42.9	15	582	38.8
RV	30	15	0.5	9	31	3.4
old	64	4	0.1	5	2	0.4
young	6	4	0.7	0	-	-

To investigate more into detail the visual observation that 2,4-D resulted in a good seed set in our intertribal crosses (Table 3), carpels of emasculated flowers were treated with 2,4-D without pollination. To our surprise, seed set occurred (Figure 4). Therefore, flow cytometry was used to compare leaf tissue and obtained fruitlets by self-pollination (control fruitlets) with fruitlets received after a 2,4-D treatment without pollination. Leaf tissue of ‘Wicabri Blue’ resulted in a clear diploid ploidy level (2×) and control peeled fruitlets had a dominant 2× peak (embryo and seed coat) and a small 3× peak (endosperm) (Figure 5a,b). Peeled fruitlets of ‘Wicabri Blue’ obtained after 2,4-D treatment without pollination resulted in a dominant 2× peak (Figure 5c) with occasionally a very small 4× peak, no 3× peak was visible, suggesting a lack of endosperm. These results, together with the abortion of the seed at maturation (data not shown) let us postulate the hypothesis that 2,4-D promotes apomixis, giving a 2× maternal embryo and a very limited or even no development of endosperm-like tissue. To complete this study, 2,4-D treated carpels were pollinated 24 h after treatment with pollen (self-pollination): most of the fruitlets (8/11) did not show a 3× peak, while some (3/11) showed a 2× and 3× peak (Figure 5d). Probably, the latter were fruitlets from sexual fertilizations.



Figure 4. Fruitlets of *A. coronaria* ‘Wicabri Blue’ after treatment of unpollinated carpels with 2,4-D (bar = 1 cm).

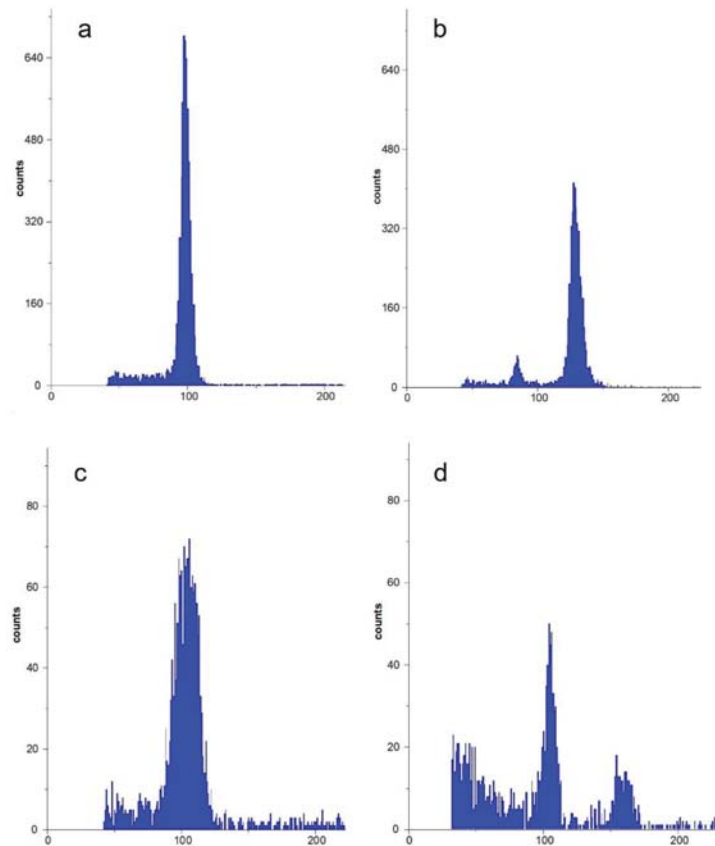


Figure 5. Flow cytometry of *A. coronaria* ‘Wicabri Blue’. (a) Flow cytometric pattern of leaf tissue of *A. coronaria* ‘Wicabri Blue’, the $2\times$ peak was set at 100. (b) Flow cytometric analysis of mature fruitlets of self-pollinated ‘Wicabri Blue’ as control, showing a diploid ploidy level (embryo and seed coat) and a triploid ploidy level (endosperm). (c) Flow cytometric analysis of immature fruitlets obtained from unpollinated 2,4-D treated carpels, showing a $2\times$ peak (embryo, seed coat). (d) Flow cytometric analysis of immature fruitlets obtained from self-pollinated 2,4-D treated carpels. The pollination was done 24 h after 2,4-D treatment. A minority (3/11) showed a $2\times$ peak (embryo, seed coat) and a $3\times$ peak (endosperm), probably the result of a sexual fertilization. The majority had the same pattern as shown in (c).

4. Discussion

Unilateral incongruity is a phenomenon often observed in distant crosses. It means that a cross is successful in one direction, whereas the reciprocal cross fails [7]. In the intertribal crosses between *A. coronaria* and *R. asiaticus*, the *Anemone* \times *Ranunculus* cross clearly resulted in higher ratios of pollen tube lengths to total style lengths than had the reciprocal cross. Some studies demonstrated a correlation between self-incompatibility and unilateral preference: pollen from self-compatible species is often rejected by self-incompatible species, whereas the reciprocal crosses are viable [6,12,29–31]. This was confirmed by interspecific crosses of *Banksia hookeriana* and *Banksia prionotes*, where seed set was only observed in *Banksia hookeriana* and in which *Banksia prionotes* showed signs of a late self-incompatibility [14]. This may partially explain the lower pollen tube to the total style length ratios of *Ranunculus* \times *Anemone* because of the self-incompatible nature of the *Ranunculus* cultivar ‘Alfa’ [19]. Besides the pollen tube inhibition observed in both

cross directions, pollen tubes also showed abnormalities such as disoriented, coiled and twisted pollen tubes with many callose plugs. Similar phenomena were observed in other interspecific crosses involving cotton and some wild relatives [22,32] and in intergeneric crosses in the Bromeliaceae family [33].

In *Anemone* and *Ranunculus*, the stigma is typically dry papillated [19]. As dry stigmas do not produce exudates, pollen adhesion is largely realized by the properties of the pollen surface [34]. Adhesion relies on the interaction between pollen coat proteins and receptors in the stigma [10]. After adhesion, mobilization of the pollen kit occurs, leading to the mixing of lipids and proteins to form a ‘foot’ of contact on the stigma surface [35]. This appressorium-like ‘foot’ appears to glue the pollen to the stigma, after which hydration takes place [8,20]. In *Arabidopsis*, it has been shown that the strength of pollen adhesion is directly proportional to the genetic distance between species [34]. In our intertribal crosses, this pollen-pistil interaction was showing no abnormalities, resulting in pollen adhesion, hydration, germination and pollen tube penetration into the stylar tissue. In several distant crosses, stigma treatments have shown their effectiveness to stimulate pollen hydration and germination. The treatment of female flowers of *Carica papaya* with 5% sucrose before pollination with the wild species *Vasconcellea cauliflora* enhanced the pollen germination and pollen tube growth [36]. On the other hand, in tobacco, the presence of cis-unsaturated triacylglycerides on the stigma has been shown to be essential and sufficient for pollen hydration, germination and penetration of the tubes into the pistil [20,37]. Olive oil (rich in cis-unsaturated triacylglycerides), pollen germination medium (sugar-rich) and sugar solutions were not very supportive in the crosses between *Anemone* and *Ranunculus*. Most probably, this is because the intertribal crosses showed no inhibition of pollen adhesion, hydration or germination. The time needed for rehydration of the pollen varies significantly between species [37] and many pollen germination percentages could be increased if pollen grains were equilibrated in a moisture environment before pollination [38,39]. Therefore, artificial pollen rehydration prior to pollination was applied in our intertribal crosses of *Anemone* and *Ranunculus*. However, without any significant effect. The system of self-incompatibility did not act in the same way as the incongruity system in wide crosses, but often similar techniques are used to overcome them. As the efficient application of saline solutions (0.25–1 M) to the stigma of *Brassica oleracea*, 30 min before pollination, inactivates the self-incompatibility barrier [18], this practice was also tested for our intertribal crosses. However, this technique was not promising. Similarly, flower age, which can have an effect on overcoming self-incompatibility [18], did not ameliorate pollen tube growth in the style compared to control crosses in our intertribal crosses.

The application of plant hormones, such as auxins, cytokinins and gibberellins, impacted the pollen tube growth or seed set in our crosses. More specifically, the combination of 2,4-D and KIN resulted in both a significant increase in pollen tube length, irrespectively of the cross direction, and a complete seed-set. The latter was also the case when the auxins 2,4-D and NAA were used alone. In interspecific hybridization in *Lens*, the application of GA₃ after fertilization increased the percentage of ovules obtained per cross, but the ovules started to turn brown and fruits dried [40]. The auxin 2,4-D is often applied in wide crosses in cereals to stimulate embryo development [41,42] and, in interspecific crosses of *Solanum*, treatment with 2,4-D on flowers after pollination improved seed set [12]. Notwithstanding 2,4-D having prevented the degeneration of the ovules and promoted the number of developing embryos, apomictic embryos were reported in some grasses and cereals after treatment with 2,4-D [21,43]. These observations are very similar to those obtained in this study. As 2,4-D-treated and pollinated carpels (24 h before or 24 h after pollination) resulted in a similar full seed set compared with unpollinated 2,4-D-treated carpels, it argues for an apomictic origin of the seeds. Moreover, flow cytometry on fruitlets obtained from unpollinated 2,4-D treated plants revealed a 2× and, occasionally, a minimal 4× peak. The 2× ploidy level is most likely derived from the apomictic embryo (and seed coat), while the absence of a 3× ploidy level can be explained by an incorrect endosperm balance number, probably triggering seed abortion. In many apomictic plants, the egg

cell begins to divide autonomously but endosperm formation often requires fertilization (pseudogamy) [44]. This could explain the abortion of these obtained seeds at maturation.

In this study, a broad range of techniques to overcome pre-zygotic barriers was used. Many of them have been successfully applied in other breeding programs. Style manipulations, such as cut-style pollination or the stylar graft technique, in which pollen is deposited on a compatible stigma, after which the upper part of the style is cut and positioned or grafted on another plant, are methods to circumvent stylar and stigmatic barriers, which can prohibit pollen tube growth [7]. Despite its success in *Lilium* [17], in the intertribal crosses of *Anemone* and *Ranunculus*, these style manipulation techniques were technically difficult to implement because of limited style length and they were of very limited success. Another technique used to overcome pre-fertilization barriers is the use of irradiated mentor pollen or mixed pollinations. The reasons for the positive effects of mentor and mixed pollination is still unknown [10]. It has been previously suggested that a high density of pollen grains induces favorable changes in the stigmatic surface and the style [45], while others proposed that congruent pollen can induce hydration and germination of normally incongruent pollen [8]. Mentor and mixed pollination techniques were both promising in some of the intertribal crosses studied here. Mixed pollinations seemed to result in a complete seed set. However, due to the relatively long period of receptivity of the stigma, it is most likely that the formed fruitlets were the result of crosses with the intrageneric pollen.

5. Conclusions

A significant effect on seed set of the use of the plant hormone auxin 2,4-D (and NAA), alone or in combination with KIN to bypass breeding barriers in intertribal crosses between *Anemone coronaria* and *Ranunculus asiaticus*, was shown in this study. Moreover, 2,4-D and KIN resulted in a significant increase in pollen tube length, irrespectively of the cross direction. However, the use of auxin can probably result in an apomictic seed set, therefore, screening of the progeny is of outmost importance.

This study shows that there are opportunities for breeding programs with genetically distant plant combinations within the Anemoneae and the Ranunculeae tribe by using stigma treatments. Treatments are, however, very cross-specific and must be elucidated empirically.

Author Contributions: Conceptualization, E.D., D.R. and M.-C.V.L.; methodology, E.D.; validation, E.D. and M.-C.V.L.; formal analysis, E.D.; investigation, E.D.; resources, D.R. and M.-C.V.L.; data curation, E.D., D.R. and M.-C.V.L.; writing—original draft preparation, E.D.; writing—review and editing, E.D., D.R. and M.-C.V.L.; visualization, E.D.; supervision, D.R. and M.-C.V.L. All authors have read and agreed to the published version of the manuscript.

Funding: This research received no external funding.

Institutional Review Board Statement: Not applicable.

Data Availability Statement: Raw data were generated at UGent. Derived data supporting the findings of this study are available from the corresponding author [E.D.] on request.

Acknowledgments: The authors thank A. Pennewaert, T. Versluys and C. Petit for their technical assistance, IRF (Istituto Regionale per la Floricoltura, Sanremo, Italy) and Biancheri Creations (Camporosso Mare, Italy) for delivering high-quality plant material and L. Van Hoorebeke and P. Vanderniepen, from the Department of Subatomic and Radiation Physics (Ghent University), for the pollen radiations. L. Leus is thanked for the flow cytometric measurements.

Conflicts of Interest: The authors declare no conflict of interest. The funders had no role in the design of the study; in the collection, analyses or interpretation of data; in the writing of the manuscript or in the decision to publish the results.

References

1. Hogenboom, N.G. A model for incongruity in intimate partner relationships. *Euphytica* **1973**, *22*, 219–233. [\[CrossRef\]](#)
2. Takayama, S.; Isogai, A. Self-Incompatibility in Plants. *Annu. Rev. Plant Biol.* **2005**, *56*, 467–489. [\[CrossRef\]](#)

3. Bhojwani, S.S.; Raste, A.P. In Vitro pollination and fertilization. In *In Vitro Haploid Production in Higher Plants*; Springer: Dordrecht, The Netherlands, 1996; pp. 237–262.
4. Orr, H.A.; Presgraves, D.C. Speciation by postzygotic isolation: Forces, genes and molecules. *BioEssays* **2000**, *22*, 1085–1094. [[CrossRef](#)]
5. Bino, R.J.; Van Creijl, M.G.M.; Van Der Leede-Plegt, L.M.; Van Tunen, A.J.; Van Tuyl, J.M. Application of in Vitro Pollination and Fertilization Techniques for Breeding and Genetic Manipulation of Lilium. In *Sexual Plant Reproduction*; Springer: Singapore, 1992; pp. 127–134.
6. Rieseberg, L.H.; Carney, S.E. Plant hybridization. *New Phytol.* **1998**, *140*, 599–624. [[CrossRef](#)] [[PubMed](#)]
7. van Tuyl, J.M.; de Jeu, M.J. Methods for overcoming interspecific crossing barriers. *Pollen Biotechnol. Crop Prod. Improv.* **1997**, *273–292*. [[CrossRef](#)]
8. Hiscock, S.J.; Allen, A.M. Diverse cell signalling pathways regulate pollen-stigma interactions: The search for consensus. *New Phytol.* **2008**, *179*, 286–317. [[CrossRef](#)]
9. Heslop-Harrison, Y.; Shivanna, K.R. The Receptive Surface of the Angiosperm Stigma. *Ann. Bot.* **1977**, *41*, 1233–1258. [[CrossRef](#)]
10. Broz, A.K.; Bedinger, P.A. Pollen-Pistil Interactions as Reproductive Barriers. *Annu. Rev. Plant Biol.* **2021**, *72*, 615–639. [[CrossRef](#)]
11. Sharma, H.C. How wide can a wide cross be? *Euphytica* **1995**, *82*, 43–64. [[CrossRef](#)]
12. Jansky, S. Overcoming hybridization barriers in potato. *Plant Breed.* **2006**, *125*, 1–12. [[CrossRef](#)]
13. Van Tuyl, J.; Lim, K.-B. Interspecific hybridisation and polyploidisation as tools in ornamental plant breeding. *Acta Hort.* **2003**, *612*, 13–22. [[CrossRef](#)]
14. Sedgley, M.; Wirthensohn, M.; Delaporte, K.L. Interspecific Hybridization between *Banksia hookeriana* Meisn. and *Banksia prionotes* Lindl. (Proteaceae). *Int. J. Plant Sci.* **1996**, *157*, 638–643. [[CrossRef](#)]
15. Sarmah, B.K.; Sarla, N. Overcoming preferentialization barriers in the cross *Diplotaxis siettiana* × *Brassica juncea* using irradiated mentor pollen. *Biol. Plant.* **1995**, *37*, 329–334.
16. Wenslaff, T.F.; Lyrene, P.M. The Use of Mentor Pollination to Facilitate Wide Hybridization in Blueberry. *HortScience* **2000**, *35*, 114–115. [[CrossRef](#)]
17. Van Tuyl, J.; Van Diën, M.; Van Creijl, M.; Van Kleinwee, T.; Franken, J.; Bino, R. Application of in vitro pollination, ovary culture, ovule culture and embryo rescue for overcoming incongruity barriers in interspecific *Lilium* crosses. *Plant Sci.* **1991**, *74*, 115–126. [[CrossRef](#)]
18. Carafa, A.M.; Carratù, G. Stigma treatment with saline solutions: A new method to overcome self-incompatibility in *Brassica oleracea* L. *J. Hort. Sci.* **1997**, *72*, 531–535. [[CrossRef](#)]
19. Dhoooge, E.; Grunewald, W.; Reheul, D.; Goetghebeur, P.; Van Labeke, M.-C. Floral characteristics and gametophyte development of *Anemone coronaria* L. and *Ranunculus asiaticus* L. (Ranunculaceae). *Sci. Hort.* **2012**, *138*, 73–80. [[CrossRef](#)]
20. Wolters-Arts, M.; Lush, W.M.; Mariani, C. Lipids are required for directional pollen-tube growth. *Nat. Cell Biol.* **1998**, *392*, 818–821. [[CrossRef](#)]
21. Matzk, F. A novel approach to differentiated embryos in the absence of endosperm. *Sex. Plant Reprod.* **1991**, *4*, 88–94. [[CrossRef](#)]
22. Ram, S.G.; Ramakrishnan, S.H.; Thiruvengadam, V.; Babu, J.R.K. Prefertilization barriers to interspecific hybridization involving *Gossypium hirsutum* and four diploid wild species. *Plant Breed.* **2008**, *127*, 295–300. [[CrossRef](#)]
23. Langlet, O.F.J. Über Chromosomen Verhältnisse und Systematik der Ranunculaceae. *Sven. Bot. Tidskr.* **1932**, *26*, 318–400.
24. Beruto, M.; Fibiani, M.; Rinino, S.; Scalzo, R.L.; Curir, P. Plant development of *Ranunculus asiaticus* L. tuberous roots is affected by different temperature and oxygen conditions during storage period. *Isr. J. Plant Sci.* **2009**, *57*, 377–388. [[CrossRef](#)]
25. Meynet, J. *Anemone*. In *The Physiology of Flower Bulbs*; De Hertogh, A., Le Nard, M., Eds.; Elsevier: Amsterdam, The Netherlands, 1993; pp. 211–218.
26. Meynet, J. *Ranunculus*. In *The Physiology of Flower Bulbs*; De Hertogh, A., Le Nard, M., Eds.; Elsevier: Amsterdam, The Netherlands, 1993; pp. 603–610.
27. Galbraith, D.W.; Harkins, K.R.; Maddox, J.M.; Ayres, N.M.; Sharma, D.P.; Firoozabady, E. Rapid Flow Cytometric Analysis of the Cell Cycle in Intact Plant Tissues. *Science* **1983**, *220*, 1049–1051. [[CrossRef](#)] [[PubMed](#)]
28. Otto, F. Chapter 11 DAPI Staining of Fixed Cells for High-Resolution Flow Cytometry of Nuclear DNA. In *Methods in Cell Biology*; Elsevier: Amsterdam, The Netherlands, 1990; Volume 33, pp. 105–110.
29. Lee, C.B.; Page, L.E.; McClure, B.A.; Holtsford, T.P. Post-pollination hybridization barriers in Nicotiana section Alatae. *Sex. Plant Reprod.* **2008**, *21*, 183–195. [[CrossRef](#)]
30. Wheeler, M.J.; Franklin-Tong, V.E.; Franklin-Tong, N. The molecular and genetic basis of pollen–pistil interactions. *New Phytol.* **2001**, *151*, 565–584. [[CrossRef](#)] [[PubMed](#)]
31. Zenkteler, M.; Nitzsche, W. Wide hybridization experiments in cereals. *Theor. Appl. Genet.* **1984**, *68*, 311–315. [[CrossRef](#)]
32. Ram, S.G.; Thiruvengadam, V.; Ramakrishnan, S.H.; Babu, J.R.K. Investigation on pre-zygotic barriers in the interspecific crosses involving *Gossypium barbadense* and four diploid wild species. *Euphytica* **2007**, *159*, 241–248. [[CrossRef](#)]
33. Parton, E. Flower Biology and Crossing Barriers in Bromeliaceae. Ph.D. Thesis, Katholieke Universiteit Leuven, Leuven, Belgium, 2001.
34. Zinkl, G.; Zwiebel, B.; Grier, D.; Preuss, D. Pollen-stigma adhesion in Arabidopsis: A species-specific interaction mediated by lipophilic molecules in the pollen exine. *Development* **1999**, *126*, 5431–5440. [[CrossRef](#)] [[PubMed](#)]

35. Edlund, A.F.; Swanson, R.; Preuss, D. Pollen and Stigma Structure and Function: The Role of Diversity in Pollination. *Plant Cell* **2004**, *16*, S84–S97. [[CrossRef](#)] [[PubMed](#)]
36. Dinesh, M.; Rekha, A.; Ravishankar, K.; Praveen, K.; Santosh, L. Breaking the intergeneric crossing barrier in papaya using sucrose treatment. *Sci. Hortic.* **2007**, *114*, 33–36. [[CrossRef](#)]
37. Wolters-Arts, M.; van der Weerd, L.; Van Aelst, A.C.; Van As, H.; Mariani, C. Water-conducting properties of lipids during pollen hydration. *Plant Cell Environ.* **2002**, *25*, 513–519. [[CrossRef](#)]
38. Boavida, L.C.; McCormick, S. Temperature as a determinant factor for increased and reproducible in vitro pollen germination in *Arabidopsis thaliana*. *Plant J.* **2007**, *52*, 570–582. [[CrossRef](#)]
39. Ma, J.-F.; Liu, Z.-H.; Chu, C.-P.; Hu, Z.-Y.; Wang, X.-L.; Zhang, X.S. Different regulatory processes control pollen hydration and germination in *Arabidopsis*. *Sex. Plant Reprod.* **2011**, *25*, 77–82. [[CrossRef](#)] [[PubMed](#)]
40. Fratini, R.; Ruiz, M.L. Interspecific Hybridization in the Genus *Lens* Applying In Vitro Embryo Rescue. *Euphytica* **2006**, *150*, 271–280. [[CrossRef](#)]
41. Matzk, F. Hybrids of Crosses between Oat and Andropogoneae or Paniceae Species. *Crop. Sci.* **1996**, *36*, 17–21. [[CrossRef](#)]
42. Sidhu, P.K.; Howes, N.K.; Aung, T.; Zwer, P.K.; Davies, P.A. Factors affecting oat haploid production following oat × maize hybridization. *Plant Breed.* **2006**, *125*, 243–247. [[CrossRef](#)]
43. Wędzony, M.; Van Lammeren, A.A.M. Pollen tube growth and early embryogenesis in wheat × maize crosses influenced by 2, 4-D. *Ann. Bot.* **1996**, *77*, 639–647. [[CrossRef](#)]
44. Koltunow, A.M.; Grossniklaus, U. Apomixis: A Developmental Perspective. *Annu. Rev. Plant Biol.* **2003**, *54*, 547–574. [[CrossRef](#)] [[PubMed](#)]
45. Mulcahy, G.B.; Mulcahy, D.L. A comparison of pollen tube growth in bi- and trinucleate pollen. *Pollen Biol. Implic. Plant Breed.* **1983**, 29–33.



Article

Dehydrins and Soluble Sugars Involved in Cold Acclimation of *Rosa wichurana* and Rose Cultivar ‘Yesterday’

Lin Ouyang^{1,2,*}, Leen Leus³, Ellen De Keyser³ and Marie-Christine Van Labeke²

¹ Institute of Urban Agriculture, Chinese Academy of Agricultural Sciences, 99 Hupan West Road, Tianfu New Area, Chengdu 610000, China

² Department of Plants and Crops, Ghent University, Coupure Links 653, 9000 Ghent, Belgium; MarieChristine.VanLabeke@UGent.be

³ Plant Sciences Unit, Flanders Research Institute for Agriculture, Fisheries and Food (ILVO), Caritasstraat 39, 9090 Melle, Belgium; leen.leus@ilvo.vlaanderen.be (L.L.); Ellen.DeKeyser@ilvo.vlaanderen.be (E.D.K.)

* Correspondence: ouyanglin@caas.cn; Tel.: +86-028-8020-3195

Abstract: Rose is the most economically important ornamental plant. However, cold stress seriously affects the survival and regrowth of garden roses in northern regions. Cold acclimation was studied using two genotypes (*Rosa wichurana* and *R. hybrida* ‘Yesterday’) selected from a rose breeding program. During the winter season (November to April), the cold hardiness of stems, soluble sugar content, and expression of dehydrins and the related key genes in the soluble sugar metabolism were analyzed. ‘Yesterday’ is more cold-hardy and acclimated faster, reaching its maximum cold hardiness in December. *R. wichurana* is relatively less cold-hardy, only reaching its maximum cold hardiness in January after prolonged exposure to freezing temperatures. Dehydrin transcripts accumulated significantly during November–January in both genotypes. Soluble sugars are highly involved in cold acclimation, with sucrose and oligosaccharides significantly correlated with cold hardiness. Sucrose occupied the highest proportion of total soluble sugars in both genotypes. During November–January, downregulation of *RhSUS* was found in both genotypes, while upregulation of *RhSPS* was observed in ‘Yesterday’ and upregulation of *RhINV2* was found in *R. wichurana*. Oligosaccharides accumulated from November to February and decreased to a significantly low level in April. *RhRS6* had a significant upregulation in December in *R. wichurana*. This study provides insight into the cold acclimation mechanism of roses by combining transcription patterns with metabolite quantification.

Keywords: cold hardiness; LT₅₀; sucrose; oligosaccharides; soluble sugar metabolism; gene expression

Citation: Ouyang, L.; Leus, L.; De Keyser, E.; Van Labeke, M.-C. Dehydrins and Soluble Sugars Involved in Cold Acclimation of *Rosa wichurana* and Rose Cultivar ‘Yesterday’. *Horticulturae* **2021**, *7*, 379. <https://doi.org/10.3390/horticulturae7100379>

Academic Editor: Anastasios Darras

Received: 30 August 2021

Accepted: 1 October 2021

Published: 8 October 2021

Publisher’s Note: MDPI stays neutral with regard to jurisdictional claims in published maps and institutional affiliations.



Copyright: © 2021 by the authors. Licensee MDPI, Basel, Switzerland. This article is an open access article distributed under the terms and conditions of the Creative Commons Attribution (CC BY) license (<https://creativecommons.org/licenses/by/4.0/>).

1. Introduction

Rose is the most economically important ornamental plant. For garden roses grown in northern regions (Northern Europe, North China, Russia, the northern regions of the US and Canada), winter temperatures restrict the geographical distribution and affect winter survival, growth, and ornamental quality of garden roses. Breeding for improved cold hardiness would allow roses to survive wintry temperatures without extra protection, an important selling point for gardeners in colder regions. The study of the mechanisms involved in cold acclimation can help future varietal development in breeding programs as well as the selection of cold-hardy garden roses. Woody plants have evolved the ability to adapt to low temperatures and develop cold hardiness. Cold hardiness has a seasonal dynamic characterized by three phases: cold acclimation during autumn–winter, mid-winter hardiness (maximum level of cold hardiness), and deacclimation (loss of tolerance) during winter–spring. Evaluation of cold hardiness using electrolyte leakage analysis is a reliable method for the stems of woody plants [1,2]. Low temperatures can lead to the loss of membrane integrity, resulting in cellular damage and solute leakage across the membrane. The level of electrolyte leakage is related to the freezing temperatures and cold tolerance of plants.

Cold acclimation, the process by which the plant achieves cold hardiness/freezing tolerance, is associated with a wide spectrum of physiological and biochemical changes that occur in response to the decrease of photoperiod, light intensity and temperatures [3–6]. The most prominent changes during cold acclimation include growth reduction, a decrease in tissue water content, changes in membrane lipid compositions, induction of stress proteins, accumulation of osmolytes (soluble sugars, proline, betaine, etc.), and enhancement of the antioxidant system [7–11]. These changes are the results of genetic adjustments starting from the signal perception and transduction to transcriptional regulation, and finally to downstream stress-responsive gene expression [12,13].

Dehydrins are highly hydrophilic proteins which belong to the late embryo-abundant (LEA and LEA-like) II group of proteins. They play multiple roles in enhancing freezing tolerance, including cryoprotection of enzymes, stabilization of cell membranes, protection of cellular components, and scavenging reactive oxygen species [14,15]. It is assumed that they repair the rigidity of the membrane by forming amphipathic α -helices to stabilize cell membranes [16,17]. Dehydrins may also prevent freeze-induced dehydration by interacting with soluble sugars in the cells [18]. This interaction may be due to the information of stable glasses [19]. The accumulation of both soluble sugars and cold stress proteins is necessary to achieve the maximum cold hardiness [20].

Soluble sugars contribute to the plant's cold hardiness level by protecting cells from freezing injury in a number of ways. Soluble sugars that function as compatible solutes (osmolytes) can stabilize the osmotic potential of cells and prevent an excessive water loss to the apoplast space, resulting in the enlargement of ice crystals. An accumulation of soluble sugars increases solute concentration and thus drops the freezing point of cells [7]; this has been observed in both herbaceous and woody plants during cold acclimation [21–24]. Soluble sugars can act as cryoprotectants, protecting cell membranes by interacting with lipid molecules [25] and protecting specific enzymes during cold-induced dehydration. Sugars may also stabilize the cell membranes by interacting with lipid molecules [26]. Several essential genes involved in the metabolism of soluble sugars were found to be responsive to cold stress: *sucrose synthase* (*SUS*), *sucrose-phosphate synthase* (*SPS*), and *invertase* (*INV*) in the sucrose metabolism pathway [27,28]; *raffinose synthase* (*RS*) and *galactinol* (*Gols*) in the RFOs (raffinose family oligosaccharides) synthesis pathway [29–31].

In the present study, two garden roses with distinct genetic backgrounds (one rose species (*R. wichurana*) and one rose cultivar (*R. hybrida* 'Yesterday')) were selected to study cold acclimation under natural conditions. This study revealed both biochemical and molecular mechanisms involved in cold acclimation of two different rose genotypes, with a main focus on the role of dehydrins and cryoprotective soluble sugars.

2. Materials and Methods

2.1. Plant Material and Experimental Field Condition

R. wichurana is one of the wild rose species. *R. hybrida* 'Yesterday', bred by Harkness (United Kingdom, 1974), is one of the modern rose cultivars and belongs to the rose type Polyantha. Both genotypes are diploid roses. The coldest USDA (United States Department of Agriculture) plant hardiness zone of *R. wichurana* is 5b (−26.1 to −23.3 °C); the hardiness zone for 'Yesterday' is 4b (31.7 to −28.9 °C) (<http://www.helpmefind.com/rose/index.php>; accessed on 4 October 2021). Plant material for *R. wichurana* and 'Yesterday' started as rooted cuttings in summer 2014. The experiment was conducted at ILVO (Melle, Belgium, 51°0' N, 3°48' E). The roses were planted outdoors in February 2015 in light sandy loam soil (pH_{KCl} 5.67, the organic matter 1.35%) and pruned in March 2015 to allow new shoots to grow. A randomized block design was arranged in two blocks; each block included 30 plants per genotype. Stems that emerged during that season were sampled on 19 November 2015, 14 December 2015, 20 January 2016, 19 February 2016, 14 March 2016, and 18 April 2016. Sampled stems were transferred on ice to the laboratory.

2.2. Controlled Freezing Test

Cold hardiness as evaluated by LT_{50} was conducted using a controlled freezing test ($n = 5$). Internodal stem segments (0.5 cm long) were taken from the middle part of the current-year stem. Stem segments were placed in a cryostat (Polystat 37, Fisher Scientific, Merelbeke, Belgium) from 0 °C to seven target temperatures (−5, −10, −15, −20, −25, −30, −35, and −80 °C) at a cooling rate of 6 °C h^{−1} (0.1 °C min^{−1}). The detailed protocol of the controlled freezing test was described by Ouyang et al. [32]. Index of injury (It) based on electrolyte leakage (EL) values were calculated according to Flint et al. [33] and transformed into the adjusted It value taking into account the It at −80 °C [34]. LT_{50} values were calculated from the injury versus temperature plot using logistic regression.

2.3. Soluble Sugars

Stem tissue samples of each replicate representing a balanced mix of the apical, median, and basal zone were ground in liquid nitrogen with a mill (IKA® A11 Basic Analytical Mill, Staufen, Germany). The analysis was done in five replicates for each genotype. Soluble sugars were extracted as described in Ouyang et al. [32]. Sucrose, hexoses (glucose and fructose), and oligosaccharides (raffinose and stachyose) were quantified via high-performance anion-exchange chromatography with pulsed amperometric detection (ACQUITY UPLC H-Class, Waters, Milford, MA, USA) using a CarboPac PA-20 analytical column and companion guard column of Dionex (Thermo Fisher Scientific, Sunnyvale, CA, USA) and an eluent of 50 mM NaOH at 22 °C.

2.4. RNA Extraction and Reverse Transcription

Stem tissue samples of each replicate representing a balanced mix of the apical, median, and basal zone were ground in liquid nitrogen. The analysis was done in three replicates for each genotype. Each replicate of the RNA sample was extracted from 100 mg of the ground tissue sample in 700 µL extraction buffer using a CTAB protocol. The RNA quality was controlled and tested by the NanoDrop (ND-1000) spectrophotometer (Isogen Life Science, Utrecht, The Netherlands). The RNA quality was further determined by the Experion™ Automated Electrophoresis System and RNA StdSens Chips (Bio-Rad Laboratories N.V., Temse, Belgium) with a random selection of about 10% of total samples spread over the two genotypes and sampling points. RNA samples (starting from 550 ng of RNA) were converted to single-stranded cDNA using the iScript™ cDNA Synthesis Kit (Bio-Rad Laboratories N.V., Temse, Belgium). Detailed protocols were based on Luyypaert et al. [35].

2.5. Gene Isolation and Expression

Candidate genes associated with dehydrins and soluble sugar metabolism were selected according to the literature (Table 1). These homologous sequences were locally BLASTed against the ILVO *Rosa hybrida* transcriptome database in CLCbio. This transcriptome database was built based on transcriptomic data of *R. wichurana* and ‘Yesterday’. BLASTx [36] was used to confirm fragment identity. Several dehydrins were found, but only *RhDHN5* and *RhDHN6* were expressed and thus retained for further study. Four key genes involved in the soluble sugar metabolism were studied—including *RhSPS1*, *RhSUS*, and *RhINV2* in the sucrose metabolism pathway, and *RhRS6* in the RFOs (raffinose family oligosaccharides) synthesis pathway (Table 1). RT-qPCR primers of target genes were designed using Primer3Plus software [37] (Table 2). The RT-qPCR analysis was performed as described in Luyypaert et al. [35]. Candidate reference genes (*PGK*, *RPS18c*, *2-UBC9*, *APT1*, *ACT*, *CAB*, *HMG1*, *HSP81*, *MDHC1*, *RBCS1A*, and *TUB*) were chosen from Pipino [38]. GeNorm analysis was conducted based on Vandesompele et al. [39], and gene-specific amplification efficiencies were determined by LinRegPCR according to Ruijter et al. [40] (Table 2). A normalization factor based on three validated reference genes (*PGK*, *PR518c*, and *2-UBC9*) was used for the calculation of calibrated normalized relative quantities (CNRQ) in the qbase+ software (Biogazelle, Ghent, Belgium) [41]. CNRQ values were exported to Microsoft Excel. Biological replicates were averaged geometrically.

Table 1. List of candidate genes in other species used to identify the putative homologue and isolate from the *Rosa* spp. transcriptome database.

Genes in Roses	Functional Annotation	Species	Acc. No.
<i>RhDHN5/6</i> *	Dehydrin	<i>Prunus persica</i>	U34809
<i>RhSPS1</i>	Sucrose-phosphate synthase	<i>Camellia sinensis</i>	KF696388
<i>RhSUS</i>	Sucrose synthase	<i>Camellia sinensis</i>	KF921302
<i>RhINV2</i>	Invertase	<i>Camellia sinensis</i>	KP053402
<i>RhRS6</i>	Raffinose synthase	<i>Camellia sinensis</i>	KP162174

* *RhDHN5/6* were chosen according to Artlip et al. [42], and other four candidate genes (*RhSPS1*, *RhSUS*, *RhINV2*, and *RhRS6*) were chosen from Yue et al. [43].

Table 2. List of RT-qPCR primer sequences and product size for *Rosa* spp. target gene fragments and reference genes.

Gene	Acc. No.	F or R	Primer Sequence 5'–3'	Amplicon Size (bp)	PCR Efficiencies
<i>RhDHN5</i>	MH249069	F	GGTACAAGGACGATCCCTA	86	1.886
		R	CCCTTATGCTCTTGGTGCTC		
<i>RhDHN6</i>	MH249070	F	CCGTGAGAATAAGGGAGTGG	106	1.914
		R	GCCGTAACCCGGTGTAGTAG		
<i>RhSUS</i>	MH249072	F	AGACCCTTCTCACTGGGACA	142	1.798
		R	GCGATCAAGGTTGGAGACA		
<i>RhINV2</i>	MH249073	F	TCTGTGGCAACTGATGTTGTT	130	1.893
		R	TTGTTTCGTCCACCTTGAGC		
<i>RhRS6</i>	MH249076	F	CATTAGTGGCGACCTGTTT	84	1.912
		R	CCGTCCGGCAATACTATCTT		
<i>RhPGK</i> *	EC586265.1	F	GCCAAAGTCATCTTGGCTTC	101	1.869
		R	CCACTCCAAGGAGCTCAGAC		
<i>RhRPS18c</i> *	BI977264.1	F	ATCTCGAGCGGTTGAAGAAG	97	1.890
		R	TGCGACCAGTAGTCTTGGTG		
<i>Rh2-UBC9</i> *	EC586612.1	F	GACCCAAATCCTGATGATCC	104	1.903
		R	CGTACTTCTGGGTCCAGCTC		

* These genes were selected from Pipino [38].

2.6. Statistical Analysis

The homoscedasticity of data was checked by Levene's test ($p \geq 0.01$) before performing a one-way analysis of variance (ANOVA). LT_{50} and soluble sugars were analyzed with a one-way ANOVA and the accompanying Scheffé's post-hoc test ($p = 0.05$). CNRQ values were log-transformed. Gene expression was analyzed using one-way ANOVA with a Scheffé's post-hoc test at a 0.05 significance level; if homoscedasticity of data was not fulfilled, a Kruskal–Wallis test was performed ($p = 0.05$). Statistics were analyzed in SPSS Statistics 24.0, and all figures were performed in SigmaPlot 13.0. Gene expression graphs are made according to non-log transformed data. Correlation analysis between LT_{50} and the concentration of sugars and between LT_{50} and gene expression were conducted by Spearman's two-tailed test ($p = 0.05$).

3. Results

3.1. Air Temperature and Day Length Condition

Cold hardiness of woody plants is a seasonal dynamic process including three phases: acclimation, mid-winter hardiness and deacclimation. As the process is mainly influenced by changes in temperature and photoperiod, the mean temperature and day length were recorded seven days before the sampling points. The air temperature was monitored on location at 30-min intervals by a sensor integrated into a weather station (HortiMaX, Maasdijk, The Netherlands) and installed near the trial field at ILVO (Melle, Belgium, 51°0' N, 3°48' E) on the greenhouse roof, 5 m above the ground level. Data for day length at Melle was based on information found at <https://www.timeanddate.com> (accessed on 4 October 2021).

The average temperatures dropped from 9.9 °C in November to 5.5 °C in December and dropped further to below zero in January (−2 °C) and February (−1.8 °C). In March the mean temperature increased to −0.1 °C then rose sharply to 5.2 °C in April. Negative minimum temperatures were noted in January, February, and March. Day length shifted from 8 h 57 min in November to 8 h 2 min in December and then lengthened to 13 h 48 min at the end of April.

3.2. Cold Hardiness

Seasonal changes in cold hardiness as estimated by LT_{50} values (i.e., the temperature that causes 50% of injury) are given in Figure 1. LT_{50} values decreased from November to December/January, remained relatively low in February–March, and increased to April. A significantly lower LT_{50} value of −26.4 °C was found in December for ‘Yesterday’ ($p < 0.05$) compared to that in other months. This indicates a strong and fast acclimation pattern, with the highest cold hardiness achieved in early winter. In contrast with ‘Yesterday’, *R. wichurana* developed maximum cold hardiness later in January and reached a lower mid-winter hardiness of −20.1 °C. It can be concluded that ‘Yesterday’ has a fast acclimation and is relatively more cold-hardy than *R. wichurana*. A certain degree of deacclimation of both genotypes was observed during January–March with a strong deacclimation observed in April.

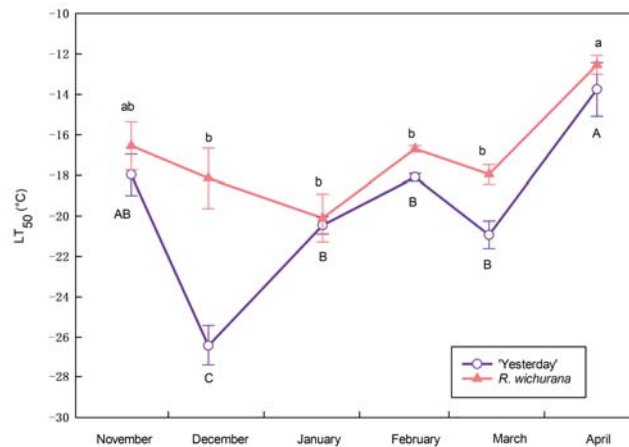


Figure 1. Seasonal changes of cold hardiness of stems expressed as LT_{50} (temperature of 50% relative electrolyte leakage) of two rose genotypes (*Rosa hybrida* ‘Yesterday’ and *R. wichurana*). Different letters indicate significant differences among sampling time points within each genotype ($p = 0.05$). Values are means \pm SE ($n = 5$).

3.3. Expression Analysis of Dehydrins

The expression of *RhDHN5* and *RhDHN6* was induced from November to January in both genotypes (Figure 2). High transcript abundance was observed in the more cold-hardy genotype ‘Yesterday’ during this period, indicating a higher induction when compared to that during February–April. The expression of *RhDHN5* and *RhDHN6* showed a similar seasonal pattern in *R. wichurana*, although transcript levels were lower than in ‘Yesterday’. In addition, the expression levels of *RhDHN5* and *RhDHN6* in ‘Yesterday’ from November to January were much higher than those in *R. wichurana*, which corresponds to the stronger development of cold hardiness (lower LT_{50} value) observed in ‘Yesterday’ during the same period. No significant correlations between gene expression of dehydrins and LT_{50} were observed in either genotype.

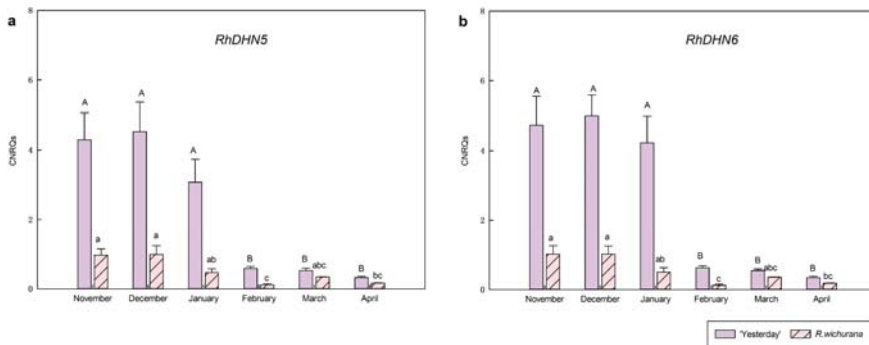


Figure 2. Seasonal changes in expression of dehydrins including *RhDHN5* (a) and *RhDHN6* (b) in the more cold-hardy genotype (*Rosa hybrida* ‘Yesterday’) and the less cold-hardy genotype (*R. wichurana*). Data were assessed by one-way ANOVA and a Scheffé post-hoc test ($p = 0.05$). Different letters (A, B, etc.; or a, b, etc.) indicate significant differences between time points within each genotype. Normalized relative quantities (CNRQs, non-log-transformed) are presented as geometric means \pm SE ($n = 3$).

3.4. Soluble Sugars

Sucrose represented the largest proportion of total soluble sugars in the test season (Figure 3). In ‘Yesterday’, the proportion of sucrose was highest in November and December at around 75%, followed by a slight decrease to 66.3–69.8% during January–February. After a recovery in March, the proportion of sucrose dropped to 53.5% in April. In *R. wichurana*, the proportion of sucrose increased sharply from 41.3% in November to 62.0% in December and remained relatively stable during December–April, varying between 61.9–65.2%. A negative correlation between sucrose and LT_{50} value was detected in ‘Yesterday’ ($r = 0.42, p < 0.05$).

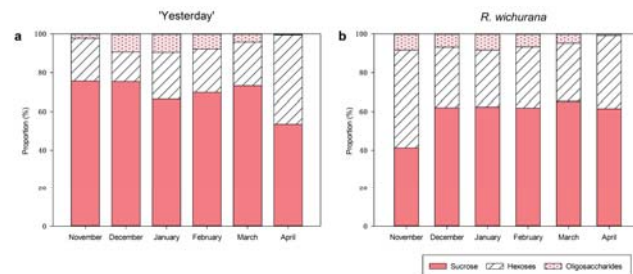


Figure 3. Proportions of sucrose, hexoses (glucose + fructose), and oligosaccharides (raffinose + stachyose) in total soluble sugars of the more cold-hardy genotype (*Rosa hybrida* ‘Yesterday’) (a) and the less cold-hardy genotype (*R. wichurana*) (b) within each sampling points. Values are means ($n = 5$).

The second-largest proportion of total soluble sugars were hexoses, measured in the range of 15.3–46.0% in ‘Yesterday’ and 30.0–50.3% in *R. wichurana* (Figure 3).

Oligosaccharides, including raffinose and stachyose, were the least abundant sugars (< 10%) in both genotypes (Figure 3). In ‘Yesterday’, oligosaccharides accumulated during December–February, measured at 7.8–9.5%. In *R. wichurana*, a higher proportion of oligosaccharides (6.7–8.4%) was also observed in November–February. In April, the oligosaccharide fraction was only 0.5% and 0.8% in ‘Yesterday’ and *R. wichurana*, respectively. Furthermore, oligosaccharides showed a significant negative correlation with LT_{50} value for both ‘Yesterday’ ($r = -0.70, p < 0.01$) and *R. wichurana* ($r = -0.68, p < 0.01$).

3.5. Expression Analysis of Sugar Metabolism-Related Genes

Sucrose is synthesized by SPS in the cytosol and is degraded either by SUS or by INV into hexoses or derivatives. The expression pattern of *RhSPS1*, *RhSUS*, and *RhINV2* is given in Figure 4a–c, respectively. For ‘Yesterday’, the expression of *RhSPS1* was upregulated from November to January; however, transcripts of *RhSPS1* were hardly detectable in *R. wichurana*. *RhSUS* transcripts were low during November–January for the two genotypes but increased towards April. This upregulation of *RhSUS* was pronounced for the cold-hardy genotype of ‘Yesterday’. For *R. wichurana*, the expression of *RhINV2* was induced during November–December and decreased after January. In contrast, for ‘Yesterday’ the expression of *RhINV2* remained relatively stable during cold acclimation. *Raffinose synthase* (*RS*) is a critical gene in the RFOs (raffinose family oligosaccharides) pathway. However, the four-fold upregulation of *RhRS6* was found only in the less cold-hardy genotype *R. wichurana* in December as compared to November and January (Figure 4d). No significant correlations were found between the expression levels of sugar metabolism-related genes and LT₅₀ values in ‘Yesterday’ and *R. wichurana*.

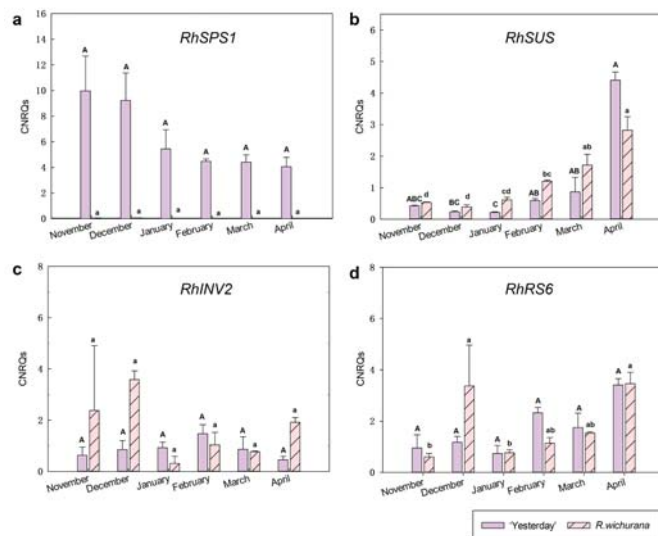


Figure 4. Seasonal changes in gene expression of *RhSPS1* (a), *RhSUS* (b), and *RhINV2* (c) in sucrose biosynthesis and *RhRS6* (d) in RFOs (raffinose family oligosaccharides) biosynthesis in the more cold-hardy genotype (*Rosa hybrida* ‘Yesterday’) and the less cold-hardy genotype (*R. wichurana*). Data were assessed by one-way ANOVA and a Scheffé post-hoc test ($p = 0.05$) except for *RhSUS* of ‘Yesterday’ by the Kruskal–Wallis test ($p = 0.05$). Different letters (A, B, etc.; or a, b, etc.) indicate significant differences between sampling time points within each genotype. Normalized relative quantities (CNRQs, non-log-transformed) are presented as geometric means \pm SE ($n = 3$).

4. Discussion

Breeding of roses with a strong freezing tolerance is necessary for application in northern climates. Cold acclimation, the ability to adapt to seasonal changes in temperature, is a prerequisite for perennial plants in temperate and boreal climate zones. Cold acclimation depends on various biochemical adaptations. The present study focused on two crucial metabolic pathways: cryoprotective dehydrins and soluble sugars.

The cold hardiness of ‘Yesterday’ and *R. wichurana* conforms to the seasonal dynamic shown in most plants. It is characterized by three phases: cold acclimation, mid-winter hardiness, and deacclimation. Two patterns of cold acclimation were observed in the roses under study. ‘Yesterday’ had a fast acclimation, reaching its highest cold hardiness level

in December, despite the relative lack of sub-zero temperatures. In contrast, *R. wichurana* reached its highest cold hardiness level in January when the average minimum temperature was below zero, suggesting that freezing events are needed for the full development of cold hardiness in this less cold-hardy genotype. The observation that ‘Yesterday’ with a higher maximum hardiness level is more cold-hardy than *R. wichurana*, conforms the published cold hardiness (USDA zone) information. The rate of deacclimation is reported as being relatively faster than cold acclimation [44], which was also confirmed in our study: the rising temperature in March–April resulted in a sharp rise of LT₅₀ and loss of cold hardiness. A faster deacclimation was found in the more cold-hardy genotype ‘Yesterday’. Rapid deacclimation has also been observed in other woody ornamentals, indicating that the pace of deacclimation is not correlated to maximum cold hardiness [45,46].

The first *dehydrin* (*ppdhn1*) found in peach (*Prunus persica*) has higher transcript levels in bark tissue during autumn and early winter [42]. We have identified *RhDHN5/6*, which are homologues of *ppdhn1*, in rose. As in peach, our results also show significant upregulation in rose during the period from November to January (Figure 2). Dehydrins in rose respond strongly to low temperatures, as also found in the bark tissue of apple (Rosaceae family) where 5 °C induced transcript levels ranging from 15-fold (*MdDhn3*) to a maximum of 122-fold (*MdDhn1*) [47]. From February to April, the decrease of *RhDHN5* and *RhDHN6* was associated with deacclimation; this correlation has also been observed in blueberry and Scots pine [48,49]. The seasonal pattern of dehydrin genes/proteins is also reported in different tissues (leaves, stem, and floral buds) of woody plants (e.g., apple, peach, birch, *Rhododendron*) during the overwintering process [50–54]. The observed seasonal dynamic of dehydrins in rose showed a positive relation to the changing pattern of cold hardiness level (determined by LT₅₀), suggesting that dehydrins might be closely associated with the freezing tolerance of rose. In Scots pine, several dehydrin genes belong to the top 50 genes. Dehydrins correlate significantly with cold hardiness of Scots pine, and were therefore selected as a marker candidate for frost tolerance in this species [55].

Soluble sugars act as osmoregulators/osmolytes under cold stress. They stabilize osmotic potential, reduce cellular dehydration, protect macromolecules, and serve as scavengers of reactive oxygen species [5,21].

Sucrose is the principal agent in cell membranes protection, as its hydroxyl groups replace water in the phospholipid groups of the membrane. The accumulation of sucrose is essential for cold acclimation [18,56]. For ‘Yesterday’, the proportion of sucrose is relatively higher in the months of November and December and much lower in April, consistent with their cold hardiness pattern. For *R. wichurana*, the proportion of sucrose gradually increased to a maximum in December, with a slight decrease noted from January to April. This slower increase and decrease of sucrose proportion are also in accordance with the rather late response of cold acclimation and deacclimation found in *R. wichurana*. The correlation between sucrose and LT₅₀ values in ‘Yesterday’ also indicate the important role of sucrose in the development of cold hardiness. The proportion of hexoses showed a reverse seasonal pattern compared to sucrose in both rose genotypes: hexoses decreased during cold acclimation and increased during deacclimation (especially in April). Compared to sucrose and raffinose, hexoses have a lower cryoprotective efficiency [57]. Oligosaccharides act as osmoprotectants and are strongly associated with the development of cold hardiness in many woody plants [58–60]. In both rose genotypes, although oligosaccharides (raffinose + stachyose) were the least abundant sugars (<10%), the accumulation of oligosaccharides during cold acclimation was prominent, while these sugars were hardly detectable in April showing a strong association with cold hardiness (Figure 3). In addition, the prominent correlation between oligosaccharides and LT₅₀ values in both genotypes showed that oligosaccharides are closely associated with cold hardiness.

SPS (sucrose-phosphate synthase) is involved in the biosynthesis of sucrose in the cytosol. The upregulation of *RhSPS1* was clearly detected in the more cold-hardy genotype ‘Yesterday’ during acclimation. Increased activities of SPS were also observed during cold acclimation in poplar [61]. Consistent with these observations, the induction of *RhSPS1*

is also associated with the apparent increase of sucrose proportion in the stem tissue of ‘Yesterday’ during November–February (Figure 3a). SUS (sucrose synthase) is associated with both sucrose synthesis and degradation but its main function is the cleavage of sucrose [62]. A similar expression pattern of *RhSUS* was found in both genotypes: it was suppressed during cold acclimation and increased steadily from February to April (Figure 4b). This regulation of *RhSUS* may help the plants to maintain a higher level of sucrose during cold acclimation (Figure 3). INVs (invertases) can cause the cleavage of sucrose into glucose and fructose and are classified into three forms based on their subcellular location, namely cell wall invertases, cytoplasmic invertases, and vacuolar invertases [28]. According to the BLASTx result, *RhINV2* might be vacuolar invertase. The upregulation of *RhINV2* in *R. wichurana* might enable the less cold-hardy genotype to maintain sufficient monosaccharide levels to support different functions in the cell. However, the lack of upregulation of *RhINV2* in ‘Yesterday’ may help the cold-hardy genotype to keep higher sucrose levels (Figure 3a). *RS* encodes the enzyme of the rate-limiting step in raffinose biosynthesis, and its regulation precedes the biosynthesis of raffinose [63]. However, the strong upregulation of *RhRS6* was only observed in *R. wichurana* in December, and the regulation pattern of *RhRS6* cannot fully reflect the accumulation of oligosaccharides which may be due to either a long sampling period or temperature fluctuations in the field. Furthermore, the present study focused on one raffinose synthase gene that was reported to be closely associated with cold hardiness in tea plants [43]. Further study of gene families of *RS* or other key genes related to the RFOs synthesis pathway might provide better explanation of the prominent accumulation of oligosaccharides during cold acclimation.

5. Conclusions

A seasonal dynamic of cold hardiness (cold acclimation, mid-winter hardiness, and deacclimation) is found in two rose genotypes that showed different patterns of cold acclimation. ‘Yesterday’ acclimated faster and achieved its maximum cold hardiness in December, while *R. wichurana* acclimated relatively slowly, only reaching its highest cold hardiness level in January. The accumulation of dehydrins in two genotypes may be closely associated with their cold acclimation. Dehydrin transcripts (*RhDHN5* and *RhDHN6*) accumulated significantly during November–January, with more pronounced accumulation in the more cold-hardy genotype ‘Yesterday’. The proportion of sucrose and oligosaccharides increased during cold acclimation in both genotypes. However, the accumulation patterns were different, possibly due to the distinct expression patterns of essential genes involved in their pathway. Sucrose and oligosaccharides are involved in cold acclimation and are associated with cold hardiness. The differences in gene regulation in the two genotypes may be due to their distinct genetic backgrounds, which led to different adaptation strategies to cold stress. A better understanding of the underlying biochemical and molecular mechanisms involved in the cold acclimation of roses will help to select hardy roses in breeding programs. In the present study, we found that dehydrins and soluble sugars played an important role in the process of cold acclimation. Sucrose and oligosaccharides are significantly associated with cold hardiness of Yesterday and *R. wichurana*.

Author Contributions: L.O. and M.-C.V.L. planned the experiment. L.O. conducted the experiment and analyzed all the data. L.O. and M.-C.V.L. interpreted the data. L.O. wrote the manuscript. M.-C.V.L., L.L. and E.D.K. revised the manuscript. All authors have read and agreed to the published version of the manuscript.

Funding: This research was funded by Sichuan Science and Technology Program, grant number 2021JDRC0140 and The Agricultural Science and Technology Innovation Program (34-IUA-05).

Institutional Review Board Statement: Not applicable.

Informed Consent Statement: Not applicable.

Data Availability Statement: All-new research data were presented in this contribution.

Acknowledgments: We acknowledge Pheno Geno Roses. BV (The Netherlands) for providing the rose material, Magali Losschaert for assistance during RT-qPCR analysis, Christophe Petit for technical support, and Miriam Levenson for English style corrections.

Conflicts of Interest: The authors have declared that the research was conducted in the absence of any commercial or financial relationships that could be construed as a potential conflict of interest.

References

- Jun, S.H.; Yu, D.J.; Hur, Y.Y.; Lee, H.J. Identifying reliable methods for evaluating cold hardiness in grapevine buds and canes. *Hortic. Environ. Biotechnol.* **2021**. [\[CrossRef\]](#)
- Kovaleski, A.P.; Grossman, J.J. Standardization of electrolyte leakage data and a novel liquid nitrogen control improve measurements of cold hardiness in woody tissue. *Plant Methods* **2021**, *17*, 1–20. [\[CrossRef\]](#)
- Huner, N.P.; Öquist, G.; Sarhan, F. Energy balance and acclimation to light and cold. *Trends Plant Sci.* **1998**, *3*, 224–230. [\[CrossRef\]](#)
- Welling, A.; Moritz, T.; Palva, E.T.; Junttila, O. Independent activation of cold acclimation by low temperature and short photoperiod in hybrid aspen. *Plant Physiol.* **2002**, *129*, 1633–1641. [\[CrossRef\]](#)
- Theocharis, A.; Clément, C.; Barka, E.A. Physiological and molecular changes in plants grown at low temperatures. *Planta* **2012**, *235*, 1091–1105. [\[CrossRef\]](#)
- Liu, B.; Xia, Y.-P.; Krebs, S.L.; Medeiros, J.; Arora, R. Seasonal responses to cold and light stresses by two elevational ecotypes of *Rhododendron catawbiense*: A comparative study of overwintering strategies. *Environ. Exp. Bot.* **2019**, *163*, 86–96. [\[CrossRef\]](#)
- Levitt, J. Chilling, Freezing, and High Temperature Stresses. In *Responses of Plants to Environmental Stresses*, 2nd ed.; Levitt, J., Ed.; Academic Press: New York, NY, USA, 1980; Volume 1, pp. 1–497.
- Uemura, M.; Joseph, R.A.; Steponkus, P.L. Cold Acclimation of *Arabidopsis thaliana* (Effect on plasma membrane lipid composition and freeze-induced lesions). *Plant Physiol.* **1995**, *109*, 15–30. [\[CrossRef\]](#) [\[PubMed\]](#)
- Luo, L.; Lin, S.-Z.; Zheng, H.-Q.; Lei, Y.; Zhang, Q.; Zhang, Z.-Y. The role of antioxidant system in freezing acclimation-induced freezing resistance of *Populus suaveolens* cuttings. *For. Stud. China* **2007**, *9*, 107–113. [\[CrossRef\]](#)
- Gusta, L.V.; Wisniewski, M. Understanding plant cold hardiness: An opinion. *Physiol. Plant.* **2012**, *147*, 4–14. [\[CrossRef\]](#) [\[PubMed\]](#)
- Masocha, V.F.; Li, Q.; Zhu, Z.; Chai, F.; Sun, X.; Wang, Z.; Yang, L.; Wang, Q.; Xin, H. Proteomic variation in *Vitis amurens* and *V. vinifera* buds during cold acclimation. *Sci. Hortic.* **2019**, *263*, 109143. [\[CrossRef\]](#)
- Wisniewski, M.; Nassuth, A.; Arora, R. Cold hardiness in trees: A mini-review. *Front. Plant Sci.* **2018**, *9*, 1394. [\[CrossRef\]](#)
- Horvath, D.P.; Zhang, J.; Chao, W.S.; Mandal, A.; Rahman, M.; Anderson, J.V. Genome-wide association studies and transcriptome changes during acclimation and deacclimation in divergent *Brassica napus* varieties. *Int. J. Mol. Sci.* **2020**, *21*, 9148. [\[CrossRef\]](#)
- Burchett, S.; Niven, S.; Fuller, M.P. The effect of cold acclimation on the water relations and freezing tolerance of *Hordeum vulgare* L. *Cryo Lett.* **2007**, *27*, 295–303.
- Graether, S.P.; Boddington, K.F. Disorder and function: A review of the dehydrin protein family. *Front. Plant Sci.* **2014**, *5*, 576. [\[CrossRef\]](#)
- Thomashow, M.F. PLANT COLD ACCLIMATION: Freezing tolerance genes and regulatory mechanisms. *Annu. Rev. Plant Biol.* **1999**, *50*, 571–599. [\[CrossRef\]](#)
- Hanin, M.; Brini, F.; Ebel, C.; Toda, Y.; Takeda, S.; Masmoudi, K. Plant dehydrins and stress tolerance. *Plant Signal. Behav.* **2011**, *6*, 1503–1509. [\[CrossRef\]](#) [\[PubMed\]](#)
- Rekarte-Cowie, I.; Ebshish, O.S.; Mohamed, K.S.; Pearce, R.S. Sucrose helps regulate cold acclimation of *Arabidopsis thaliana*. *J. Exp. Bot.* **2008**, *59*, 4205–4217. [\[CrossRef\]](#) [\[PubMed\]](#)
- Wolkers, W.F.; McCreedy, S.; Brandt, W.F.; Lindsey, G.G.; Hoekstra, F.A. Isolation and characterization of a D-7 LEA protein from pollen that stabilizes glasses in vitro. *Biochim. Biophys. Acta Protein Struct. Mol. Enzym.* **2001**, *1544*, 196–206. [\[CrossRef\]](#)
- Trischuk, R.G.; Schilling, B.S.; Low, N.H.; Gray, G.R.; Gusta, L.V. Cold acclimation, de-acclimation and re-acclimation of spring canola, winter canola and winter wheat: The role of carbohydrates, cold-induced stress proteins and vernalization. *Environ. Exp. Bot.* **2014**, *106*, 156–163. [\[CrossRef\]](#)
- Wanner, L.A.; Junttila, O. Cold-induced freezing tolerance in Arabidopsis. *Plant Physiol.* **1999**, *120*, 391–400. [\[CrossRef\]](#)
- Yu, D.J.; Hwang, J.Y.; Chung, S.W.; Oh, H.D.; Yun, S.K.; Lee, H.J. Changes in cold hardiness and carbohydrate content in peach (*Prunus persica*) trunk bark and wood tissues during cold acclimation and deacclimation. *Sci. Hortic.* **2017**, *219*, 45–52. [\[CrossRef\]](#)
- Winde, J.; Sønderkær, M.; Nielsen, K.L.; Pagter, M. Is range expansion of introduced Scotch broom (*Cytisus scoparius*) in Denmark limited by winter cold tolerance? *Plant Ecol.* **2020**, *221*, 709–723. [\[CrossRef\]](#)
- Deslauriers, A.; Garcia, L.; Charrier, G.; Buttò, V.; Pichette, A.; Paré, M. Cold acclimation and deacclimation in wild blueberry: Direct and indirect influence of environmental factors and non-structural carbohydrates. *Agric. For. Meteorol.* **2021**, *301–302*, 108349. [\[CrossRef\]](#)
- Carpenter, J.F.; Hand, S.C.; Crowe, L.M.; Crowe, J.H. Cryoprotection of phosphofructokinase with organic solutes: Characterization of enhanced protection in the presence of divalent cations. *Arch. Biochem. Biophys.* **1986**, *250*, 505–512. [\[CrossRef\]](#)
- Uemura, M.; Steponkus, P.L. Cold acclimation in plants: Relationship between the lipid composition and the cryostability of the plasma membrane. *J. Plant Res.* **1999**, *112*, 245–254. [\[CrossRef\]](#)
- Zhang, L.-L.; Zhao, M.-G.; Tian, Q.-Y.; Zhang, W.-H. Comparative studies on tolerance of *Medicago truncatula* and *Medicago falcata* to freezing. *Planta* **2011**, *234*, 445–457. [\[CrossRef\]](#)

28. Ruan, Y.-L. Sucrose metabolism: Gateway to diverse carbon use and sugar signaling. *Annu. Rev. Plant Biol.* **2014**, *65*, 33–67. [[CrossRef](#)]
29. Zuther, E.; Buchel, K.; Hundertmark, M.; Stitt, M.; Hinch, D.K.; Heyer, A.G. The role of raffinose in the cold acclimation response of *Arabidopsis thaliana*. *FEBS Lett.* **2004**, *576*, 169–173. [[CrossRef](#)] [[PubMed](#)]
30. Unda, F.; Canam, T.; Preston, L.; Mansfield, S.D. Isolation and characterization of galactinol synthases from hybrid poplar. *J. Exp. Bot.* **2011**, *63*, 2059–2069. [[CrossRef](#)] [[PubMed](#)]
31. Wang, X.; Chen, Y.; Jiang, S.; Xu, F.; Wang, H.; Wei, Y.; Shao, X. PpINH1, an invertase inhibitor, interacts with vacuolar invertase PpVIN2 in regulating the chilling tolerance of peach fruit. *Hortic. Res.* **2020**, *7*, 168. [[CrossRef](#)]
32. Ouyang, L.; Leus, L.; Van Labeke, M.-C. Three-year screening for cold hardiness of garden roses. *Sci. Hortic.* **2018**, *245*, 12–18. [[CrossRef](#)]
33. Flint, H.L.; Boyce, B.R.; Beattie, D.J. Index of injury—A useful expression of freezing injury to plant tissues as determined by the electrolytic method. *Can. J. Plant Sci.* **1967**, *47*, 229–230. [[CrossRef](#)]
34. Lim, C.C.; Arora, R.; Townsend, E.C. Comparing Gompertz and Richards Functions to Estimate Freezing Injury in *Rhododendron* Using Electrolyte Leakage. *J. Am. Soc. Hortic. Sci.* **1998**, *123*, 246–252. [[CrossRef](#)]
35. Luypaert, G.; Witters, J.; Van Huylenbroeck, J.; De Clercq, P.; De Riek, J.; De Keyser, E. Induced expression of selected plant defence related genes in pot azalea, *Rhododendron simsii* hybrid. *Euphytica* **2017**, *213*, 227. [[CrossRef](#)]
36. Altschul, S.F.; Madden, T.L.; Schäffer, A.A.; Zhang, J.; Zhang, Z.; Miller, W.; Lipman, D.J. Gapped BLAST and PSI-BLAST: A new generation of protein database search programs. *Nucleic Acids Res.* **1997**, *25*, 3389–3402. [[CrossRef](#)] [[PubMed](#)]
37. Untergasser, A.; Nijveen, H.; Rao, X.; Bisseling, T.; Geurts, R.; Leunissen, J.A.M. Primer3Plus, an enhanced web interface to Primer3. *Nucleic Acids Res.* **2007**, *35*, W71–W74. [[CrossRef](#)]
38. Pipino, L. Improving Seed Production Efficiency for Hybrid Rose Breeding. Doctoral Dissertation, Ghent University, Ghent, Belgium, 2011.
39. Vandesompele, J.; De Preter, K.; Pattyn, F.; Poppe, B.; Van Roy, N.; De Paepe, A.; Speleman, F. Accurate normalization of real-time quantitative RT-PCR data by geometric averaging of multiple internal control genes. *Genome Biol.* **2002**, *3*, RESEARCH0034. [[CrossRef](#)] [[PubMed](#)]
40. Ruijter, J.M.; Ramakers, C.; Hoogaars, W.M.H.; Karlen, Y.; Bakker, O.; Van den Hoff, M.J.B.; Moorman, A.F.M. Amplification efficiency: Linking baseline and bias in the analysis of quantitative PCR data. *Nucleic Acids Res.* **2009**, *37*, e45. [[CrossRef](#)]
41. Hellemans, J.; Mortier, G.; De Paepe, A.; Speleman, F.; Vandesompele, J. qBase relative quantification framework and software for management and automated analysis of real-time quantitative PCR data. *Genome Biol.* **2007**, *8*, R19. [[CrossRef](#)]
42. Artlip, T.S.; Callahan, A.M.; Bassett, C.L.; Wisniewski, M. Seasonal expression of a dehydrin gene in sibling deciduous and evergreen genotypes of peach (*Prunus persica* [L.] Batsch). *Plant Mol. Biol.* **1997**, *33*, 61–70. [[CrossRef](#)]
43. Yue, C.; Cao, H.-L.; Wang, L.; Zhou, Y.-H.; Huang, Y.-T.; Hao, X.; Wang, Y.-C.; Wang, B.; Yang, Y.-J.; Wang, X.-C. Effects of cold acclimation on sugar metabolism and sugar-related gene expression in tea plant during the winter season. *Plant Mol. Biol.* **2015**, *88*, 591–608. [[CrossRef](#)]
44. Kalberer, S.R.; Wisniewski, M.; Arora, R. Deacclimation and reacclimation of cold-hardy plants: Current understanding and emerging concepts. *Plant Sci.* **2006**, *171*, 3–16. [[CrossRef](#)]
45. Kalberer, S.R.; Leyva-Estrada, N.; Krebs, S.L.; Arora, R. Frost dehardening and rehardening of floral buds of deciduous azaleas are influenced by genotypic biogeography. *Environ. Exp. Bot.* **2007**, *59*, 264–275. [[CrossRef](#)]
46. Pagter, M.; Hausman, J.-F.; Arora, R. Deacclimation kinetics and carbohydrate changes in stem tissues of *Hydrangea* in response to an experimental warm spell. *Plant Sci.* **2011**, *180*, 140–148. [[CrossRef](#)] [[PubMed](#)]
47. Wisniewski, M.; Bassett, C.; Norelli, J.; Macarasin, D.; Artlip, T.; Gasic, K.; Korban, S. Expressed sequence tag analysis of the response of apple (*Malus × domestica* ‘Royal Gala’) to low temperature and water deficit. *Physiol. Plant.* **2008**, *133*, 298–317. [[CrossRef](#)] [[PubMed](#)]
48. Kontunen-Soppela, S.; Taulavuori, K.; Taulavuori, E.; Lähdesmäki, P.; Laine, K. Soluble proteins and dehydrins in nitrogen-fertilized Scots pine seedlings during deacclimation and the onset of growth. *Physiol. Plant.* **2000**, *109*, 404–409. [[CrossRef](#)]
49. Arora, R.; Rowland, L.J.; Ogdan, E.L.; Dhanaraj, A.L.; Marian, C.O.; Ehlenfeldt, M.K.; Vinyard, B. Dehardening kinetics, bud development, and dehydrin metabolism in blueberry cultivars during deacclimation at constant, warm temperatures. *J. Am. Soc. Hortic. Sci.* **2004**, *129*, 667–674. [[CrossRef](#)]
50. Arora, R.; Wisniewski, M. Accumulation of a 60-kD dehydrin protein in peach xylem tissues and its relationship to cold acclimation. *HortScience* **1996**, *31*, 923–925. [[CrossRef](#)]
51. Marian, C.O.; Eris, A.; Krebs, S.L.; Arora, R. Environmental regulation of a 25 kDa dehydrin in relation to *Rhododendron* cold Acclimation. *J. Am. Soc. Hortic. Sci.* **2004**, *129*, 354–359. [[CrossRef](#)]
52. Welling, A.; Rinne, P.; Viherä-Aarnio, A.; Kontunen-Soppela, S.; Heino, P.; Palva, E.T. Photoperiod and temperature differentially regulate the expression of two dehydrin genes during overwintering of birch (*Betula pubescens* Ehrh.). *J. Exp. Bot.* **2004**, *55*, 507–516. [[CrossRef](#)] [[PubMed](#)]
53. Liang, N.; Xia, H.; Wu, S.; Ma, F. Genome-wide identification and expression profiling of dehydrin gene family in *Malus domestica*. *Mol. Biol. Rep.* **2012**, *39*, 10759–10768. [[CrossRef](#)]
54. Shin, H.; Oh, S.-I.; Kim, M.-A.; Yun, S.K.; Oh, Y.; Son, I.-C.; Kim, H.-S.; Kim, D. Relationship between cold hardiness and dehydrin gene expression in peach shoot tissues under field conditions. *Hortic. Environ. Biotechnol.* **2015**, *56*, 280–287. [[CrossRef](#)]

55. Joosen, R.V.L.; Lammers, M.; Balk, P.A.; Brønnum, P.; Konings, M.C.J.M.; Perks, M.; Stattin, E.; Van Wordragen, M.F.; Van Der Geest, A.H.M. Correlating gene expression to physiological parameters and environmental conditions during cold acclimation of *Pinus sylvestris*, identification of molecular markers using cDNA microarrays. *Tree Physiol.* **2006**, *26*, 1297–1313. [[CrossRef](#)]
56. Koster, K.; Leopold, A.C. Sugars and desiccation tolerance in seeds. *Plant Physiol.* **1988**, *88*, 829–832. [[CrossRef](#)]
57. Crowe, J.H.; Carpenter, J.F.; Crowe, L.M.; Anchooguy, T.J. Are freezing and dehydration similar stress vectors? A comparison of modes of interaction of stabilizing solutes with biomolecules. *Cryobiology* **1990**, *27*, 219–231. [[CrossRef](#)]
58. Pagter, M.; Jensen, C.R.; Petersen, K.K.; Liu, F.; Arora, R. Changes in carbohydrates, ABA and bark proteins during seasonal cold acclimation and deacclimation in *Hydrangea* species differing in cold hardiness. *Physiol. Plant.* **2008**, *134*, 473–485. [[CrossRef](#)]
59. Palonen, P.; Buszard, D.; Donnelly, D. Changes in carbohydrates and freezing tolerance during cold acclimation of red raspberry cultivars grown in vitro and in vivo. *Physiol. Plant.* **2008**, *110*, 393–401. [[CrossRef](#)]
60. Van Labeke, M.-C.; Volckaert, E. Evaluation of electrolyte leakage for detecting cold acclimatization in six deciduous tree species. *Acta Hort.* **2010**, *885*, 403–410. [[CrossRef](#)]
61. Schrader, S.; Sauter, J.J. Seasonal changes of sucrose-phosphate synthase and sucrose synthase activities in poplar wood (*Populus × canadensis* Moench ‘robusta’) and their possible role in carbohydrate metabolism. *J. Plant Physiol.* **2002**, *159*, 833–843. [[CrossRef](#)]
62. Goldner, W.; Thom, M.; Maretzki, A. Sucrose metabolism in sugarcane cell suspension cultures. *Plant Sci.* **1991**, *73*, 143–147. [[CrossRef](#)]
63. Kaplan, F.; Kopka, J.; Sung, D.Y.; Zhao, W.; Popp, M.; Porat, R.; Guy, C.L. Transcript and metabolite profiling during cold acclimation of *Arabidopsis* reveals an intricate relationship of cold-regulated gene expression with modifications in metabolite content. *Plant J.* **2007**, *50*, 967–981. [[CrossRef](#)]



Article

Morphological Characterization of Tetraploids of *Limonium sinuatum* (L.) Mill. Produced by Oryzalin Treatment of Seeds

Shiro Mori ^{1,*}, Masaki Yahata ², Ayano Kuwahara ¹, Yurina Shirono ¹, Yasufumi Ueno ¹, Misaki Hatanaka ¹, Yoshimi Honda ¹, Keita Sugiyama ³, Naho Murata ³, Yoshihiro Okamoto ¹ and Takahiro Wagatsuma ¹

¹ College of Agriculture, Food and Environment Sciences, Rakuno Gakuen University, Ebetsu 069-8501, Japan; s21451147@g.rakuno.ac.jp (A.K.); s21551002@g.rakuno.ac.jp (Y.S.); s21651270@g.rakuno.ac.jp (Y.U.); s21651030@g.rakuno.ac.jp (M.H.); s21751088@g.rakuno.ac.jp (Y.H.); yokamoto@rakuno.ac.jp (Y.O.); wagatsuma@rakuno.ac.jp (T.W.)

² Academic Institute, College of Agriculture, Shizuoka University, Shizuoka 422-8529, Japan; yahata.masaki@shizuoka.ac.jp

³ Hokkaido Agricultural Research Center, NARO, Sapporo 062-8555, Japan; keita@affrc.go.jp (K.S.); xuanwu@affrc.go.jp (N.M.)

* Correspondence: mori@rakuno.ac.jp; Tel.: +81-11-388-4858

Abstract: *Limonium sinuatum* (L.) Mill. ($2n = 2x = 16$) is a popular ornamental plant with dimorphism of pollen grains (type A and type B) and stigmas (papilla and *cob*-like). We applied polyploidy breeding to this species in order to introduce desirable traits. Tetraploid and mixoploid *L. sinuatum* plants were successfully obtained with oryzalin treatment of *L. sinuatum* ‘Early Blue’ seeds. All three tetraploids had increased leaf width, stomatal size, flower length, and pollen width compared to those of the diploid, and tetraploids had four germinal pores of pollen grains, whereas the diploid had three. All tetraploids had type A pollen grains and *cob*-like stigmas. Furthermore, the growth of cultivated tetraploid plants was slow, with later bolting and flowering times. Mixoploids Mixo-1 and Mixo-3 were estimated to be polyploidy periclinal chimeric plants consisting of a tetraploid L1 layer and diploid L2 layer, and Mixo-2 was estimated to be a polyploidy periclinal chimeric plant consisting of the diploid L1 layer and tetraploid L2 layer. Mixo-4 had tetraploid L1 and L2 layers. Mixoploids, except Mixo-4, had type A pollen grains and *cob*-like stigmas, whereas Mixo-4 had type B pollen grains and papilla stigmas. These polyploids will be useful as polyploidy breeding materials.

Keywords: bolting; cut flower; germinal pore; ornamental plant; polyploidy periclinal chimera; Plumbaginaceae; polyploidy breeding

Citation: Mori, S.; Yahata, M.; Kuwahara, A.; Shirono, Y.; Ueno, Y.; Hatanaka, M.; Honda, Y.; Sugiyama, K.; Murata, N.; Okamoto, Y.; et al. Morphological Characterization of Tetraploids of *Limonium sinuatum* (L.) Mill. Produced by Oryzalin Treatment of Seeds. *Horticulturae* **2021**, *7*, 248. <https://doi.org/10.3390/horticulturae7080248>

Academic Editor: Sergio Ruffo Roberto

Received: 16 June 2021

Accepted: 10 August 2021

Published: 15 August 2021

Publisher’s Note: MDPI stays neutral with regard to jurisdictional claims in published maps and institutional affiliations.



Copyright: © 2021 by the authors. Licensee MDPI, Basel, Switzerland. This article is an open access article distributed under the terms and conditions of the Creative Commons Attribution (CC BY) license (<https://creativecommons.org/licenses/by/4.0/>).

1. Introduction

Limonium sinuatum (L.) Mill., commonly known as statice, which belongs to the family Plumbaginaceae native to the Mediterranean area, is a popular ornamental plant because of its wide range of flower colors and long vase life. This species is diploid with $2n = 16$ [1]. In the genus *Limonium*, pollen- and stigma-dimorphism can be observed and is related to the self-incompatibility system. *L. sinuatum* produces type A and type B pollen as well as papilla stigmas and *cob*-like stigmas. The combination of type A pollen and *cob*-like stigma and the combination of type B pollen and papilla stigma do not lead to fertilization [2–5].

Generally, polyploids grow vigorously and their organs are larger than those of diploids. Polyploidization is commonly carried out to introduce novel attractive features to ornamental plants such as plant size, flower enlargement, and intense color of leaves and flowers [6,7]. Phenotypic changes due to chromosome doubling are thought to be caused by increased cell size, allele diversification, gene silencing, and gene dosage effects [6]. Chromosome doubling of plants can be achieved by treatment with polyploidizing agents including colchicine, oryzalin, amiprofos-methyl, and trifluralin. Among them, colchicine is the most commonly used agent [8], whereas oryzalin is recognized as an alternative

because of its high chromosome doubling efficiency and low toxicity [9–13]. To date, polyploids of ornamental plants including *Agastache foeniculum* [14], *Alocasia* sp. [10], *Gerbera jamesonii* [15], *Lychnis senno* [9], *Rhododendron* spp. [16,17], and *Rosa* spp. [12,13] have been obtained by oryzalin treatment.

L. sinuatum is difficult to crossbreed with different species except for some, and polyploid breeding is expected as a method to drastically change the morphology of this species. In the genus *Limonium*, there are a few reports regarding chromosome doubling using polyploidizing agents [18]. Morgan et al. [19] produced allotetraploids of an interspecific hybrid between *L. perezii* and *L. sinuatum* by oryzalin treatment of in vitro shoots. Mori et al. [20] treated the seeds of *L. bellidifolium* with colchicine and obtained autotetraploids, which tended to produce wider, thicker leaves and larger flowers than diploid plants. To the best of our knowledge in the related literature, there are no reports on the production of autotetraploids or detailed morphological characterization of tetraploid plants in *L. sinuatum*.

Enhancing the desired traits in *L. sinuatum* polyploids is a way to create new cultivars with novel attractive traits. Thus, in the present study, we examined the concentration and treatment time of oryzalin required for chromosome doubling in the seeds of *L. sinuatum* in order to achieve polyploidy breeding in *L. sinuatum*. We also investigated the morphology of *L. sinuatum* polyploids.

2. Materials and Methods

2.1. Plant Materials and Oryzalin Treatments

We used the seeds of *L. sinuatum* ‘Early Blue’ (Fukukaen Nursery & Bulb Co. Ltd., Nagoya, Japan). The treatment of seeds with oryzalin was carried out in February 2017. The seeds were surface-disinfected with 70% ethanol for 30 s, immersed in a 1% sodium hypochlorite (NaClO) solution for 10 min, and then rinsed with distilled water. They were treated with 0, 0.0005, 0.001, or 0.005% oryzalin (Wako Pure Chemical Industries Ltd., Osaka, Japan), which was dissolved in dimethyl sulfoxide (DMSO) for 24, 48, or 72 h at 25 °C in the dark on a device (Triple shaker NR-80; Taitec Corporation, Koshigaya, Japan) for shaking culture (80 rpm). Forty seeds were used in one treatment, and five independent experiments were performed. The treated seeds washed with tap water were sown in soil in the cell trays. The cell trays were placed in a greenhouse heated to 20 °C. The grown plants were potted into 7.5-cm plastic pots two months after cultivation, and their survival rate was recorded.

2.2. Flow Cytometry Analysis and Chromosome Count

A flow cytometer (CyFlow PA; Partec GmbH, Görlitz, Germany) was used in flow cytometry (FCM) analysis to estimate the ploidy level of the plants according to the method described by Mori et al. [20] with some modifications. For the analysis, a leaf disc of approximately 1 cm was cut out from a young leaf of plants potted in 7.5-cm pots. Extraction of nuclear DNA and DAPI staining were carried out using a commercial kit (CyStain UV Precise P; Sysmex Corporation, Kobe, Japan). The sample solution filtered using a 40- μ m mesh filter was analyzed using a flow cytometer.

To confirm the ploidy level, the chromosomes in the root tip cells of diploid and putative tetraploid plants were observed by using previously reported methods [20]. The prepared samples were examined under a light microscope (CX41; Olympus Corporation, Tokyo, Japan).

2.3. Morphological Characterization

The polyploids potted in 7.5-cm pots were sequentially transferred to 24-cm clay pots from the summer until the autumn of 2017, and then replanted into 45-cm large plastic pots in the summer of 2018.

Morphological characterization of the leaves was performed in October 2017. Five leaves were randomly selected from each plant, and their leaf length, leaf width, leaf

soil plant analysis development (SPAD) value, stomatal size, and stomatal density were examined. A chlorophyll meter (SPAD-502 plus; Konica Minolta, Inc., Tokyo, Japan) was used to measure leaf SPAD values. Guard cells that make up the stomata were observed under a scanning electron microscope (Miniscope[®] TM3030Plus; Hitachi High-Tech Corporation, Tokyo, Japan). The growth of tetraploids at the flowering stage was examined in March 2018. The plant height, number of shoots per plant, stem wing width, flower length, calyx length, pollen size, pollen shape, stigma shape, and its pollen fertility were examined. Pollens and stigmas were observed under a scanning electron microscope (Miniscope[®] TM3030Plus). Carmine acetate staining was used for pollen fertility testing.

In June 2019, morphological characterization of mixoploids cultivated for two years in a greenhouse was carried out by examining its stomatal size, stomatal density, pollen size, pollen shape, and stigma shape. The methods of examination were described as above. In addition, the leaf ploidy level was investigated again using a flow cytometer.

2.4. Spike Culture and Growth Characteristics of Regenerated Tetraploid Plants

Spikes were cultured to reproduce the tetraploids of *L. sinuatum* according to a previous report [21]. Since the spikes are larger than the axillary buds, they are easy to handle and have high reproductive efficiency. The younger the spike, the higher the differentiation rate. Spikes with uncolored calyxes, approximately 1 cm in length, were excised from the bolted flower stalk and surface-disinfected with 70% ethanol for 60 s and immersed in a 2% (*w/v*) NaClO solution containing 0.1% (*v/v*) Tween 20 for 20 min. After three rinses with sterile distilled water, the spikes were cut to approximately 2 mm in length and placed on a shoot regeneration medium, which consisted of the MS medium [22], 1 mg L⁻¹ 6-benzyladenine, 30 g L⁻¹ sucrose, and 8 g L⁻¹ agar, in a test tube. They were cultured in a growth chamber at 20 °C under a 16 h day length (photosynthetic photon flux density 35 μmol m⁻² s⁻¹) with light-emitting diode lights. Multiple regenerated shoots were subcultured every four weeks with the shoot regeneration medium under the conditions described above. Each shoot excised from multiple shoots was placed on the MS medium without plant growth regulators for four weeks and was then placed on the root regeneration medium, which consisted of the MS medium, 1 mg L⁻¹ α-naphthaleneacetic acid, 30 g L⁻¹ sucrose, and 8 g L⁻¹ agar, in a test tube. Diploid or tetraploid plantlets were cultured for four or six weeks, respectively, under the same culture conditions as those for shoot regeneration.

The regenerated plants were acclimated in a growth chamber at 15 °C under 12 h day length (photosynthetic photon flux density 35 μmol m⁻² s⁻¹) with fluorescent lights for three weeks. The cultured plants were potted in 24-cm pots on 15 June 2020, and cultivated in a greenhouse at a ventilation temperature of 10 °C. The number of flower stalks and leaves were recorded every two weeks, and the bolting and flowering days were recorded. Three plants from each strain were investigated.

3. Results

3.1. Oryzalin Treatment

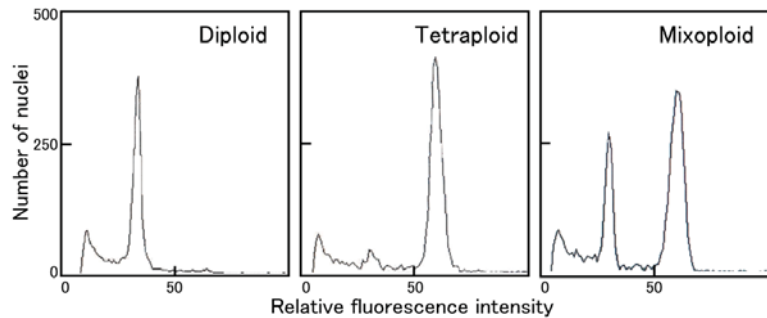
The survival rate of seedlings treated with oryzalin tended to decrease with the increase in treatment time regardless of the treatment concentration (Table 1). The DNA levels of all surviving plants were analyzed using a flow cytometer. Figure 1 presents the histograms from the FCM analysis of the control diploid, tetraploid, and mixoploid plants. A peak of tetraploid was the position with twice that in diploid. Mixoploid plants showed double peaks.

The root tip cells of tetraploid plants had 32 chromosomes, which was twice as high than that of diploid plants. Our analysis showed that three tetraploids were obtained by the seed treatments of oryzalin at 0.001% for 24 h, 0.001% for 72 h, and 0.005% for 48 h. In addition, seven mixoploids were obtained (Table 1).

Table 1. Effect of oryzalin seed treatment on the survival and ploidy level of *Limonium sinuatum* seedlings¹.

Concentration (%)	Period (h)	No. of Seeds Treated	% of Surviving Seedlings	No. of Seedlings at Each Ploidy Level ²		
				Diploid (2x)	Tetraploid (4x)	Mixoploids (2x + 4x)
0 (control)	0	200	66.0 a ³	123	0	0
0.0005	24	200	43.5 ab	94	0	0
0.0005	48	200	26.5 bc	50	0	1
0.0005	72	200	22.5 bc	31	0	2
0.001	24	200	38.5 bc	74	1	0
0.001	48	200	33.0 bc	62	0	1
0.001	72	200	16.0 cc	16	1	1
0.005	24	200	39.0 bc	74	0	0
0.005	48	200	28.5 bc	49	1	2
0.005	72	200	18.5 bc	25	0	0

¹ Data were recorded two months after the oryzalin treatment. ² Ploidy level was determined by flow cytometry using one leaf from each plant. ³ Values represent the means of five independent experiments, each consisting of 40 seeds. Values within the same column followed by different letters were significantly different at the level of 0.05 according to the Tukey–Kramer test.

**Figure 1.** Histograms from the flow cytometry (FCM) analysis of nuclear DNA content in diploid, tetraploid, and mixoploid *Limonium sinuatum* plants.

3.2. Morphological Characteristics of Tetraploid Leaves

A comparison of the morphological characteristics of leaves in tetraploids, which were named Tetra-1, 2, and 3, is shown in Table 2. The leaf width of all three tetraploids was significantly greater than that of the control plant, Cont-A, and the leaves of tetraploids were rounder (Figure 2A). The leaf SPAD values of tetraploids Tetra-2 and Tetra-3 were significantly higher than those of the diploid. The stomatal size of three tetraploids was significantly greater than that of diploids, and the stomatal density of tetraploids was significantly lower than that of the control plant (Figure 2B).

Table 2. Comparison of leaf morphological characteristics of tetraploid *Limonium sinuatum*¹.

Plant Strain	Ploidy Level	Leaf Length (mm)	Leaf Width (mm)	Leaf Index ²	Leaf SPAD Value ³	Stomatal Size (μm)		Stomatal Density (no. mm ⁻²)
						Length	Width	
Cont-A	2x	98.2 b ⁴	26.2 b	0.26 b	39.6 b	33.4 c	23.4 b	67.0 a
Tetra-1	4x	119.0 ab	51.8 a	0.44 a	39.3 b	46.0 b	30.5 a	51.7 b
Tetra-2	4x	125.0 a	49.4 a	0.40 a	53.0 a	47.2 a	30.4 a	39.0 c
Tetra-3	4x	133.8 a	52.6 a	0.39 a	52.4 a	47.4 a	30.3 a	26.9 d

¹ Five randomly selected leaves were measured from each plant. ² Leaf index represents leaf width/leaf length. ³ SPAD = Soil Plant Analysis Development. ⁴ Values within the same column followed by different letters were significantly different at the 0.05 level according to the Tukey–Kramer test.

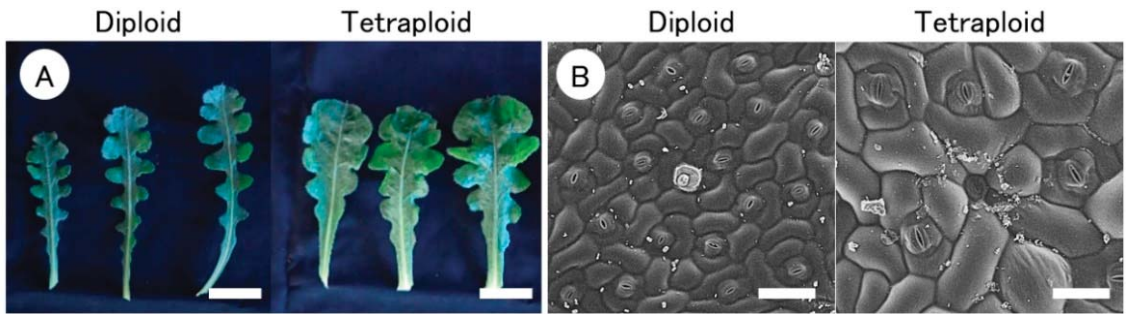


Figure 2. Morphological characteristics of leaves (A), bars = 5 cm and guard cells (B), bars = 100 μ m in diploid and tetraploid *Limonium sinuatum* plants.

3.3. Morphological Characteristics of Tetraploids at the Flowering Stage

A comparison of the morphological characteristics of tetraploids at the flowering stage is shown in Table 3. The stem wings of tetraploids Tetra-1 and Tetra-2 were more than three times wider than those of the control plant. Although the flower length of all tetraploids was significantly longer than that of the diploid plant, there was no difference in calyx length, which is the main part for ornamental use, between the diploids and tetraploids (Figure 3A,B).

Table 3. Comparison of the morphological characteristics of tetraploid *Limonium sinuatum* plants at the flowering stage ¹.

Plant Strain	Ploidy Level	Plant Height (cm)	No. of Shoot per Plant	Stem Wing (mm) ²	Flower Length (mm)	Calyx Length (mm)	Pollen Size (μ m)		No. of Germinal Pores ³	Type of Pollen Grain	Type of Stigma in Pistils
							Length	Width			
Cont-A	2x	52	14	2.2 b	14.2 b ⁴	12.6 a	54.4 a	39.9 b	3	A	cob-like
Tetra-1	4x	59	12	7.9 a	16.5 a	11.7 a	53.9 a	48.5 a	4	A	cob-like
Tetra-2	4x	55	10	8.2 a	17.2 a	13.4 a	56.4 a	52.8 a	4	A	cob-like
Tetra-3	4x	45	12	4.5 b	17.3 a	12.3 a	56.7 a	51.5 a	4	A	cob-like

¹ Five randomly selected shoots, flowers, and pollen grains were investigated from each plant. ² The stem wing width was measured from the center of the stem to the end of the wing. ³ Number of germinal pores of pollen grains was observed. ⁴ Values within the same column followed by different letters were significantly different at the 0.05 level according to the Tukey–Kramer test.

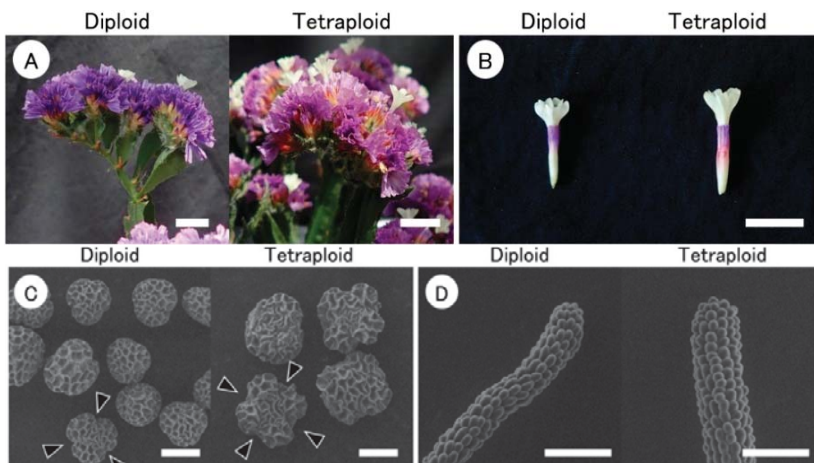


Figure 3. Morphological characteristics of flower clusters (A), bars = 10 mm, flowers (B), bar = 10 mm, pollen grains (C), bars = 30 μ m, and stigmas (D), bars = 100 μ m in diploid and tetraploid *Limonium sinuatum* plants. Arrows indicate the germinal pore.

Pollen and stigma types are involved in cross-compatibility. This information is important when using the obtained polyploids for future breeding. There are two pollen types in *L. sinuatum*: type A with coarse pollen surface, and type B with fine pollen surface. All pollen grains of tetraploids investigated in the present study coincidentally belonged to type A. The pollen width of tetraploids was significantly higher than that of the control, and the tetraploid pollen grains was close to a spherical shape. The pollen grains of diploids were tricolpate with three germinal pores, whereas some observed pollen grains of tetraploids were stephanocolporate with four germinal pores (Figure 3C). There are two types of stigmas in this species: *cob*-like stigmas and papilla stigmas. Both control diploids and tetraploid stigmas investigated in the present study were *cob*-like stigmas (Figure 3D). The pollen fertility of Cont-A, Tetra-1, Tetra-2, and Tetra-3 was 86, 66, 82, and 87%, respectively, and the pollen fertility of Tetra-1 was significantly lower than that of the others (data not shown).

3.4. Morphological Characteristics of Mixoploids

The morphological characteristics of survived mixoploids, which were named Mixo-1, 2, 3, 4, 5, and 6, at the flowering stage in the second year are shown in Table 4. Ploidy levels in the leaves were analyzed by FCM again at the flowering stage in the second year; Mixo-1, Mixo-2, Mixo-3, Mixo-5, and Mixo-6 were polyploid chimeras consisting of diploid and tetraploid cells, and Mixo-4 was detected only in tetraploid cells. Mixoploids investigated in this study, except for Mixo-4, had type A pollen grains and *cob*-like stigmas. However, Mixo-4 contained type B pollen grains and papilla stigmas (Figure 4A,B). The stomatal sizes of Mixo-1, Mixo-3, and Mixo-4 were significantly greater than those of the control diploid, and the stomatal density of Mixo-1 and Mixo-3 was significantly lower than that of the diploid. Mixo-2 had a wide range of pollen grains with four germinal pores. Mixo-4 had large pollen grains with four germinal pores.

Table 4. Comparison of the morphological characteristics of mixoploid *Limonium sinuatum* plants at the flowering stage in the second year ¹.

Plant Strain	Stomatal Size (μm)		Stomatal Density (no. mm^{-2})	Pollen Size (μm)		No. of Germinal Pores ²	Type of Pollen Grains	Type of Stigma of Pistils	Ploidy Level of Leaf ³	L1-L2 Putative Ploidy Level
	Length	Width		Length	Width					
Cont-A	35.1 d ⁴	21.1 de	77.2 bc	52.5 bc	42.5 bc	3	A	<i>cob</i> -like	2x	-
Mixo-1	45.8 b	28.9 b	42.7 d	56.5 ab	46.7 ab	3	A	<i>cob</i> -like	2x + 4x	4x – 2x
Mixo-2	33.1 d	21.9 cd	80.4 bc	57.4 ab	48.9 a	4	A	<i>cob</i> -like	2x + 4x	2x – 4x
Mixo-3	55.8 a	31.4 a	26.9 d	52.0 bc	42.3 bc	3	A	<i>cob</i> -like	2x + 4x	4x – 2x
Mixo-4	40.6 c	24.1 c	58.9 cd	60.8 a	44.9 ab	4	B	papilla	4x	4x – 4x
Mixo-5	27.8 e	19.2 e	130.3 a	49.6 c	39.6 c	3	A	<i>cob</i> -like	2x + 4x	2x – 2x
Mixo-6	28.6 e	20.3 de	100.8 ab	52.6 bc	42.7 bc	3	A	<i>cob</i> -like	2x + 4x	2x – 2x

¹ Three randomly selected leaves and 12 randomly selected pollen grains were investigated from each plant. ² Number of germinal pores of pollen grains was observed. ³ Ploidy levels of leaves were analyzed by flow cytometry at the flowering stage in the second year. ⁴ Values within the same column followed by different letters were significantly different at the 0.05 level according to the Tukey–Kramer test.

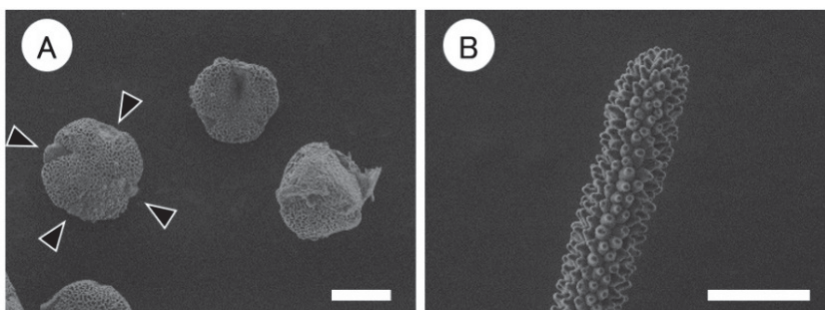


Figure 4. Pollen grains (A), bar = 30 μm and a stigma (B), bar = 100 μm in mixoploid Mixo-4 of *Limonium sinuatum*. Pollens are type B, and stigma is papilla. Arrows indicate the germinal pore.

3.5. Growth of Cultivated Tetraploid Plants

Diploid- and tetraploid-derived cultures except Tetra-2, which were propagated by spike culture, were successfully acclimatized and planted in pots. Tetra-2 could not be successfully cultivated due to complications. In the Cont-A-derived strain (i.e., in the control diploid plants), the leaves were vigorously differentiated, and the plants developed early and produced a large number of flower stalks. The number of leaves and flower stalks of tetraploid Tetra-1- and Tetra-3-derived strains were significantly lower than that of diploids after the middle stage of growth. The number of days from planting to flowering in the Tetra-3-derived strain was high. In the Tetra-1-derived strain, there were few flower stalks, and none reached flowering during the experimental period because of physiological disorders (Figures 5 and 6).

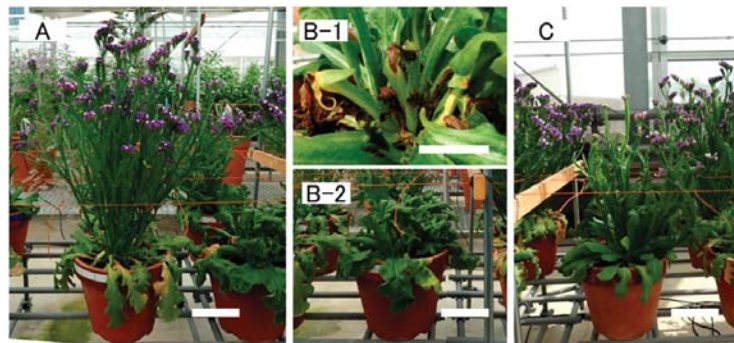


Figure 5. Plants cultivated from diploid Cont-A (A), tetraploid Tetra-1 (B1,B2), and Tetra-3 (C) of *Limonium sinuatum*. The photos were taken three months after planting. Scale bars: all except B1 = 10 cm, B2 = 5 cm.

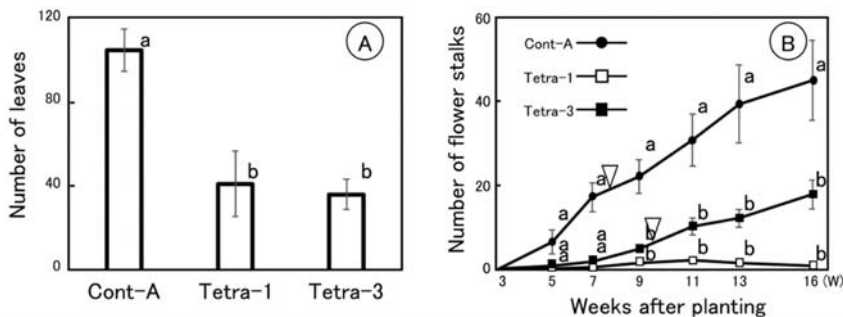


Figure 6. Number of leaves seven weeks after planting (A) and changes in the number of flower stalks (B) in diploid Cont-A-derived strain, tetraploid Tetra-1-derived strain, and Tetra-3-derived strain of *Limonium sinuatum*. Arrows in figure (B) indicate the flowering day. Bars indicate standard errors ($n = 3$). Values followed by different letters were significantly different at the 0.05 level according to the Tukey–Kramer test.

4. Discussion

Our *in vivo* seed treatments with oryzalin successfully produced polyploids of *L. sinuatum* (Table 1). Morgan et al. [19,23] produced interspecific hybrids of *L. perezii* and *L. sinuatum* and obtained allotetraploids after an oryzalin treatment of their embryos. These findings indicate that oryzalin treatment is effective for producing polyploid plants in *Limonium* spp. However, Mori et al. [20] produced tetraploids using *in vivo* colchicine treatment in *L. bellidifolium*, and the production rate of tetraploids was higher than that in the present study using *in vivo* oryzalin treatment in *L. sinuatum*. In the future, it is

necessary to consider the use of colchicine in chromosome doubling of *L. sinuatum* for its further improvement. In addition, in vitro treatments of spindle toxins may increase the efficiency of chromosome doubling in this species because this treatment has been successfully used to produce tetraploids in various ornamental plant species [9,10,24,25].

Tetraploids of *L. sinuatum* have wide leaves, large stomata, low stomata density, and large flowers, and these morphological characteristics were consistent with those of polyploid *L. bellidifolium* [20]. In addition, leaf ovalization [10], stomatal enlargement [26–28], and flower enlargement [29–34] as a consequence of chromosome doubling has been reported in other ornamental plants. Thick stem wings and inflorescence clogging in the tetraploids obtained in this study are not desirable from an ornamental point of view. The ornamental value of the tetraploids is low, and we consider that these need to be improved by breeding. On the other hand, chromosomal doubling is known to bring resistance to environmental stresses such as drought, salt stress, cold, and heat, in addition to morphological changes [35]. Drought tolerance of tetraploids will be associated with low stomatal density [25]. Environmental stress tolerance is also a desirable trait in ornamental plants and future research is expected to explore this aspect deeper.

Generally, pollen grains of the genus *Limonium* have three germinal pores. In this study, the pollen grains of diploids had three germinal pores, whereas those of tetraploids had four germinal pores. An increase in the germinal pore number by chromosome doubling has been widely reported in plants [36,37]. In *L. sinuatum*, the number of germinal pores as well as pollen size in pollen grains is useful as an index to determine the ploidy of pollen.

The cultured *Limonium* tetraploid strains grew slowly and had a later bolting and flowering times. Polyploid plants have lower growth rates and tend to flower later than the related diploids [38]. Pei et al. [39] reported that tetraploid radishes have later bolting and flowering times than those of diploid radishes, and the levels of endogenous phytohormones gibberellin (GA) 1 and GA4, which are presumed to promote flowering, were higher in diploids than in tetraploids, whereas the amount of abscisic acid, which is considered as a floral repressor, was higher in tetraploids than in diploids. Such physiological changes may also occur in tetraploid *Limonium* species.

The shoot apical meristem of many higher plants consists of three cell layers: the outermost epidermal layer (L1), the subepidermal layer (L2), and the inner corpus region (L3) [40–42]. Cells of the L1 layer form the epidermis, those of the L2 layer form the subepidermal mesophyll and germ cells, and those of the L3 layer form the internal and vascular tissues [40,41,43]. In the present study, we estimated the ploidy of the L1 and L2 layers in *Limonium* mixoploids based on morphological observations. Mixo-1 and Mixo-3 were estimated to be polyploidy periclinal chimeric plants consisting of tetraploid L1 tissue and diploid L2 tissue (layer constitution: L1-L2 = 4x – 2x), because they had larger stomata, and their pollen grains had three germinal pores and were about the same size as those of diploids. Mixo-2 was estimated to be a polyploidy periclinal chimeric plant consisting of diploid L1 tissue and tetraploid L2 tissue (L1-L2 = 2x – 4x) because the stomatal sizes were approximately the same as those of the diploids, and the pollen grains had four germinal pores and were larger than those of diploids. The second FCM analysis and observation indicated that Mixo-4 had tetraploid leaves and flower stalks. This plant was determined to be a mixoploid according to the first FCM analysis in the early growth period, but it was estimated that tetraploid tissue grew more vigorously than diploid tissue during the two-year cultivation period. In Mixo-5 and Mixo-6, no tetraploid tissues were found in our morphological observations, and detailed investigation is required in the future. The mixoploids obtained in the present study will be useful as breeding materials in *Limonium* polyploidy breeding programs.

In conclusion, tetraploid and mixoploid *L. sinuatum* plants were successfully obtained by oryzalin treatment of the seeds. However, the chromosomal doubling in *L. sinuatum* did not provide a sufficient improvement in ornamental value. In the future, we would like to cross a tetraploid with a diploid to create a triploid with desirable traits such as voluminous inflorescence. On the other hand, it is known that chromosomal doubling may

affect resistance to stress [38]. We want to investigate the physiological characteristics of polyploidy.

Author Contributions: Conceptualization, S.M. and M.Y.; Formal analysis, S.M. and M.Y.; Investigation, S.M., M.Y., A.K., Y.S., Y.U., M.H., Y.H. and N.M.; Resources, M.Y., K.S., N.M., Y.O. and T.W.; Data curation, S.M. and M.Y.; Writing—original draft preparation, S.M.; Writing—review and editing, S.M., M.Y., K.S., N.M., Y.O. and T.W.; Visualization, S.M., M.Y. and N.M.; Supervision, S.M. and M.Y.; Project administration, S.M. All authors have read and agreed to the published version of the manuscript.

Funding: This research received no external funding.

Conflicts of Interest: The authors declare no conflict of interest.

References

1. Brullo, S.; Pavone, P. Chromosome numbers in the Sicilian species of *Limonium* Miller (*Plumbaginaceae*). *An. Jard. Bot. Madr.* **1981**, *37*, 535–555.
2. Baker, H.G. Dimorphism and monomorphism in the Plumbaginaceae: I. A survey of the family. *Ann. Bot.* **1948**, *12*, 207–219. [[CrossRef](#)]
3. Baker, H.G. Dimorphism and monomorphism in the Plumbaginaceae. II. Pollen and stigmata in the genus *Limonium*. *Ann. Bot.* **1953**, *17*, 433–446. [[CrossRef](#)]
4. Baker, H.G. The evolution, functioning and breakdown of heteromorphic incompatibility systems. I. The Plumbaginaceae. *Evolution* **1966**, *20*, 349–368. [[CrossRef](#)]
5. Róis, A.S.; Teixeira, G.; Sharbel, T.F.; Fuchs, J.; Martins, S.; Espírito-Santo, D.; Caperta, A.D. Male fertility versus sterility, cytotype, and DNA quantitative variation in seed production in diploid and tetraploid sea lavenders (*Limonium* sp., *Plumbaginaceae*) reveal diversity in reproduction modes. *Sex Plant Reprod.* **2012**, *25*, 305–318. [[CrossRef](#)]
6. Manzoor, A.; Ahmad, T.; Bashir, M.A.; Hafiz, I.A.; Silvestri, C. Studies on colchicine induced chromosome doubling for enhancement of quality traits in ornamental plants. *Plants* **2019**, *8*, 194. [[CrossRef](#)]
7. Niazian, M.; Nalouisi, A.M. Artificial polyploidy induction for improvement of ornamental and medicinal plants. *Plant Cell Tissue Organ Cult.* **2020**, *142*, 447–469. [[CrossRef](#)]
8. Hancock, J.F. The colchicine story. *HortScience* **1997**, *32*, 1011–1012. [[CrossRef](#)]
9. Nonaka, T.; Oka, E.; Asano, M.; Kuwayama, S.; Tasaki, H.; Han, D.S.; Godo, T.; Nakano, M. Chromosome doubling of *Lychnis* spp. by in vitro spindle toxin treatment of nodal segments. *Sci. Hortic.* **2011**, *129*, 832–839. [[CrossRef](#)]
10. Thao, N.T.P.; Ureshino, K.; Miyajima, I.; Ozaki, Y.; Okubo, H. Induction of tetraploids in ornamental *Alocasia* through colchicine and oryzalin treatments. *Plant Cell Tissue Organ Cult.* **2003**, *72*, 19–25. [[CrossRef](#)]
11. Sree Ramulu, K.; Verhoeven, H.A.; Dijkhuis, P. Mitotic blocking, micronucleation, and chromosome doubling by oryzalin, amiprofos-methyl, and colchicine in potato. *Protoplasma* **1991**, *160*, 65–71. [[CrossRef](#)]
12. Kermani, M.J.; Sarasan, V.; Roberts, A.V.; Yokoya, K.; Wentworth, J.; Sieber, V.K. Oryzalin-induced chromosome doubling in *Rosa* and its effect on plant morphology and pollen viability. *Theor. Appl. Genet.* **2003**, *107*, 1195–1200. [[CrossRef](#)]
13. Allum, J.F.; Bringloe, D.H.; Roberts, A.V. Chromosome doubling in a *Rosa rugosa* Thunb. hybrid by exposure of in vitro nodes to oryzalin: The effects of node length, oryzalin concentration and exposure time. *Plant Cell Rep.* **2007**, *26*, 1977–1984. [[CrossRef](#)] [[PubMed](#)]
14. Talebi, S.F.; Saharkhiz, M.J.; Kermani, M.J.; Sharafi, Y.; Raouf Fard, F. Effect of different antimitotic agents on polyploid induction of anise hyssop (*Agastache foeniculum* L.). *Caryologia* **2017**, *70*, 184–193. [[CrossRef](#)]
15. Tosca, A.; Pandolfi, R.; Citterio, S.; Fasoli, A.; Sgorbati, S. Determination by flow cytometry of the chromosome doubling capacity of colchicine and oryzalin in gynogenic haploids of *Gerbera*. *Plant Cell Rep.* **1995**, *14*, 455–458. [[CrossRef](#)]
16. Väinölä, A. Polyploidization and early screening of *Rhododendron* hybrids. *Euphytica* **2000**, *112*, 239–244. [[CrossRef](#)]
17. Mo, L.; Chen, J.H.; Chen, F.; Xu, Q.W.; Tong, Z.K.; Huang, H.H.; Dong, R.H.; Lou, X.Z.; Lin, E.P. Induction and characterization of polyploids from seeds of *Rhododendron fortunei* Lindl. *J. Integr. Agric.* **2020**, *19*, 2016–2026. [[CrossRef](#)]
18. Morgan, E.R.; Funnell, K.A. *Limonium*. In *Ornamental Crops*; Rajcan, I., Vollmann, J., Eds.; Handbook of Plant Breeding 11; Springer: Cham, Switzerland, 2018; pp. 513–527. [[CrossRef](#)]
19. Morgan, E.R.; Burge, G.K.; Seelye, J.F. *Limonium* breeding: New options for a well known genus. *Acta Hortic.* **2001**, *552*, 39–42. [[CrossRef](#)]
20. Mori, S.; Yamane, T.; Yahata, M.; Shinoda, K.; Murata, N. Chromosome doubling in *Limonium bellidifolium* (Gouan) Dumort. by colchicine treatment of seeds. *Hort. J.* **2016**, *85*, 366–371. [[CrossRef](#)]
21. Hoshi, N.; Abe, J. Micropropagation system of *Limonium sinuatum* “I-star” series. *Tohoku Agric. Res.* **2002**, *55*, 255–256. (In Japanese)
22. Murashige, T.; Skoog, F. A revised medium for rapid growth and bioassays with tobacco tissue cultures. *Physiol. Plant.* **1962**, *15*, 473–497. [[CrossRef](#)]

23. Morgan, E.R.; Burge, G.K.; Seelye, J.F.; Hopping, M.E.; Grant, J.E. Production of inter-specific hybrids between *Limonium perezii* (Stapf) Hubb. and *Limonium sinuatum* (L.) Mill. *Euphytica* **1998**, *102*, 109–115. [[CrossRef](#)]
24. Cohen, D.; Yao, J.L. In vitro chromosome doubling of nine Zantedeschia cultivars. *Plant Cell Tissue Organ Cult.* **1996**, *47*, 43–49. [[CrossRef](#)]
25. Fetouh, M.I.; Deng, Z.; Wilson, S.B.; Adams, C.R.; Knox, G.W. Induction and characterization of tetraploids in Chinese Privet (*Ligustrum sinense* Lour.). *Sci. Hortic.* **2020**, *271*, 109482. [[CrossRef](#)]
26. Chen, C.; Hou, X.; Zhang, H.; Wang, G.; Tian, L. Induction of *Anthurium andraeanum* “Arizona” tetraploid by colchicine in vitro. *Euphytica* **2011**, *181*, 137–145. [[CrossRef](#)]
27. Gantait, S.; Mandal, N.; Bhattacharyya, S.; Das, P.K. Induction and identification of tetraploids using in vitro colchicine treatment of *Gerbera jamesonii* Bolus cv. Sciella. *Plant. Cell Tissue Organ. Cult.* **2011**, *106*, 485–493. [[CrossRef](#)]
28. Otani, M.; Ishibe, M.; Inthima, P.; Supaibulwatana, K.; Mori, S.; Niki, T.; Nishijima, T.; Koshioka, M.; Nakano, M. Horticultural characterization of a tetraploid transgenic plant of *Tricyrtis* sp. carrying the gibberellin 2-oxidase gene. *Plant. Biotechnol.* **2014**, *31*, 335–340. [[CrossRef](#)]
29. Chen, C.H.; Goeden-Kallemeyn, Y. In vitro induction of tetraploid plants from colchicine-treated diploid daylily callus. *Euphytica* **1979**, *28*, 705–709. [[CrossRef](#)]
30. Ishizaka, H.; Uematsu, J. Amphidiploids between *Cyclamen persicum* Mill. and *C. hederifolium* Aiton induced through colchicine treatment of ovules in vitro and plants. *Breed. Sci.* **1994**, *44*, 161–166. [[CrossRef](#)]
31. Lindsay, G.C.; Hopping, M.E.; O’Brien, I.E.W. Detection of protoplast-derived DNA tetraploid Lisianthus (*Eustoma grandiflorum*) plants by leaf and flower characteristics and by flow cytometry. *Plant. Cell Tissue Organ. Cult.* **1994**, *38*, 53–55. [[CrossRef](#)]
32. Nakano, M.; Nomizu, T.; Mizunashi, K.; Suzuki, M.; Mori, S.; Kuwayama, S.; Hayashi, M.; Umehara, H.; Oka, E.; Kobayashi, H. Somaclonal variation in *Tricyrtis hirta* plants regenerated from 1-year-old embryogenic callus cultures. *Sci. Hortic.* **2006**, *110*, 366–371. [[CrossRef](#)]
33. Nimura, M.; Kato, J.; Horaguchi, H.; Mii, M.; Sakai, K.; Katoh, T. Induction of fertile amphidiploids by artificial chromosome-doubling in interspecific hybrid between *Dianthus caryophyllus* L. and *D. japonicus* Thunb. *Breed. Sci.* **2006**, *56*, 303–310. [[CrossRef](#)]
34. Takamura, T.; Miyajima, I. Colchicine induced tetraploids in yellow-flowered cyclamens and their characteristics. *Sci. Hortic.* **1996**, *65*, 305–312. [[CrossRef](#)]
35. del Pozo, J.C.; Ramirez-Parra, E. Whole genome duplications in plants: An overview from *Arabidopsis*. *J. Exp. Bot.* **2015**, *66*, 6991–7003. [[CrossRef](#)]
36. Laws, H.M. Pollen-grain morphology of polyploid *Oenotheras*. *J. Hered.* **1965**, *56*, 18–21. [[CrossRef](#)]
37. Najčevska, C.M.; Speckmann, G.J. Number of chloroplasts and pollen grain pores in diploid and tetraploid varieties of some *Trifolium* species. *Euphytica* **1968**, *17*, 357–362. [[CrossRef](#)]
38. Sattler, M.C.; Carvalho, C.R.; Clarindo, W.R. The polyploidy and its key role in plant breeding. *Planta* **2016**, *243*, 281–296. [[CrossRef](#)] [[PubMed](#)]
39. Pei, Y.; Yao, N.; He, L.; Deng, D.; Li, W.; Zhang, W. Comparative study of the morphological, physiological and molecular characteristics between diploid and tetraploid radish (*Raphanus sativus* L.). *Sci. Hortic.* **2019**, *257*, 108739. [[CrossRef](#)]
40. Aida, R.; Sasaki, K.; Yoshioka, S.; Noda, N. Chimerism of chrysanthemum stems changes at the nodes during vegetative growth. *Plant. Biotechnol.* **2020**, *37*, 373–375. [[CrossRef](#)]
41. Huala, E.; Sussex, I.M. Determination and cell interactions in reproductive meristems. *Plant. Cell* **1993**, *5*, 1157–1165. [[CrossRef](#)]
42. Satina, S.; Blakeslee, A.F.; Avery, A.G. Demonstration of the three germ layers in the shoot apex of *Datura* by means of induced polyploidy in periclinal chimeras. *Am. J. Bot.* **1940**, *27*, 895–905. [[CrossRef](#)]
43. Hantke, S.S.; Carpenter, R.; Coen, E.S. Expression of *floricaula* in single cell layers of periclinal chimeras activates downstream homeotic genes in all layers of floral meristems. *Development* **1995**, *121*, 27–35. [[CrossRef](#)] [[PubMed](#)]



Article

The Senescence-Associated Endonuclease, *PhENDO1*, Is Upregulated by Ethylene and Phosphorus Deficiency in Petunia

Michelle L. Jones ^{*}, Shuangyi Bai [†], Yiyun Lin and Laura J. Chapin

Department of Horticulture and Crop Science, The Ohio State University, 1680 Madison Avenue, Wooster, OH 44691, USA; shyibai@wsu.edu (S.B.); lin.2266@buckeyemail.osu.edu (Y.L.); chapin.23@osu.edu (L.J.C.)

^{*} Correspondence: jones.1968@osu.edu; Tel.: +1-330-263-3885

[†] Current address: Paul G. Allen School for Global Animal Health, College of Veterinary Medicine, Washington State University, Pullman, WA 99164, USA.

Abstract: The upregulation of endonuclease activities and subsequent decreases in the nucleic acid content of leaves and petals are characteristics of senescence that allow for nutrient remobilization from dying organs. We previously identified a 43-kDa endonuclease activity (PhNUC1) that was upregulated in *Petunia × hybrida* petals during senescence. PhNUC1 has optimal activity at neutral pH, is enhanced by Co²⁺, and degrades both DNA and RNA. The peptide sequence of a 43-kDa endonuclease identified from senescing petals by 2-dimensional gel electrophoresis was used to clone the gene (*PhENDO1*) encoding the senescence-associated protein. *PhENDO1* expression was upregulated in petals during the senescence of unpollinated and pollinated flowers and by ethylene treatment. When petunias were grown under nutrient deficient conditions, P-starvation, and to a lesser extent N-starvation, induced expression of *PhENDO1*. The endogenous expression of *PhENDO1* was down regulated using virus induced gene silencing (VIGS), and in-gel endonuclease assays confirmed that the activity of the 43-kDa PhNUC1 was decreased in senescing corollas from *PhENDO1*-silenced (pTRV2:*PhCHS:PhENDO1*) plants compared to controls (pTRV2:*PhCHS*). Down regulating *PhENDO1* in petunias did not alter flower longevity. While *PhENDO1* may be involved in nucleic acid catabolism during senescence, down regulating this gene using VIGS was not sufficient to delay flower senescence.

Citation: Jones, M.L.; Bai, S.; Lin, Y.; Chapin, L.J. The Senescence-Associated Endonuclease, *PhENDO1*, Is Upregulated by Ethylene and Phosphorus Deficiency in Petunia. *Horticulturae* **2021**, *7*, 46. <https://doi.org/10.3390/horticulturae7030046>

Academic Editors: Johan Van Huylenbroeck, Kenneth W. Leonhardt, Teresita D. Amore and Krishna Bhattarai

Received: 10 February 2021
Accepted: 4 March 2021
Published: 6 March 2021

Publisher's Note: MDPI stays neutral with regard to jurisdictional claims in published maps and institutional affiliations.



Copyright: © 2021 by the authors. Licensee MDPI, Basel, Switzerland. This article is an open access article distributed under the terms and conditions of the Creative Commons Attribution (CC BY) license (<https://creativecommons.org/licenses/by/4.0/>).

Keywords: flower senescence; nuclease; nutrient deficiency; petals; programmed cell death; virus induced gene silencing

1. Introduction

Senescence is a highly regulated process that represents a developmental transition from anabolism and growth to catabolism and cell death in organs, tissues, or whole plants. Developmental age, in combination with various endogenous and exogenous signals, determines the timing of senescence [1]. Ethylene is the primary hormonal signal regulating the initiation and progression of senescence in both leaves and flowers. External signals that influence senescence include environmental stresses like drought, nutrient limitations, low light levels, and temperature extremes, as well as biotic factors like pathogens [2,3].

Leaf and petal senescence are both accompanied by the upregulation of thousands of genes, and the progression of senescence in these organs requires de novo protein synthesis. Many of the upregulated genes encode enzymes involved in the degradation of proteins, nucleic acids, cell wall carbohydrates, and membrane lipids [4–7]. While organic molecules are degraded, organelles like the mitochondria and the nucleus must be maintained until late in the senescence process to allow for transcription of senescence-associated genes (SAGs) and to provide energy for cellular catabolism. This organized disassembly of macromolecules allows nutrients to be remobilized from older leaves and flowers to new sink tissues [8–10]. In pollinated flowers, senescence allows nutrients to be reallocated from

the dying petals to the developing ovary before the corolla is shed [11,12]. In both leaves and petals, cell death and associated macromolecule degradation starts in the margins and spreads inward, allowing for the maintenance of the vascular system until the final stages of senescence to facilitate nutrient remobilization via the phloem [2,13–15].

A characteristic feature of senescence is the hydrolysis of nucleic acids. Leaf and petal senescence are accompanied by large decreases in extractable RNA and DNA. Programmed cell death (PCD) at the advanced stages of senescence involves the fragmentation of nuclear DNA, which can be visualized as internucleosomal fragments or DNA ladders [2,16]. Senescence-associated nucleases hydrolyze the phosphodiester linkages in nucleic acids, releasing nucleotide bases that can serve as a source of nitrogen and phosphorus for remobilization to developing tissues [17,18]. Most of the nucleases that are involved in PCD are endonucleases, and activities against RNA, double-stranded DNA (dsDNA) and single-stranded DNA (ssDNA) are upregulated during petal and leaf senescence [19–26].

Plants have two major types of endonucleases, which are distinguished by their divalent cation cofactors and pH optima. Zn²⁺-dependent endonucleases (type I) require Zn²⁺ for catalytic activity and typically have an acidic pH optimum, while Ca²⁺-dependent endonucleases (type II) have a requirement for Ca²⁺ and are more active in the neutral pH range. Many Ca²⁺-dependent endonucleases preferentially degrade ssDNA over RNA, and Zn²⁺-dependent endonucleases prefer RNA and ssDNA to dsDNA as substrate. Both types of endonucleases are upregulated during senescence [17,27].

While most of the work on characterizing endonuclease activity and gene expression during senescence has been in leaves, endonucleases are also upregulated during the senescence of flower petals [7,19,21,23,28]. The upregulation of endonucleases with activity against RNA, ssDNA and dsDNA is observed during the age-related senescence of petals from unpollinated flowers and during pollination-induced senescence in petunias. This increased nuclease activity occurs later in the senescence program concomitant with DNA fragmentation, ethylene production, and corolla wilting [21,23]. Multiple senescence induced endonucleases with activity against RNA, ssDNA, and dsDNA are enhanced by Ca²⁺ in *Petunia inflata* petals [21]. In-gel activity assays show that some nucleases are detected constitutively in non-senescent petals with increasing activity during senescence, while some senescence-specific nucleases are detected only in senescing petals [21,23]. In *Petunia × hybrida*, a senescence-specific endonuclease was identified that has activity against ssDNA, dsDNA, and RNA [23]. This 43-kDa bifunctional endonuclease, which was identified from in-gel activity assays, was named PhNUC1. PhNUC1 activity is detected in the presence of Ca²⁺ and activity is inhibited by Zn²⁺, suggesting it could be a Ca²⁺-dependent endonuclease. Interestingly, the activity of PhNUC1 is greatly enhanced by the addition of Co²⁺, and Co²⁺ can overcome inhibition of the activity by Zn²⁺. The activity of PhNUC1 is induced by ethylene, and it is a glycoprotein with a pH optimum around 7.5 [23]. Only a few other endonuclease activities have been shown to be enhanced by Co²⁺ [25,26]. Senescence-associated genes encoding endonucleases have also been identified from daylily (*Heemerocallis* sp.) and carnation (*Dianthus caryophyllus*) flowers [29,30].

The senescence specific activity of PhNUC1 and its regulation by ethylene suggest that this endonuclease may catalyze the degradation of nucleic acids during petal senescence, but further investigation is needed to confirm this role. A proteomic analysis of pollination-induced corolla senescence identified an endonuclease (protein 14-12) with an observed molecular mass (*Mr*) of 43-kDa, that was detected only in senescing petals at 48 and 72 h after pollination [31]. The goal of this paper was to clone the gene encoding the senescence specific protein (14-12) and determine if the cobalt-enhanced, bifunctional endonuclease PhNUC1 is a product of that gene. The gene was named *PhENDO1* according to the nomenclature recommendations by Triques et al. [32]. Down-regulating *PhENDO1* in petunia using virus induced gene silencing (VIGS) demonstrated that PhNUC1 was a product of the *PhENDO1* gene. Down regulating this senescence specific activity was not sufficient to delay flower senescence. *PhENDO1* gene expression was upregulated during

petal senescence, by ethylene treatment, and during phosphorus (P) starvation, supporting a role in nutrient remobilization during developmental and stress induced PCD.

2. Materials and Methods

2.1. Plant Material

Petunia × *hybrida* ‘Mitchell Diploid’ (MD) were used in all experiments unless otherwise stated. Comparative analyses using MD plants transformed with 35S:*etr1-1* (line 44568; referred to as *etr1-1* petunias) were conducted to evaluate the role of ethylene in gene expression. *Etr1-1* petunia seeds were obtained from Dr. David Clark (University of Florida). Seeds were treated with 100 mg L⁻¹ GA₃ for 24 h and sown in cell-packs on top of soil-less mix (Promix BX, Premier Horticulture, Quakertown, PA, USA). All plants were established in the greenhouse after germination and plants were transferred to 16-cm pots after 4 weeks. Plants were fertilized at each watering with 150 mg L⁻¹ Nitrogen (N) from Scott’s Excel 15N-2.2P-12.5K-3.6Ca-1.2Mg (The Scotts Co., Marysville, OH, USA). A one-time treatment of Soluble Trace Element Mix (S.T.E.M., The Scotts Co.) was applied four weeks after transferring to 16-cm pots. Temperature in the greenhouse was set at 24/16 °C (day/night) with a 13-h photoperiod supplemented by high pressure sodium and metal halide lights.

2.2. Collection of Senescing Corollas

Flowers were emasculated 1 d before opening to prevent self-pollination. To study pollination-induced senescence, flowers were pollinated on the day of flower opening by brushing pollen from freshly dehisced anthers onto the stigma. Alternatively, flowers were emasculated and left unpollinated to senesce naturally. Zero h after pollination (hap) and 0 d represent unpollinated flowers on the day of flower opening. *Petunia* corollas (the fused petals on a *petunia* flower are collectively called the corolla) were collected from pollinated flowers at 0, 24, 48, and 72 h after flower opening, flash frozen in liquid nitrogen, and stored at −80 °C for subsequent RNA or protein extraction. Corollas from unpollinated flowers were collected from MD and *etr1-1* petunias on various days from flower opening through corolla wilting to evaluate natural senescence. Four replicates, each containing eight corollas from at least three different plants, were collected at each time point. Tissue was flash frozen in liquid nitrogen and stored at −80 °C prior to RNA extraction.

2.3. Ethylene and Cycloheximide Treatment of Flowers

Flowers were removed from plants 1 d after flower opening and placed in vials of deionized water or 50 μM cycloheximide, an inhibitor of protein synthesis. Flowers were then sealed in 24-L chambers and treated with air (control 0 μL L⁻¹ ethylene) or 0.1 μL L⁻¹ ethylene for 4 h (n = 12). The control chambers contained potassium permanganate (Ethylene Control, Selma, CA, USA) to absorb any ethylene produced by the flowers. After 4 h of treatment, corollas were harvested, flash frozen in liquid nitrogen, and stored at −80 °C. Four biologicals replicates, each containing three corollas were pooled for subsequent RNA extraction.

2.4. Nutrient Deficiency Treatments

Petunia seeds were germinated as previously described. Four-week-old seedlings were transplanted, three seedlings per pot, into 11-cm pots containing coarse perlite mixed with a wetting polymer (Soil Moist, JRM Chemicals, Cleveland, OH, USA). Treatments included complete nutrient solution, -N, -P and -K. Six pots received the different treatments. Pots contained a capillary wick and nutrient solutions were applied to trays for capillary uptake as well as top watered with fresh solution daily for 4 weeks. Nutrient solutions were prepared according to the recipes in Machlis and Torrey [33] and as previously described in Quijia Pilajio et al. [34]. After four weeks of treatment, all the leaves from each plant were harvested, and the leaves from the three plants in a single pot were pooled, frozen in liquid nitrogen, and stored at −80 °C for RNA extraction.

2.5. Cloning the Gene Encoding the Senescence-Specific Endonuclease PhNUC1

Total proteins were extracted from corollas, separated by two-dimensional gel electrophoresis (2-DE), and identified by mass spectrometry as described previously [31]. Protein profiles of pollinated corollas were compared to unpollinated corollas at the same developmental age and during the progression of pollination-induced senescence to identify differentially expressed proteins for sequence analysis. Mass spectrometry was conducted at the Cleveland Clinic Proteomics Laboratory (Cleveland Clinic Foundation, Cleveland, OH, USA). Protein abundance was calculated using PDQuest v7.40 (Bio-Rad Laboratories, Hercules, CA, USA) as described in Bai et al. [31].

RT-PCR was used to clone the gene (*PhENDO1*) encoding a senescence-specific endonuclease (14-12) previously identified in a large-scale proteomic analysis of senescing versus non senescing petunia corollas [31]. Total RNA was isolated from senescing petunia corollas at 72 h after pollination and first-strand cDNA was synthesized using the Omniscript Reverse Transcriptase kit (Qiagen, Valencia, CA, USA). Additional details on RNA extraction and cDNA synthesis can be found below in the section RNA extraction and gene expression analysis. Specific primers were designed based on the peptide sequences of 14-12 and other senescence-associated nucleases (Table S1). Using 2 µg cDNA as template, a fragment of a petunia endonuclease was amplified. The remaining 5' and 3' cDNA sequences were isolated by rapid amplification of cDNA ends (RACE) (SMART RACE kit, Clontech, Mountain View, CA, USA), and the full-length *PhENDO1* cDNA was then isolated by RT-PCR. Primer sequences can be found in Table S1. Sequence information for the full-length cDNA was obtained by capillary sequencing at the Molecular and Cellular Imaging Center (The Ohio State University/OARDC, Wooster, OH, USA) and analyzed with ChromasPro and the BLAST algorithm from NCBI non-redundant database. Sequence for *PhENDO1* can be found in the GenBank database Accession No. MW247148.

The open reading frame and amino acid sequence of the predicted PhENDO1 protein was determined using ORF Finder (<http://www.ncbi.nlm.nih.gov/projects/gorf/>, accessed on 15 January 2008). Putative signal peptides and glycosylation sites were predicted using TargetP 2.0 (<http://www.cbs.dtu.dk/services/TargetP>, accessed on 15 January 2008) and NetNGlyc 1.0 (<http://www.cbs.dtu.dk/services/NetNGlyc-1.0>, accessed on 15 January 2008), respectively. PhENDO1 and the predicted amino acid sequences of other plant endonucleases were aligned using Clustal Omega (<https://www.ebi.ac.uk/Tools/msa/clustalo/>, accessed on 21 October 2020) and formatted for viewing using BOXSHADE 3.21 (https://embnet.vital-it.ch/software/BOX_form.html, accessed on 21 October 2020).

2.6. RNA Extraction and Gene Expression Analysis

Total RNA was extracted from petunia tissue using TRIzol reagent (Invitrogen, Carlsbad, CA, USA), and RNA was treated with RQ1 RNase-free DNase (Promega, Madison, WI, USA). Complementary DNA (cDNA) was synthesized from 2 µg RNA using the Omniscript Reverse Transcriptase kit (Qiagen). Quantitative PCR was performed in a 20 µL reaction volume using B-R SYBR Green Master Mix (Quanta BioSciences, Gaithersburg, MD, USA). One microliter cDNA was used as template, and all reactions were performed in triplicate. PCR was conducted for 40 cycles of 94 °C for 10 s, 60 °C for 30 s, 72 °C for 15 s using the iQ5 Thermocycler (BioRad, Hercules, CA, USA). *PhCP10*, a senescence-specific cysteine protease from petunia (Genbank #AY662996; [35]), was used as a molecular marker for senescence [36]. Primers (Table S1) were designed to amplify transcripts using IDT primer Quest.

Melt curves were generated to check amplification specificity, and standard curves were generated to determine reaction efficiencies. An optimized delta delta CT method was used to determine relative target gene expression by using the reaction efficiencies and normalizing target gene expression to that of the reference gene *PhACTIN* (Actin2/7 GenBank #CV299322). In the second VIGS experiment (described below), the normalized relative expression was calculated using arithmetic means of relative quantity for the target gene and two reference genes: *PhACTIN* and *PhRPS13* (SGN# U209515). Both genes have

previously been shown to be stable targets for normalizing gene expression in senescing corollas and leaves from petunia [36,37].

2.7. Down Regulating *PhENDO1* in *Petunias* Using Virus Induced Gene Silencing (VIGS)

Two independent experiments were conducted in petunia to characterize the function of *PhENDO1* in petal senescence. The TRV1 (TRV RNA1) and TRV2 (TRV RNA2) vectors from tobacco rattle virus were used for VIGS in petunia [38]. The pTRV2:*PhCHS* (or pTRV2:*PhCHS:GFP*) construct was used as a control to visualize successful silencing in the corollas. Silencing the chalcone synthase gene (*CHS*) causes purple flowers to turn fully white or have white sectors [39].

In the first experiment, to generate the pTRV2:*PhCHS:PhENDO1* construct, a 303 bp fragment of *PhENDO1* was amplified by RT-PCR from petunia corolla cDNA using a forward primer with a *NcoI* restriction site and a reverse primer with a *KpnI* restriction site (Table S1). The fragment was chosen from the region corresponding to bases 304–606 to include both DNase and RNase active sites. The amplified fragment was ligated into pTRV2:*PhCHS* following double digestion using the respective restriction enzymes. The constructed plasmids, pTRV1, pTRV2, pTRV2:*PhCHS*, and pTRV2:*PhCHS:PhENDO1* were transformed into *Agrobacterium tumefaciens* GV3101 by heat shock.

In the second VIGS experiment RNAi designer (<https://rnaidesigner.lifetechnologies.com/rnaiexpress/design.do>, accessed on 15 March 2018) was used to identify siRNA regions in *PhENDO1* to increase silencing efficiency, and a second construct with a 245-bp fragment was amplified using a forward primer with a *BamHI* site and a reverse primer with an *XbaI* restriction site (Table S1). PCR products were ligated into pTRV2:*PhCHS* following double digestion with the respective restriction enzymes. A pTRV2:*PhCHS* construct including a 265-bp fragment of the *GFP* gene was used as the control in the second experiment [40]. The constructed plasmids, pTRV1, pTRV2:*PhCHS:GFP*, and pTRV2:*PhCHS:PhENDO1* were transformed into *Agrobacterium tumefaciens* GV3101 by electroporation.

To prepare for plant inoculation, the transformed *Agrobacterium* cultures were grown overnight at 30 °C in liquid LB media containing 25 mg·L⁻¹ gentamicin, 10 mg·L⁻¹ rifampin, and 50 mg·L⁻¹ kanamycin. The overnight cultures were used to inoculate (1:100 ratio) the LB-MESA media containing 10 mM MES pH 5.7 and 20 µM acetosyringone in addition to the antibiotics mentioned above. Once the OD₆₀₀ of the cultures reached 0.8–1.0, the cells were harvested at 4 °C and resuspended to an OD₆₀₀ of 2.0 in agroinduction media containing 10 mM MES pH 5.7, 10 mM MgCl₂, and 200 µM acetosyringone. The cultures were incubated overnight at room temperature and the cultures containing pTRV1 and pTRV2 or its derivatives were mixed at a 1:1 ratio as inoculum.

In the first experiment, *Petunia × hybrida* ‘Fantasy Blue’ 4-week old seedlings were inoculated via leaf infiltration using a needleless syringe. Treatments included mock inoculation (agroinduction media only), pTRV1+pTRV2 (empty vector), pTRV1+pTRV2:*PhCHS* (control), and pTRV1+pTRV2:*PhCHS:PhENDO1* inoculation. In the second experiment, *Petunia × hybrida* ‘Picobella Blue’ 4-week old seedlings were inoculated via apical meristem inoculation following optimized methods in Broderick and Jones [40]. Syngenta Flowers (formerly Goldsmith Seeds) replaced ‘Fantasy Blue’ with the improved variety ‘Picobella Blue’ that has the same plant profile, but different genetic background. Treatments for the second experiment included pTRV1+pTRV2:*PhCHS:GFP* (control) and pTRV1+pTRV2:*PhCHS:PhENDO1*.

The inoculated plants were maintained in a growth chamber (Conviron, Winnipeg, Canada) at Ohio Agricultural Research and Development Center, The Ohio State University, Wooster, OH for the duration of these experiments. Growing conditions in the growth chamber were 24 °C/20 °C (day/night) with a 13-h photoperiod from high pressure sodium lights for the first experiment and 20 °C/18 °C (day/night) with a 16-h photoperiod supplemented by metal halide lights for the second experiment.

To analyze the longevity of flowers from *PhENDO1*-silenced plants, flowers were emasculated one day prior to flower opening to avoid self-pollination. Flower longevity

was defined as the number of days from flower opening until the flower had senesced and the corolla was wilted. Flower longevity was measured using 48 flowers per treatment in the first experiment and 24 flowers per treatment in the second experiment. Corollas from senescing and non-senescing flowers were also harvested ($n = 4$), flash frozen in liquid nitrogen, and stored at $-80\text{ }^{\circ}\text{C}$ for extraction of RNA to confirm the down regulation of the *PhENDO1* transcript levels and for extraction of total protein to determine endonuclease activity. RNA extraction and qPCR were conducted as previously described.

2.8. Protein Extraction and Nuclease Activity Assays

Total protein was extracted from corollas collected from VIGS plants to use for both in-gel nuclease assays to separate individual activities and activity assays to quantify total nuclease activity. Corollas were collected at 0 d (non-senescing) and on the day of wilting (senescing) from mock inoculated, pTRV2 empty vector, pTRV2:*PhCHS* control, and pTRV2:*PhCHS:PhENDO1* plants for in-gel nuclease activity assays. A protein sample contained one corolla, and all collections, extractions, and gels were replicated five times. For quantifying total nuclease activity, corollas were collected from pTRV2:*PhCHS:GFP* controls and pTRV2:*PhCHS:PhENDO1* plants. Three corollas from each treatment were pooled together for each of the four biological replicates. Corollas were flash frozen and stored at $-80\text{ }^{\circ}\text{C}$. Frozen corollas were ground to a fine powder in a chilled mortar and pestle and extracted in 50 mM Tris-HCl (pH 7.4) amended with 20 mM DTT. Total protein was quantified using Coomassie Bradford Protein Assay (Pierce Biotechnology Thermo Scientific, Rockford, IL, USA).

In-gel nuclease activity assays were conducted as previously reported in Langston et al. [23]. Briefly, total proteins were resolved on a 15% (*w/v*) SDS-PAGE gel containing $100\text{ }\mu\text{g mL}^{-1}$ BSA. To identify DNase activities, the gels contained either $15\text{ }\mu\text{g mL}^{-1}$ double-stranded salmon sperm DNA (Invitrogen, Grand Island, NY, USA) or DNA that had been boiled for 3 min to make it single stranded. To identify RNase activities, gels contained $40\text{ }\mu\text{g mL}^{-1}$ total RNA from petunia corollas. SDS-PAGE was run at 120 V for 2 h at $25\text{ }^{\circ}\text{C}$. After separation, nucleases were renatured by incubating the gels in renaturation buffer [0.1 M Tris-HCl (pH 7.4), 1% Triton X-100] with shaking at $37\text{ }^{\circ}\text{C}$ for 1 h. Following two rinses in 0.1 M Tris-HCl (pH 7.4), gels were incubated overnight at $37\text{ }^{\circ}\text{C}$ in development buffer supplemented with cobalt to optimize activity of the senescence specific endonuclease previously identified [23] [50 mM Tris-HCl (pH 7.5), 20 mM NaCl , $100\text{ }\mu\text{M CoCl}_2$]. Gels were stained for 1 h at room temperature in 50 mM Tris (pH 7.0) containing $0.5\text{ }\mu\text{g mL}^{-1}$ ethidium bromide to visualize the bands of nuclease activity.

Total nuclease activity was measured for each corolla protein extract in nuclease reaction buffer containing 50 mM Tris-HCl (pH 7.5), 20 mM NaCl, $20\text{ }\mu\text{M CaCl}_2$, $10\text{ }\mu\text{M MgCl}_2$, $20\text{ }\mu\text{M CoCl}_2$, $10\text{ }\mu\text{M MnCl}_2$ and either heat-treated, single-stranded salmon sperm DNA (Invitrogen) or petunia leaf RNA as substrate. Each reaction consisted of 50 μL protein extract, $0.2\text{ }\mu\text{g mL}^{-1}$ heat-treated DNA or $0.5\text{ }\mu\text{g mL}^{-1}$ RNA, 0.1 mg mL^{-1} BSA and nuclease reaction buffer to a final volume of 350 μL . The reaction was incubated at $37\text{ }^{\circ}\text{C}$ for 20 min and terminated with the addition of 350 μL chilled 3.4% (*w/v*) perchloric acid followed by 10 min incubation on ice. Precipitates were removed by centrifugation ($5000\times g$ for 20 min at $4\text{ }^{\circ}\text{C}$). Supernatant was assayed for change in absorbance at 260 nm compared to the blank sample. One unit of DNase or RNase activity is the amount of enzyme liberating acid soluble material at a rate of 1.0 absorbance unit per min. Four biological replicates were assayed for each treatment and each sample was run in triplicate.

2.9. Statistical Analysis

All statistical analyses in this study were conducted in R 3.3.1. An analysis of variance (ANOVA) was performed followed by mean separation via Fisher's Least Significant Difference (LSD) test using R package agricolae ($\alpha = 0.05$). When data was not normally distributed, a log-transformation of the data was conducted. A statistical model was used for analyses: $Y = \mu + \text{Treat} + \text{Rep} + \varepsilon$, where μ is the mean across all experiments and

treatments, Treat is the effect of treatment (e.g., buffer or VIGS construct), Rep is the effect of replicates in each experiment, and ϵ is the uncontrolled error. All effects in the model were considered fixed.

3. Results

3.1. *PhENDO1* Is a Senescence-Associated Gene

Proteomics experiments identified a putative endonuclease (14-12) that was differentially expressed in senescing corollas (Figure 1A,B and [31]). Spot 14-12 in the 2-DE gels had an observed molecular mass of 43-kDa. This protein spot was not detected in unpollinated corollas at 0 h after flower opening (Figure 1B,C). In pollinated flowers, the spot was not detected at 24 h but was detected at 48 h with an increase in abundance at 72 h (Figure 1B,C). RT-PCR was used to clone the gene encoding this senescence-specific protein by using the peptide sequences obtained from MS analysis of spot 14-12. Quantitative PCR showed that the transcript levels of *PhENDO1* also increased in corollas during pollination-induced senescence (Figure 1D). Transcripts of *PhENDO1* were detected in corollas on the day of flower opening (0 h). Transcript levels increased slightly at 24 h after pollination and peaked at 48 h after pollination when corollas were visibly wilted (Figure 1A,D).

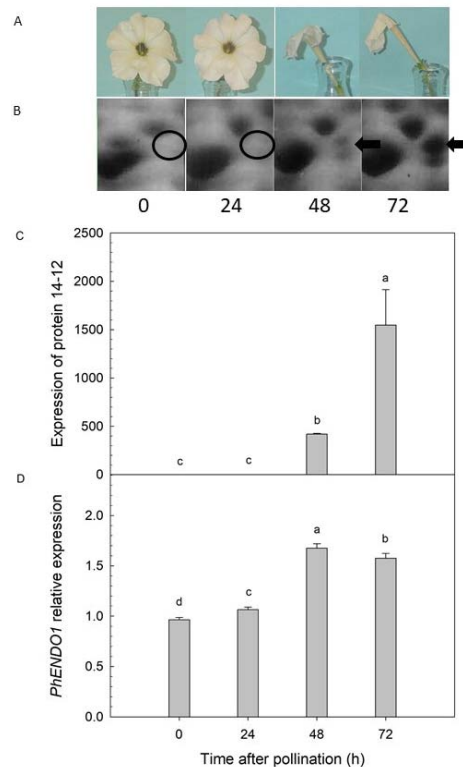


Figure 1. Endonuclease protein and gene expression is up regulated during petunia corolla senescence. (A) *Petunia × hybrida* 'Mitchell Diploid' (MD) flowers at 0, 24, 48, and 72 h after pollination. (B) Protein 14-12 is an endonuclease detected only in senescing corollas at 48 and 72 h after pollination. (C) Changes in the abundance of a 43-kDa protein (endonuclease14-12) and (D) gene expression of *PhENDO1* in corollas during pollination-induced senescence. Bars represent mean \pm SE. Protein abundance is presented as the spot volume from the replicated 2-DE gels ($n = 3$) and gene expression was evaluated by qPCR ($n = 3$). Different letters indicate significant difference between the means.

The full-length *PhENDO1* cDNA was 1100 bp, with an opening reading frame (ORF) encoding 301 amino acids (Figure S1). The predicted PhENDO1 protein had a molecular mass of 34.1-kDa and PI of 5.2. The first 25 amino acids of PhENDO1 are predicted to encode a signal peptide that leads the protein to a secretory pathway [41,42]. After the signal peptide is cleaved, the mature peptide of PhENDO1 would be 31.4-kDa. PhENDO1 has three N-glycosylation sites at amino acids 119, 137 and 211, based on the presence of the consensus sequence Asn-Xaa-Ser/Thr (Figure S1).

Multiple alignment of the deduced amino acid sequences of PhENDO1 and other endonucleases showed that PhENDO1 shares many common features with other bifunctional endonucleases in plants including the residues that bind zinc atoms, the residues that form disulfide bonds, the three glycosylation sites, and the sites of RNase and DNase activity (Figure S2). PhENDO1 is most homologous to endonucleases from other Solanaceae plants, and it shares the highest amino acid identity (91%) with endonuclease 1 from *Nicotiana attenuata* (XP_019234897). Among the Arabidopsis endonucleases (AtENDO1-5), PhENDO1 shares the highest amino acid identity (74.8%) with AtENDO1 (NP_172585, previously called BFN1). Homology to the other Arabidopsis endonucleases is much lower, with PhENDO1 sharing only 53.14%, 52.57%, 47.43%, and 47.25% amino acid identity with AtENDO2, AtENDO4, AtENDO3, and AtENDO5, respectively (Alignment shown in Figure S2).

3.2. *PhENDO1* Is Upregulated during Natural Flower Senescence and by Exogenous Ethylene

Quantitative PCR showed that *PhENDO1* transcript abundance increased at 7 d after flower opening as MD corollas were starting to show the first signs of wilting and senescence (Figure 2). Expression peaked at 8 d and decreased at 9 d after flower opening. Expression in corollas from *etr1-1* ethylene insensitive transgenic plants also increased, but to a much lesser extent at 21 d after opening when these corollas were wilted. Treating flowers with a low level of ethylene ($0.1 \mu\text{L L}^{-1}$) for only 4 h resulted in a 152-fold increase in *PhENDO1* transcripts in MD corollas (Figure 3). This increase was completely prevented by treating flowers with the protein synthesis inhibitor cycloheximide. There was no significant upregulation of *PhENDO1* by exogenous ethylene treatment in *etr1-1* corollas.

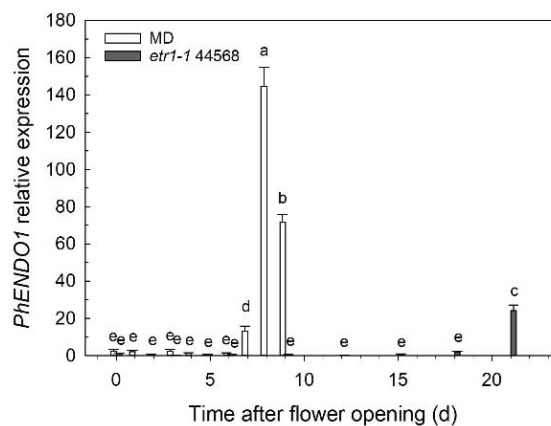


Figure 2. Expression of *PhENDO1* is upregulated during corolla senescence in unpollinated MD and *etr1-1* petunias. *PhENDO1* relative expression was measured during the natural senescence of unpollinated corollas from *Petunia × hybrida* wild type ‘Mitchell Diploid’ (MD) and transgenic petunia with reduced sensitivity to ethylene (35S:*etr1-1*, line 44568). Expression analysis was conducted by qPCR. Samples were run in triplicate (n = 3) and normalized to *PhACTIN*. Bars represent mean relative expression level ± SE. Different letters indicate significant difference between the means.

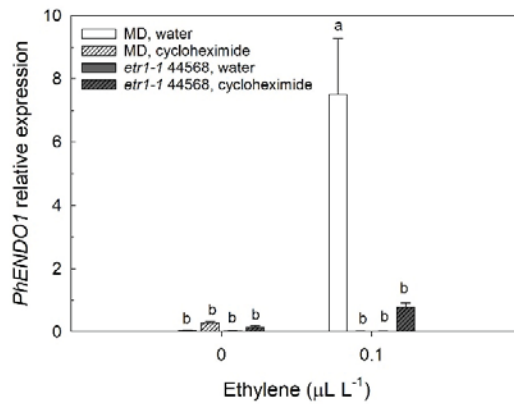


Figure 3. Expression of *PhENDO1* is upregulated by ethylene treatment in MD petunias. Relative *PhENDO1* expression was measured in corollas from *Petunia* \times *hybrida* ‘Mitchell Diploid’ (MD) and transgenic petunia with reduced sensitivity to ethylene (35S:*etr1-1*, line 44568) following treatment of detached flowers with the protein synthesis inhibitor, cycloheximide (0 μM or 50 μM), and exposure to 0.1 $\mu\text{L L}^{-1}$ ethylene for 4 h. Expression analysis was conducted by qPCR. Samples were run in triplicate ($n = 3$) and normalized to *PhACTIN*. Bars represent mean relative expression level \pm SE. Different letters indicate significant difference between the means.

3.3. *PhENDO1* Is Upregulated by P Starvation

When MD plants were grown under individual nutrient deficiencies, N and P starvation increased the expression of *PhENDO1* in leaves, but there was not a significant up regulation by potassium (K) starvation. P starvation resulted in the greatest up regulation of *PhENDO1*, with an 88-fold increase in transcript abundance compared to control plants receiving a complete fertilizer solution (Figure 4). Plants grown under N deficiency were smaller and had chlorotic leaves compared to control plants. P deficiency also resulted in stunted growth and purpling of the leaves.

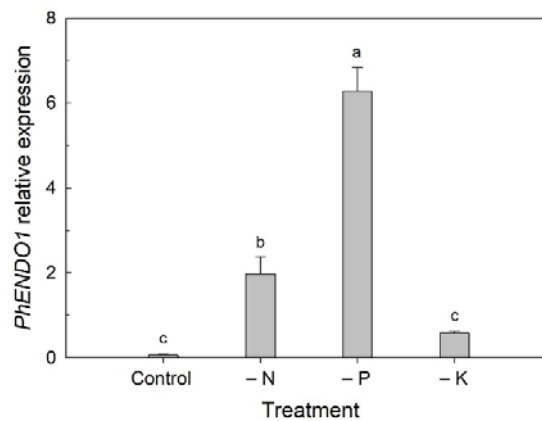


Figure 4. Expression of *PhENDO1* in response to nutrient deficiency. Petunia plants were irrigated with complete nutrient solution or solutions deficient in N, P or K. Leaves were collected after 4 weeks of treatment. Expression of *PhENDO1* in the leaves was determine by qPCR. Samples were run in triplicate ($n = 3$) and normalized to *PhACTIN*. Bars represent mean \pm SE. Different letters indicate significant difference between the means.

3.4. *PhENDO1* Encodes a Previously Identified 43-kDa Senescence-Specific, Cobalt-Enhanced Endonuclease Activity

VIGS was used to down regulate the expression of *PhENDO1* in petunias. A senescence specific endonuclease activity previously identified and called PhNUC1 was detected in senescing corollas from mock inoculated plants, pTRV2 empty vector and pTRV2-*PhCHS* control plants at 43-kDa (Figure 5). This cobalt-enhanced, bifunctional endonuclease was previously reported in senescing petunia corollas [23]. This activity was senescence specific and was not detected in the non-senescing corollas on the day of flower opening (Figure 5E). The 43-kDa activity corresponding to this endonuclease was greatly reduced in corollas from *PhENDO1*-silenced petunias, confirming that *PhENDO1* encoded for the endonuclease responsible for this activity. The 43-kDa endonuclease had activity against ssDNA, dsDNA and RNA, and a reduction in activity was detected in *PhENDO1*-silenced corollas against all three substrates.

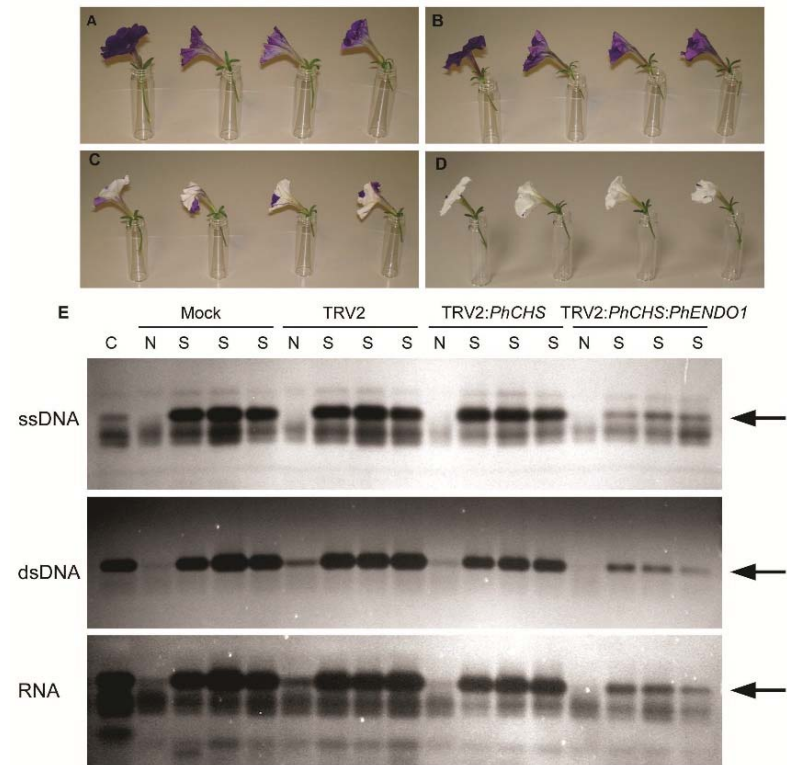


Figure 5. Activity of the 43-kDa senescence-specific, Co^{2+} -enhanced endonuclease (PhNUC1) decreased in senescing corollas of pTRV2:*PhCHS*:*PhENDO1* plants. Photos of the single flowers from (A) mock inoculated, (B) pTRV2 empty vector, (C) pTRV2:*PhCHS* and (D) pTRV2:*PhCHS*:*PhENDO1* used for protein extraction and in-gel nuclease activity assays in Figure 5E. The first flower in each group was a non-senescing flower collected on the day of flower opening and the next three flowers were wilted, senescing flowers at 48 h after pollination. (E) Nuclease in-gel activity assays with single stranded DNA (ssDNA), double stranded DNA (dsDNA), or RNA as substrates. Control (C) samples were proteins extracted from wild type ‘MD’ corollas 48 h after pollination; N, non-senescing; S, senescing corollas. The 43-kDa endonuclease previously identified as PhNUC1 [23] in each assay is indicated by an arrow.

Quantitative PCR was used to confirm the down regulation of *PhENDO1* gene expression in the VIGS plants. *PhENDO1* transcript abundance was reduced by 66% in senescing corollas from pTRV2:*PhCHS*:*PhENDO1* plants when compared to senescing corollas from control (pTRV:*PhCHS*) plants (Figure S3). Down regulating *PhENDO1* did not have a significant effect on flower longevity. *PhENDO1*-silenced plants had an average flower longevity of 8.5 d compared to 8.7 d for the control flowers (n = 48 flowers) (Table 1). A second experiment was conducted using VIGS protocols that had been optimized to improve silencing efficiency in petunia [40]. This second experiment confirmed that silencing *PhENDO1* did not accelerate or delay corolla senescence (n = 24 flowers) (Table 1). Gene silencing in the second experiment was more efficient and resulted in an 88.4% decrease in the expression of *PhENDO1* in pTRV2:*PhCHS*:*PhENDO1* (*PhENDO1*-silenced) senescing corollas compared to pTRV2:*PhCHS*:*GFP* (control) senescing corollas (Figure 6A). *PhENDO1* transcripts were upregulated during the senescence of control corollas, but a significant senescence-associated increase in transcript abundance was not detected in *PhENDO1*-silenced corollas. The expression of the senescence marker *PhCP10* (*Petunia* × *hybrida* *Cysteine Protease 10*) was similar in the senescing corollas of control and *PhENDO1*-silenced petunias (Figure 6B). Total endonuclease activity against ssDNA (DNase activity) and RNA (RNase activity) increased in senescing corollas compared to non-senescing corollas, but both DNase (Figure 6C) and RNase (Figure 6D) activity was similar in *PhENDO1*-silenced corollas and control corollas.

Table 1. Flower longevity comparisons among *Petunia* × *hybrida* inoculated pTRV2:*PhCHS* or pTRV2:*PhCHS*:*GFP* (control) and pTRV2:*PhCHS*:*PhENDO1* in two independent experiments. Flower longevity of each flower was determined as the number of days from flower opening until the corolla showed more than half of the tissue as wilted. Flower longevity reported represents the means. Mean separations were analyzed based on ANOVA protected least significant difference (LSD) test at 0.05 level. Means with the same letters are not significantly different.

Treatment	Experiment 1 (n = 48)	Experiment 2 (n = 24)
Control *	8.7 a	10.9 a
pTRV2: <i>PhCHS</i> : <i>PhENDO1</i>	8.5 a	10.7 a

* Plants inoculated with pTRV2:*PhCHS* were used as the control in experiment 1, and plants inoculated with pTRV2:*PhCHS*:*GFP* were used as the control in experiment 2.

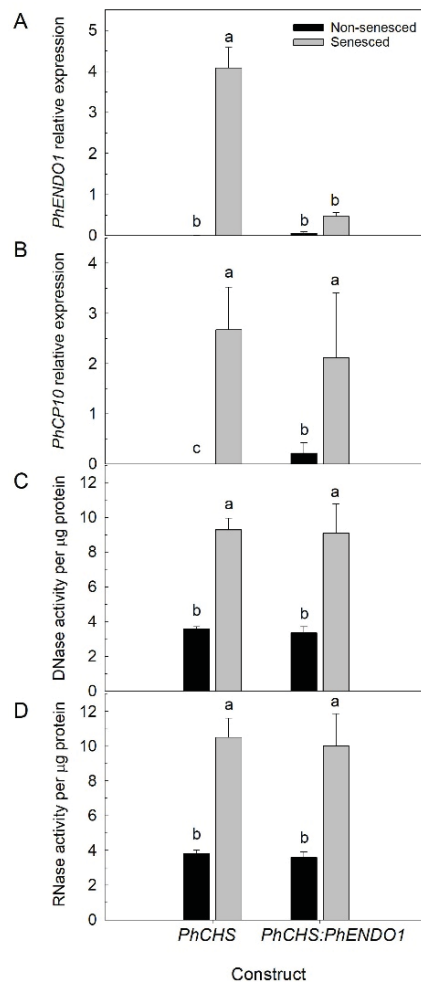


Figure 6. Gene expression and endonuclease activity in *PhENDO1*-silenced corollas. Relative abundance of *PhENDO1* (A) and *PhCP10* (B) in non-senesced and senesced corollas was determined by qPCR in pTRV:*PhCHS:GFP* (controls) and pTRV2:*PhCHS:PhENDO1* petunias. Bars represent mean \pm SE (n = 4) and least squared means were evaluated at $p < 0.05$. Different letters indicate significant difference between the means. Total protein extracts from non-senesced and senesced corollas of control and *PhENDO1*-silenced petunias were assayed for ssDNase (C) and RNase (D) activity. Each treatment had 4 biological replicates and each extract was run in triplicate. Bars represent mean \pm SE with different letters indicating significance differences ($p < 0.05$).

4. Discussion

The programmed senescence of petunia petals is accompanied by increases in DNA fragmentation and the induction of various nuclease activities as evidenced by in-gel activity assays. An increase in total endonuclease activity accompanies the decrease in RNA and DNA content of the petals, which occurs late in the senescence program concomitant with corolla wilting (Figure 6 [21,23]). The degradation of nucleic acids provides N and P that can be reallocated during nutrient starvation or during the senescence of plant organs. The N and P content of petals decreases during the senescence of pollinated and

unpollinated flowers, supporting the remobilization function of programmed cell death in the corolla [9–12,37,43].

Multiple constitutive and senescence upregulated endonuclease activities have been reported in flowers that could be involved in the large-scale degradation of genomic DNA and RNA during programmed cell death in petals [19,21,23]. Xu and Hanson [21] reported the activity of two constitutive and two upregulated activities against RNA, five upregulated activities against ssDNA, and four upregulated activities against dsDNA during the pollination-induced senescence of *Petunia inflata* corollas. One of these was a senescence-specific endonuclease (46-kDa) with activity against only ssDNA. The divalent cation requirements and pH optimum of this endonuclease were not reported. In *Petunia × hybrida*, a senescence-specific, 43-kDa endonuclease (PhNUC1) was identified in corollas that had activity against DNA (both ss and ds) and RNA. This bifunctional endonuclease has low levels of activity in the presence of Ca^{2+} , but the addition of Co^{2+} enhances activity against all substrates much beyond that of Ca^{2+} . Cobalt restores the activity that is inhibited by the chelating agent EDTA, while Ca^{2+} does not [23]. The inhibition by Zn^{2+} and pH optimum around 7.5 suggest that PhNUC1 is a type II Ca^{2+} -dependent endonuclease. Similar bifunctional endonucleases, that are upregulated during leaf senescence in parsley (*Petroselinum crispum*) (PcNUC1, 43-kDa and PcNUC2, 40-kDa) and tomato (*Solanum lycopersicum*) (LeNUC1, 41-kDa) also have neutral pH optima and Co^{2+} -enhanced activity [25,26].

Two-dimensional gel electrophoresis (2-DE) was used to identify proteins that were differentially expressed between senescing and nonsenescing petunia corollas [31]. A protein with a predicted molecular mass of 43-kDa was detected only in senescing petals at 48 and 72 h after pollination (Figure 1B). Liquid chromatography-tandem mass spectrometry (LC-MS/MS) identified this senescence-specific protein as a putative endonuclease (protein 14-12) [31]. The peptide sequence for that putative endonuclease was successfully used to clone the corresponding cDNA, which was named *PhENDO1* (Figure S1). *PhENDO1* has all the features of an endonuclease, and it has high amino acid identity to other senescence-associated endonucleases like BFN1 (now called AtENDO1) from Arabidopsis (*Arabidopsis thaliana*) (Figure S2). The gene expression pattern for *PhENDO1* corresponded with the senescence-associated expression of the endonuclease protein 14-12 [31] and with the activity of the bifunctional endonuclease PhNUC1 [23] in senescing corollas from pollinated flowers (Figure 1). *PhENDO1* expression was also upregulated during the age-related senescence of unpollinated petunia corollas, peaking at 8 days after flower opening when the corolla was visibly wilting (Figure 2). This also mirrors the pattern of PhNUC1 activity observed against both DNA and RNA in unpollinated corollas [23]. The activities of the bifunctional endonucleases, LeNUC1 (tomato), AtENDO1/BFN1 (Arabidopsis), PcNUC1 and 2 (parsley), and PVN2 and 5 (French bean, *Phaseolus vulgaris*) are all upregulated during natural leaf senescence [20,24–26]. Few papers report specifically on expression in senescing petals, but AtENDO1/BFN1 and AtENDO3 are expressed in petals, with expression of AtENDO1 increasing during flower aging [20,28,44].

The predicted molecular mass of *PhENDO1* is 34.1-kDa, while the observed M_r of both the endonuclease 14-12 [31] and the bifunctional endonuclease activity PhNUC1 [23] is 43-kDa. Arabidopsis endonucleases have observed molecular masses of 30–40 kDa in SDS-PAGE activity gels, which is also higher than the molecular masses estimated from their amino acid sequences [44]. The electrophoretic mobility of AtENDO1 and AtENDO2 were shown to be reduced due to the glycosylation state of the proteins [45]. PhNUC1 and the other cobalt-enhanced endonucleases from tomato and parsley are also glycoproteins [23,25,26], which can explain the difference between the observed size of the activity bands and the predicted molecular masses of the proteins.

The expression pattern of *PhENDO1* (and endonuclease 14-12) corresponded well with the activity of PhNUC1 during corolla senescence, suggesting that this endonuclease activity is encoded by *PhENDO1*. Down regulating the expression of *PhENDO1* using VIGS confirmed that PhNUC1 activity was a product of the *PhENDO1* gene (Figure 5).

Overexpressing recombinant AtENDO1 and AtENDO2 in protoplasts reveals that some of the Arabidopsis endonucleases appear as more than one activity band, and that there can be multiple post-translationally modified forms of the proteins with endonuclease activity [44]. It is possible that there are also other variants of PhENDO1 that we did not observe were down-regulated in petunia corollas, because the conditions used for the in-gel activity assays were those optimized previously for PhNUC1 activity (i.e., pH 7.5, plus Co^{2+}). The Arabidopsis *ENDO2* knockout mutant (*endo2*) was used to confirm which nuclease activities are products of the *AtENDO2* gene [46]. In-gel activity assays show that *endo2* protoplasts lack activity corresponding to both a 34-kDa (N1) and a 36-kDa (N2) endonuclease [46]. The N2 variant of AtENDO2 is not glycosylated, while the N1 variant is glycosylated. AtENDO2-N1 is localized in the cytoplasm in healthy cells, and the de-glycosylated form (AtENDO2-N2) is localized in the nucleus where it is believed to play a role in DNA fragmentation [46].

Down regulating the *PhENDO1* gene did not result in any visible differences in growth and development. *PhENDO1*-deficient petunias had similar plant biomass, flower size, flower numbers, and flower longevity as control plants (Table 1 and data not shown). Corolla senescence in these flowers was also accompanied by upregulation of the senescence marker, *PhCP10*, to similar levels as the control corollas (Figure 6B). *PhCP10* encodes a cysteine protease believed to be involved in protein degradation during petal senescence. It is an ortholog of *AtSAG12*, which serves as a molecular marker for senescence [47]. Arabidopsis plants lacking a functional AtENDO1/BFN1 do not have any visible differences in leaf senescence or other aspects of growth and development [48]. Similarly, overexpressing *AtENDO1* has no effect on leaf senescence [20].

PhENDO1 transcript levels in senescing flowers were reduced, as was the specific nuclease activity corresponding to the 43-kDa bifunctional endonuclease PhNUC1 (Figures 5 and 6A and data not shown). In contrast, the total endonuclease activity against RNA and ssDNA was not reduced in senescing corollas from *PhENDO1*-deficient flowers (Figure 6C,D), suggesting that there were other nucleases that were upregulated during corolla senescence to compensate for the reduced expression of *PhENDO1* and its product PhNUC1. Searching the *Petunia axillaris* predicted protein database at the Sol Genomics Network (<https://solgenomics.net/>, accessed on 4 February 2021) identified two putative endonucleases (Peaxi162Scf00527g00026.1 and Peaxi162Scf00753g00440.1) that had 81% and 44.8% amino acid identity, respectively, with PhENDO1.

Plant endonucleases are encoded by a multi gene family, and studies show some tissue specificity and differential expression during plant development and stress responses among the individual family members [44,49,50]. In French bean, *PVN4* and *PVN5* are upregulated during cotyledon senescence and *PVN2* and *PVN5* are upregulated during the natural and dark-induced senescence of leaves, suggesting that there are also some functional redundancies between the family members [49,50]. Senescence involves a complex network of genes involved in a highly coordinated program of cellular disassembly and resource remobilization. Manipulating individual components of this network often does not alter the initiation or progression of senescence [51].

Ethylene is a key regulator of senescence in both leaves and flowers [52,53]. In ethylene-insensitive transgenic petunias (35S:*etr1-1*), where petal senescence is delayed, expression of *PhENDO1* (Figure 2) and PhNUC1 activity [23] were similarly delayed until the corollas of those flowers were wilted. A similar pattern of delayed expression in senescing petals from 35S:*etr1-1* transgenic petunias was observed with the senescence-associated gene *PhCP10* [35]. Treating petunia flowers with ethylene induced expression of *PhENDO1* (Figure 3) and the activity of PhNUC1 in the corollas [23]. The progression of senescence requires the de novo synthesis of proteins and treating flowers with cycloheximide delays senescence [54]. Labeling experiments in morning glory (*Ipomea tricolor*) provide evidence that ribonuclease is de novo synthesized during the senescence of the corolla [55]. The upregulation of *PhENDO1* by ethylene was prevented by treating flowers with the protein synthesis inhibitor, cycloheximide (Figure 3). Similarly, the induction

of *PhCP10* is also prevented by treating petunia flowers with cycloheximide [36]. These experiments suggest that both the upregulation of *PhENDO1* and *PhCP10* are secondary responses to the ethylene stimulus. The activities of LeNUC1 and PcNUC1 and PcNUC2 are induced by treating young, attached leaves or green, detached leaves, respectively, with ethylene [25,26]. Senescence-associated endonuclease genes are also upregulated by other plant hormones including jasmonic acid, salicylic acid, gibberellic acid, and abscisic acid [29,56,57].

Many senescence-associated nucleases are also induced by phosphate starvation [18,49,50,58–60]. In tomato, *LE* and *LX* RNase genes are induced at the late stage of senescence and during phosphate starvation in cell cultures, suggesting a dual role in nutrient remobilization during developmental senescence and phosphate scavenging during nutrient stress [18]. We found that the expression of *PhENDO1* was also upregulated when plants were grown under nutrient deficient conditions (Figure 4). The greatest upregulation was seen under P-deficient conditions, but N deficiency also resulted in upregulation of *PhENDO1* expression in leaves to a lesser extent. Interestingly, expression of *PhCP10* is highly upregulated in petunia leaves under N-deficient conditions and to a lesser extent under P-deficient conditions [34]. *PVN4* and *PVN5*, endonucleases in French bean that are upregulated during cotyledon senescence, are also upregulated when seedlings are grown under nutrient deficient conditions (minus P and N) [50]. Other senescence-associated bifunctional nucleases, like *AtENDO1/BFN1* are not induced by phosphate starvation [20].

A decrease in nucleic acid content and increased DNA fragmentation during corolla senescence is accompanied by an increase in endonuclease activities against both DNA and RNA in petunias. A senescence-specific, bifunctional endonuclease, whose activity is enhanced by cobalt was identified in petunia corollas (PhNUC1). In the present study, we cloned the gene (*PhENDO1*) encoding this endonuclease activity. *PhENDO1* gene expression mirrored activity of the endonuclease PhNUC1 during corolla senescence. *PhENDO1* was upregulated in corollas from both pollinated and unpollinated flowers, and its induction by ethylene required de novo protein synthesis. Virus induced silencing of *PhENDO1* proved an effective way to confirm that PhNUC1 activity was a product of the *PhENDO1* gene, and it demonstrated that down regulating this endonuclease did not delay senescence or decrease the total endonuclease activity in senescing corollas. *PhENDO1* expression was also upregulated in leaves of plants grown under P-deficient and to a lesser extent N-deficient conditions, confirming a functional role in both nutrient remobilization during senescence and nutrient salvaging during starvation responses. This work increases our understanding of the molecular and biochemical changes accompanying flower petal senescence and their role in programmed cell death and nutrient recycling.

Supplementary Materials: The following are available online at <https://www.mdpi.com/2311-7524/7/3/46/s1>, Figure S1: The sequences of the *PhENDO1* coding region and the predicted protein, Figure S2: Alignment of the deduced amino acid sequences of endonuclease enzymes.

Author Contributions: M.L.J.: Conceptualization, Resources, Writing—original draft preparation, Writing—reviewing and editing, Supervision, Project administration, Funding acquisition. S.B.: Conceptualization, Methodology, Formal analysis, Investigation, Visualization, Writing—reviewing and editing. Y.L.: Conceptualization, Methodology, Formal analysis, Investigation, Visualization, Writing—reviewing and editing. L.J.C.: Conceptualization, Methodology, Formal analysis, Investigation, Visualization, Writing—reviewing and editing. All authors have read and agreed to the published version of the manuscript.

Funding: This work was supported by The Ohio State University D.C. Kiplinger Floriculture Endowment and the American Floral Endowment. Salaries and research support were provided in part by State and Federal funds appropriated to the Ohio Agriculture Research and Development Center (OARDC), The Ohio State University. Journal Article Number HCS 20-09.

Data Availability Statement: Sequence for *PhENDO1* can be found in the GenBank database Accession No. MW247148.

Acknowledgments: We would like to thank Karli Shultz and Kesia Hartzler for their excellent greenhouse support.

Conflicts of Interest: The authors declare no conflict of interest.

References

- Kim, J.; Kim, J.H.; Lyu, J., II; Woo, H.R.; Lim, P.O. New insights into the regulation of leaf senescence in Arabidopsis. *J. Exp. Bot.* **2018**, *69*, 787–799. [[CrossRef](#)] [[PubMed](#)]
- Pyung, O.L.; Kim, H.J.; Nam, H.G. Leaf senescence. *Annu. Rev. Plant Biol.* **2007**, *58*, 115–136.
- Shibuya, K. Molecular aspects of flower senescence and strategies to improve flower longevity. *Breed. Sci.* **2018**, *68*, 99–108. [[CrossRef](#)]
- Gepstein, S.; Sabehi, G.; Carp, M.J.; Hajouj, T.; Neshet, M.F.O.; Yariv, I.; Dor, C.; Bassani, M. Large-scale identification of leaf senescence-associated genes. *Plant J.* **2003**, *36*, 629–642. [[CrossRef](#)]
- Broderick, S.R.; Wijeratne, S.; Wijeratn, A.J.; Chapin, L.J.; Meulia, T.; Jones, M.L. RNA-sequencing reveals early, dynamic transcriptome changes in the corollas of pollinated petunias. *BMC Plant Biol.* **2014**, *14*, 1–21. [[CrossRef](#)]
- Breeze, E.; Harrison, E.; McHattie, S.; Hughes, L.; Hickman, R.; Hill, C.; Kiddle, S.; Kim, Y.S.; Penfold, C.A.; Jenkins, D.; et al. High-resolution temporal profiling of transcripts during Arabidopsis leaf senescence reveals a distinct chronology of processes and regulation. *Plant Cell* **2011**, *23*, 873–894. [[CrossRef](#)] [[PubMed](#)]
- Price, A.M.; Orellana, D.F.A.; Salleh, F.M.; Stevens, R.; Acock, R.; Buchanan-Wollaston, V.; Stead, A.D.; Rogers, H.J. A comparison of leaf and petal senescence in wallflower reveals common and distinct patterns of gene expression and physiology. *Plant Physiol.* **2008**, *147*, 1898–1912. [[CrossRef](#)] [[PubMed](#)]
- Himelblau, E.; Amasino, R.M. Nutrients mobilized from leaves of Arabidopsis thaliana during leaf senescence. *J. Plant Physiol.* **2001**, *158*, 1317–1323. [[CrossRef](#)]
- Verlinden, S. Changes in mineral nutrient concentrations in petunia corollas during development and senescence. *HortScience* **2003**, *38*, 71–74. [[CrossRef](#)]
- Jones, M.L. Mineral nutrient remobilization during corolla senescence in ethylene-sensitive and insensitive flowers. *AoB Plants* **2013**, *5*, 1–11. [[CrossRef](#)] [[PubMed](#)]
- Chapin, L.; Jones, M. Nutrient Remobilization during Pollination-Induced Corolla Senescence in Petunia. In Proceedings of the International Conference on Quality Management in Supply Chains of Ornamentals, Bangkok, Thailand, 3 December 2007; Volume 755, pp. 181–190.
- Shibuya, K.; Niki, T.; Ichimura, K. Pollination induces autophagy in petunia petals via ethylene. *J. Exp. Bot.* **2013**, *64*, 1111–1120. [[CrossRef](#)]
- Van Doorn, W.G.; Balk, P.A.; Van Houwelingen, A.M.; Hoeberichts, F.A.; Hall, R.D.; Vorst, O.; Van Der School, C.; Van Wordragen, M.F. Gene expression during anthesis and senescence in Iris flowers. *Plant Mol. Biol.* **2003**, *53*, 845–863. [[CrossRef](#)] [[PubMed](#)]
- Wagstaff, C.; Malcolm, P.; Rafiq, A.; Leverenz, M.; Griffiths, G.; Thomas, B.; Stead, A.; Rogers, H. Programmed cell death (PCD) processes begin extremely early in Alstroemeria petal senescence. *N. Phytol.* **2003**, *160*, 49–59. [[CrossRef](#)]
- Battelli, R.; Lombardi, L.; Rogers, H.J.; Picciarelli, P.; Lorenzi, R.; Ceccarelli, N. Changes in ultrastructure, protease and caspase-like activities during flower senescence in Lilium longiflorum. *Plant Sci.* **2011**, *180*, 716–725. [[CrossRef](#)] [[PubMed](#)]
- Van Doorn, W.G.; Woltering, E.J. Physiology and molecular biology of petal senescence. *J. Exp. Bot.* **2008**, *59*, 453–480. [[CrossRef](#)]
- Sugiyama, M.; Ito, J.; Aoyagi, S.; Fukuda, H. Endonucleases. *Plant Mol. Biol.* **2000**, *44*, 387–397. [[CrossRef](#)]
- Lers, A.; Khalchitski, A.; Lomaniec, E.; Burd, S.; Green, P.J. Senescence-induced RNases in tomato. *Plant Mol. Biol.* **1998**, *36*, 439–449. [[CrossRef](#)]
- Panavas, T.; LeVangie, R.; Mistler, J.; Reid, P.D.; Rubinstein, B. Activities of nucleases in senescing daylily petals. *Plant Physiol. Biochem.* **2000**, *38*, 837–843. [[CrossRef](#)]
- Perez-Amador, M.A.; Abler, M.L.; De Rocher, E.J.; Thompson, D.M.; Van Hoof, A.; LeBrasseur, N.D.; Lers, A.; Green, P.J. Identification of BFN1, a bifunctional nuclease induced during leaf and stem senescence in Arabidopsis. *Plant Physiol.* **2000**, *122*, 169–179. [[CrossRef](#)]
- Xu, Y.; Hanson, M.R. Programmed cell death during pollination-induced petal senescence in petunia. *Plant Physiol.* **2000**, *122*, 1323–1333. [[CrossRef](#)] [[PubMed](#)]
- Lehmann, K.; Hause, B.; Altmann, D.; Köck, M. Tomato ribonuclease LX with the functional endoplasmic reticulum retention motif HDEF is expressed during programmed cell death processes, including xylem differentiation, germination, and senescence. *Plant Physiol.* **2001**, *127*, 436–449. [[CrossRef](#)] [[PubMed](#)]
- Langston, B.J.; Bai, S.; Jones, M.L. Increases in DNA fragmentation and induction of a senescence-specific nuclease are delayed during corolla senescence in ethylene-insensitive (etr1-1) transgenic petunias. *J. Exp. Bot.* **2005**, *56*, 15–23. [[CrossRef](#)] [[PubMed](#)]
- Lambert, R.; Quiles, F.A.; Gálvez-Valdivieso, G.; Piedras, P. Nucleases activities during French bean leaf aging and dark-induced senescence. *J. Plant Physiol.* **2017**, *218*, 235–242. [[CrossRef](#)] [[PubMed](#)]
- Lers, A.; Lomaniec, E.; Burd, S.; Khalchitski, A. The characterization of LeNUC1, a nuclease associated with leaf senescence of tomato. *Physiol. Plant* **2001**, *112*, 176–182. [[CrossRef](#)]
- Canetti, L.; Lomaniec, E.; Elkind, Y.; Lers, A. Nuclease activities associated with dark-induced and natural leaf senescence in parsley. *Plant Sci.* **2002**, *163*, 873–880. [[CrossRef](#)]

27. Sakamoto, W.; Takami, T. Nucleases in higher plants and their possible involvement in DNA degradation during leaf senescence. *J. Exp. Bot.* **2014**, *65*, 3835–3843. [[CrossRef](#)] [[PubMed](#)]
28. Farage-Barhom, S.; Burd, S.; Sonogo, L.; Perl-Treves, R.; Lers, A. Expression analysis of the BFN1 nuclease gene promoter during senescence, abscission, and programmed cell death-related processes. *J. Exp. Bot.* **2008**, *59*, 3247–3258. [[CrossRef](#)]
29. Panavas, T.; Pikula, A.; Reid, P.D.; Rubinstein, B.; Walker, E.L. Identification of senescence-associated genes from daylily petals. *Plant Mol. Biol.* **1999**, *40*, 237–248. [[CrossRef](#)] [[PubMed](#)]
30. Narumi, T.; Sudo, R.; Satoh, S. Cloning and characterization of a cDNA encoding a putative nuclease related to petal senescence in carnation (*Dianthus caryophyllus* L.) flowers. *J. Jpn. Soc. Hortic. Sci.* **2006**, *75*, 323–327. [[CrossRef](#)]
31. Bai, S.; Willard, B.; Chapin, L.J.; Kinter, M.T.; Francis, D.M.; Stead, A.D.; Jones, M.L. Proteomic analysis of pollination-induced corolla senescence in petunia. *J. Exp. Bot.* **2010**, *61*, 1089–1109. [[CrossRef](#)]
32. Triques, K.; Sturbois, B.; Gallais, S.; Dalmais, M.; Chauvin, S.; Clepet, C.; Aubourg, S.; Rameau, C.; Caboche, M.; Bendahmane, A. Characterization of *Arabidopsis thaliana* mismatch specific endonucleases: Application to mutation discovery by TILLING in pea. *Plant J.* **2007**, *51*, 1116–1125. [[CrossRef](#)]
33. Machlis, L.; Torrey, J.G. *Plants in Action: A Laboratory Manual of Plant Physiology*; Freeman: San Francisco, CA, USA, 1956.
34. Quijia Pillajo, J.O.; Chapin, L.J.; Jones, M.L. Senescence and abiotic stress induce expression of autophagy-related genes in petunia. *J. Am. Soc. Hortic. Sci.* **2018**, *143*, 154–163. [[CrossRef](#)]
35. Jones, M.L.; Chaffin, G.S.; Eason, J.R.; Clark, D.G. Ethylene-sensitivity regulates proteolytic activity and cysteine protease gene expression in petunia corollas. *J. Exp. Bot.* **2005**, *56*, 2733–2744. [[CrossRef](#)] [[PubMed](#)]
36. Chapin, L.J.; Moon, Y.; Jones, M.L. Downregulating a type I metacaspase in petunia accelerates flower senescence. *J. Am. Soc. Hortic. Sci.* **2017**, *142*, 405–414. [[CrossRef](#)]
37. Chapin, L.J.; Jones, M.L. Ethylene regulates phosphorus remobilization and expression of a phosphate transporter (PhPT1) during petunia corolla senescence. *J. Exp. Bot.* **2009**, *60*, 2179–2190. [[CrossRef](#)] [[PubMed](#)]
38. Liu, Y.; Schiff, M.; Marathe, R.; Dinesh-Kumar, S.P. Tobacco Rar1, EDS1 and NPR1/NIM1 like genes are required for N-mediated resistance to tobacco mosaic virus. *Plant J.* **2002**, *30*, 415–429. [[CrossRef](#)] [[PubMed](#)]
39. Chen, J.C.; Jiang, C.Z.; Gookin, T.E.; Hunter, D.A.; Clark, D.G.; Reid, M.S. Chalcone synthase as a reporter in virus-induced gene silencing studies of flower senescence. *Plant Mol. Biol.* **2004**, *55*, 521–530. [[CrossRef](#)]
40. Broderick, S.R.; Jones, M.L. An optimized protocol to increase virus-induced gene silencing efficiency and minimize viral symptoms in Petunia. *Plant Mol. Biol. Rep.* **2014**, *32*, 219–233. [[CrossRef](#)]
41. Nielsen, H.; Engelbrecht, J.; Brunak, S.; VonHeijne, G. Identification of prokaryotic and eukaryotic signal peptides and prediction of their cleavage sites. *Protein Eng.* **1997**, *10*, 1–6. [[CrossRef](#)] [[PubMed](#)]
42. Emanuelsson, O.; Nielsen, H.; Brunak, S.; Von Heijne, G. Predicting subcellular localization of proteins based on their N-terminal amino acid sequence. *J. Mol. Biol.* **2000**, *300*, 1005–1016. [[CrossRef](#)]
43. Trivellini, A.; Ferrante, A.; Vernieri, P.; Carmassi, G.; Serra, G. Spatial and temporal distribution of mineral nutrients and sugars throughout the lifespan of *Hibiscus rosa-sinensis* L. flower. *Cent. Eur. J. Biol.* **2011**, *6*, 365–375. [[CrossRef](#)]
44. Lesniewicz, K.; Karlowski, W.M.; Pienkowska, J.R.; Krzykowski, P.; Poreba, E. The plant s1-like nuclease family has evolved a highly diverse range of catalytic capabilities. *Plant Cell Physiol.* **2013**, *54*, 1064–1078. [[CrossRef](#)] [[PubMed](#)]
45. Ko, C.Y.; Lai, Y.L.; Lin, C.H.; Chen, Y.T.; Chen, L.F.; Lin, T.Y.; Shaw, S.F. *Arabidopsis* ENDO2: It's catalytic role and requirement of N-glycosylation for function. *J. Agric. Food Chem.* **2012**, *60*, 5169–5179. [[CrossRef](#)]
46. Givaty-Rapp, Y.; Yadav, N.S.; Khan, A.; Grafi, G. S1-type endonuclease 2 in dedifferentiating *Arabidopsis* protoplasts: Translocation to the nucleus in senescing protoplasts is associated with de-glycosylation. *PLoS ONE* **2017**, *12*, 1–16. [[CrossRef](#)]
47. Grbić, V.; Bleecker, A.B. Ethylene regulates the timing of leaf senescence in *Arabidopsis*. *Plant J.* **1995**, *8*, 595–602. [[CrossRef](#)]
48. Matallana-Ramirez, L.P.; Rauf, M.; Farage-Barhom, S.; Dortay, H.; Xue, G.P.; Dröge-Laser, W.; Lers, A.; Balazadeh, S.; Mueller-Roeber, B. NAC transcription factor ORE1 and Senescence-Induced Bifunctional Nuclease1 (BFN1) constitute a regulatory cascade in *Arabidopsis*. *Mol. Plant* **2013**, *6*, 1438–1452. [[CrossRef](#)] [[PubMed](#)]
49. Lambert, R.; Quiles, F.A.; Cabello-Díaz, J.M.; Piedras, P. Purification and identification of a nuclease activity in embryo axes from French bean. *Plant Sci.* **2014**, *224*, 137–143. [[CrossRef](#)]
50. Lambert, R.; Cabello-Díaz, J.M.; Quiles, F.A.; Piedras, P. Identification of nucleases related to nutrient mobilization in senescing cotyledons from French bean. *Acta Physiol. Plant.* **2016**, *38*, 1–13. [[CrossRef](#)]
51. Otegui, M.S.; Noh, Y.S.; Martínez, D.E.; Vila Petroff, M.G.; Staehelin, L.A.; Amasino, R.M.; Guimnet, J.J. Senescence-associated vacuoles with intense proteolytic activity develop in leaves of *Arabidopsis* and soybean. *Plant J.* **2005**, *41*, 831–844. [[CrossRef](#)]
52. Rogers, H.J. From models to ornamentals: How is flower senescence regulated? *Plant Mol. Biol.* **2013**, *82*, 563–574. [[CrossRef](#)]
53. Thomas, H. Senescence, ageing and death of the whole plant. *N. Phytol.* **2013**, *197*, 696–711. [[CrossRef](#)] [[PubMed](#)]
54. Wulster, G.; Sacalis, J.; Janes, H.W. Senescence in Isolated Carnation Petals. *Plant Physiol.* **1982**, *70*, 1039–1043. [[CrossRef](#)] [[PubMed](#)]
55. Baumgartner, B.; Kende, H.; Matile, P. Ribonuclease in Senescing Morning Glory: Purification and Demonstration of de Novo Synthesis. *Plant Physiol.* **1975**, *55*, 734–737. [[CrossRef](#)]
56. Aoyagi, S.; Sugiyama, M.; Fukuda, H. BEN1 and ZEN1 cDNAs encoding S1-type DNases that are associated with programmed cell death in plants. *FEBS Lett.* **1998**, *429*, 134–138. [[CrossRef](#)]

57. Krupinska, K.; Hausstühl, K.; Schäfer, A.; Van der Kooij, T.A.W.; Leckband, G.; Lörz, H.; Falk, J. A novel nucleus-targeted protein is expressed in barley leaves during senescence and pathogen infection. *Plant Physiol.* **2002**, *130*, 1172–1180. [[CrossRef](#)]
58. Taylor, C.B.; Bariola, P.A.; Delcardayre, S.B.; Raines, R.T.; Green, P.J. RNS2: A Senescence-Associated RNase of Arabidopsis that Diverged from the S-RNases before Speciation. *Proc. Natl. Acad. Sci. USA* **1993**, *90*, 5118–5122. [[CrossRef](#)] [[PubMed](#)]
59. Kock, M.; Stenzel, I.; Zimmer, A. Tissue-specific expression of tomato Ribonuclease LX during phosphate starvation-induced root growth. *J. Exp. Bot.* **2006**, *57*, 3717–3726. [[CrossRef](#)] [[PubMed](#)]
60. Liang, L.; Lai, Z.; Ma, W.; Zhang, Y.; Xue, Y. AhSL28, a senescence- and phosphate starvation-induced S-like RNase gene in *Antirrhinum*. *Biochim. Biophys. Acta-Gene Struct. Expr.* **2002**, *1579*, 64–71. [[CrossRef](#)]



Article

Genomic Resource Development for Hydrangea (*Hydrangea macrophylla* (Thunb.) Ser.)—A Transcriptome Assembly and a High-Density Genetic Linkage Map

Xingbo Wu ^{1,2}, Amanda M. Hulse-Kemp ^{1,3}, Phillip A. Wadl ⁴, Zach Smith ⁵, Keithanne Mockaitis ⁶, Margaret E. Staton ⁷, Timothy A. Rinehart ⁸ and Lisa W. Alexander ^{2,*}

¹ Department of Crop and Soil Sciences, North Carolina State University, Raleigh, NC 27695, USA; xwu33@ncsu.edu (X.W.); amanda.hulse-kemp@usda.gov (A.M.H.-K.)

² USDA-ARS, U.S. National Arboretum, Floral and Nursery Plants Research Unit, Otis L. Floyd Nursery Research Center, McMinville, TN 37110, USA

³ USDA-ARS, Genomics and Bioinformatics Research Unit, Raleigh, NC 27695, USA

⁴ USDA-ARS, U. S. Vegetable Laboratory, Charleston, SC 29414, USA; phillip.wadl@usda.gov

⁵ Beckman Coulter Life Sciences, Indianapolis, IN 46268, USA; ZSMITH@beckman.com

⁶ Root Cause Scientific Inc., Indianapolis, IN 46268, USA; km13@cornell.edu

⁷ Department of Entomology and Plant Pathology, University of Tennessee, Knoxville, TN 37996, USA; mstaton1@utk.edu

⁸ USDA-ARS, Crop Production and Protection, Beltsville, MD 20705, USA; tim.rinehart@usda.gov

* Correspondence: lisa.alexander@usda.gov

Citation: Wu, X.; Hulse-Kemp, A.M.; Wadl, P.A.; Smith, Z.; Mockaitis, K.; Staton, M.E.; Rinehart, T.A.; Alexander, L.W. Genomic Resource Development for Hydrangea (*Hydrangea macrophylla* (Thunb.) Ser.)—A Transcriptome Assembly and a High-Density Genetic Linkage Map. *Horticulturae* **2021**, *7*, 25. <https://doi.org/10.3390/horticulturae7020025>

Academic Editor: Johan Van Huylbroeck
Received: 11 January 2021
Accepted: 2 February 2021
Published: 5 February 2021

Publisher's Note: MDPI stays neutral with regard to jurisdictional claims in published maps and institutional affiliations.

Abstract: Hydrangea (*Hydrangea macrophylla*) is an important ornamental crop that has been cultivated for more than 300 years. Despite the economic importance, genetic studies for hydrangea have been limited by the lack of genetic resources. Genetic linkage maps and subsequent trait mapping are essential tools to identify and make markers available for marker-assisted breeding. A transcriptomic study was performed on two important cultivars, Veitchii and Endless Summer, to discover simple sequence repeat (SSR) markers and an F₁ population based on the cross 'Veitchii' × 'Endless Summer' was established for genetic linkage map construction. Genotyping by sequencing (GBS) was performed on the mapping population along with SSR genotyping. From an analysis of 42,682 putative transcripts, 8780 SSRs were identified and 1535 were validated in the mapping parents. A total of 267 polymorphic SSRs were selected for linkage map construction. The GBS yielded 3923 high quality single nucleotide polymorphisms (SNPs) in the mapping population, resulting in a total of 4190 markers that were used to generate maps for each parent and a consensus map. The consensus linkage map contained 1767 positioned markers (146 SSRs and 1621 SNPs), spanned 1383.4 centiMorgans (cM), and was comprised of 18 linkage groups, with an average mapping interval of 0.8 cM. The transcriptome information and large-scale marker development in this study greatly expanded the genetic resources that are available for hydrangea. The high-density genetic linkage maps presented here will serve as an important foundation for quantitative trait loci mapping, map-based gene cloning, and marker-assisted selection of *H. macrophylla*.

Keywords: *Hydrangea macrophylla*; SSR; SNP; linkage map



Copyright: © 2021 by the authors. Licensee MDPI, Basel, Switzerland. This article is an open access article distributed under the terms and conditions of the Creative Commons Attribution (CC BY) license (<https://creativecommons.org/licenses/by/4.0/>).

1. Introduction

Hydrangea is one of the most widely cultivated plants in the horticulture industry and is grown for floriculture, nursery, landscape, and cut flower markets. Introduced as a cultivated ornamental into Europe from Asia around 1788 by Sir Joseph Banks [1], *Hydrangea macrophylla* is now represented by more than 500 extant cultivars in the United States and Europe. Among the twenty-three *Hydrangea* species that are recognized, less than half are common in cultivation and the most economically important among these by far is *H. macrophylla* [2]. In recent years, hydrangeas have become a dominant product

in the flowering shrub market in the United States (US), worth 91.3 million US dollars in 2014 [3]. The economic value has stimulated an increasing demand for specialized hydrangeas, such as the remontant type (blooming more than once per year), and thus has energized hydrangea breeding in the US.

As a typical woody plant, hydrangea breeding requires a long generation time in a conventional breeding process. Traits that are most important to *H. macrophylla* breeding are unique inflorescence architecture and flower color variation for all markets, floral induction (reblooming for landscape use and year-round floral production for florist's hydrangeas), drought and sun tolerance in landscape breeding, and powdery mildew resistance for greenhouse and landscape grown plants. Selections in hydrangea breeding historically have focused mainly on novel flower types that can be chosen in the first generation for incremental improvements [4]. An additional, current goal of hydrangea breeding is to introduce resistance to existing and emerging diseases and pests for nursery producers [5]. As a highly heterozygous horticultural crop, hydrangea breeding is mainly based on phenotypic selection, which is a long and difficult process, particularly when coupled with long generation times [4].

Conventional breeding can be improved and generation interval times can be reduced by incorporating marker-assisted selection (MAS) or marker-assisted breeding. One prerequisite of MAS is the development of genomic resources, such as genetic markers, that can be used to identify markers linked to the traits of interest to segregate populations through genetic mapping analyses [6]. Codominant markers such as microsatellites (simple sequence repeats, SSRs) and single nucleotide polymorphisms (SNPs) are markers of choice for such an application as they occur randomly throughout the genome in relatively abundant levels that can allow for estimation of additive and dominance allelic effects. However, little genetic information is currently known for *H. macrophylla*. Development of genetic information has been difficult given its highly heterozygous genomic composition, differing ploidy levels with base chromosome number ($n = 18$), and large diploid genome size (~2.2 Gbp) [7].

A previous transcriptomic study focusing on aluminum stress of hydrangea discovered thousands of SSRs; however, none were validated [8,9]. Only 39 SSR markers were available for hydrangea through 2010 [10–12]. Even with 226 newly developed SSR markers in 2018 [13], the total number of SSRs is still under 300, which is too low for most genetic studies in hydrangea. The insufficient number of molecular markers and unavailability of any genotyping platform has largely hampered the ability to perform linkage and association mapping for molecular-trait dissection studies in hydrangea. To date, only one linkage map was reported in hydrangea, but with low SSR marker density [13], which is much lower than the number of linkage maps reported in roses (eight) [14], peony (three) [15], and chrysanthemum (three) [16]. In addition to providing tools for MAS, high-density linkage maps could also be used to assist genome assembly in scaffolding and quality assessments [17]. Further marker development and high-density genetic linkage maps are needed for potential genetic improvement as well as genomic studies in hydrangea.

Transcriptome sequencing is an efficient and economical way to capture sequences of the genic regions in plants with complex, large genomes. Specialty crops such as *H. macrophylla* benefit from this approach, which creates massive expression datasets that include candidate coding sequences that can be used to produce an abundance of markers. Recent advances in the next-generation sequencing (NGS) methods have also made detection of SNPs, the most abundant marker type in the largest numbers, possible through high-throughput sequence-based genotyping. Sequence-based genotyping is a powerful tool for plant breeding and is especially helpful for those plant species that lack genome information [18]. Genotyping by sequencing (GBS) allows for the detection and genotyping of tens of thousands of SNPs in many individuals simultaneously, resulting in an unparalleled cost per data point when screening for codominant polymorphisms in large panels and for constructing highly saturated genetic maps [19]. GBS has been employed for linkage mapping in woody ornamentals such as roses [20] and apples [21]. In hydrangea,

it has been used for genetic diversity [22] and association mapping studies [23,24], but no linkage map was constructed with this method.

Genomic resource development is urgently needed for future genetic mapping and quantitative genetics studies in *H. macrophylla*. Genomics approaches to hydrangea breeding offer opportunities to make immediate advances in trait improvement, especially for complex traits such as environmental tolerance and disease resistance. The objectives of this study were to generate genomic resources through transcriptome sequencing and genotyping by sequencing for *H. macrophylla*, and to demonstrate the utility of these resources with a high-density linkage map.

2. Materials and Methods

2.1. Plant Materials and Sample Preparation

Two important hydrangea cultivars, Veitchii and Endless Summer, were chosen as representatives for genomic resource development. 'Veitchii' is a lacecap cultivar used for the cut flower market and is tolerant to powdery mildew and *Cercospora* leaf spot but only flowers once a year (once-flowering), while 'Endless Summer' (formerly also identified as 'Bailmer') is a mophead cultivar which can flower twice or more per year (remontant) and is popular in the floriculture market but susceptible to powdery mildew [25,26]. In order to get broader representation in gene expression and better coverage of the genome, four tissue types (leaves, stems, buds, and open flowers) were collected for transcriptome sequencing from three year old 'Veitchii' and 'Endless Summer' plants grown in three gallon plastic containers (24.1 × 27.9 × 27.9 cm) containing composted pine bark medium under drip irrigation and 50% shade at the United States Department of Agriculture Agricultural Research Service (USDA-ARS) Thad Cochran Southern Horticultural Laboratory, Poplarville, MS, USA (30° 50' 02.68" N 89° 32' 50.54" W) (Figure 1). The tissues were collected in spring 2010 and immediately frozen in liquid nitrogen and stored at −80 °C. Total RNA was isolated from the tissues using the RNeasy Plant Mini Kit (Qiagen; Valencia, CA, USA) according to the manufacturer's instructions. The isolated RNA was treated with DNase I (New England BioLabs; Ipswich, MA, USA). RNA quantity and quality were determined by fluorimetry and by microfluidic electrophoresis (BioAnalyzer, Agilent; Santa Clara, CA, USA).

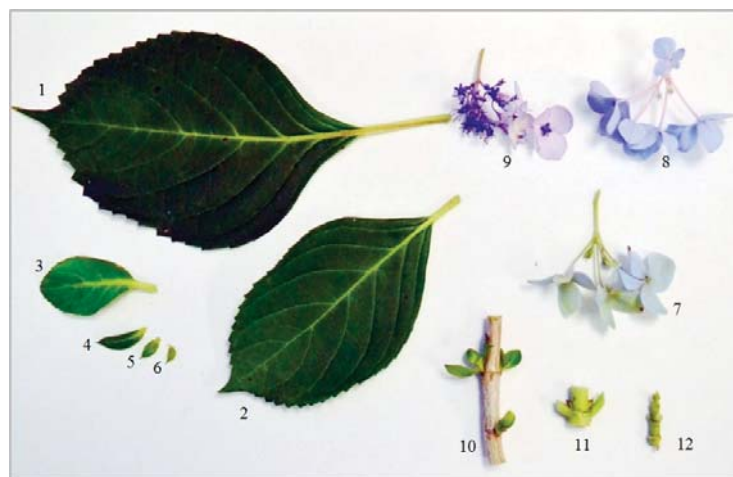


Figure 1. Example of tissue types sampled from a single plant of 'Veitchii' and 'Endless Summer' for transcriptome sequencing. 1–6: leaf tissues collected at different developmental stages. 7–9: flower tissues collected at different flowering times; 10–12: stem tissues collected from different positions. Bud tissues are not listed in this figure.

For genotyping by sequencing, an F₁ mapping population comprising 90 individuals, as well as the two parents, 'Veitchii' and 'Endless Summer', were used to construct a genetic linkage map. Trifoliate leaves of both parents and the F₁ population were collected into 2 mL Eppendorf tubes with lysate buffer and ground in a homogenizer (FastPrep-24 5G; MP Biomedicals, Santa Ana, CA, USA). Genomic DNA was isolated from the lysed tissue using the DNeasy Plant Mini Kit, followed by RNase treatment (Qiagen, Valencia, CA, USA). Nucleic acid was evaluated in 1% agarose gel and quantified using a spectrometer (NanoDrop 2000; Thermo Scientific, Wilmington, DE, USA). Enzyme activity was evaluated using 6 U of EcoRI on 300 ng DNA of eight randomly selected samples for 2 h at 37 °C and separation using gel electrophoresis on a 1% agarose gel. A lyophilized aliquot of 1.5 mg DNA was prepared for each sample for subsequent SSR genotyping and GBS.

2.2. Transcriptome Sequencing, Assembly, and Analyses

Total RNA from each cultivar was pooled in approximately equimolar amounts prior to construction of a customized cDNA library enriched for polyA and 5'cap containing transcripts, with the double-stranded cDNA library intermediate partially normalized by DSN treatment (Evrogen, Moscow, Russia) to reduce representation of the high abundance transcripts. Prior to adaptor ligation, the library was sheared by nebulization to optimize template length distribution for the sequencing system and assessed on a Bioanalyzer DNA7500 chip (Agilent; Santa Clara, CA, USA). According to the manufacturer (Roche/454 Sequencing, Branford, CT, USA) emulsion PCR was performed and the library sequenced to below saturation on a GS FLX Titanium PicoTitr™ plate to 800 cycles.

2.3. Transcriptome Assembly

Sequence reads were cleaned of adaptor sequences [27] and assembled into isotigs using NEWBLER v2.3 GS De Novo Assembler [28] (Roche 454 Sequencing, Branford, CT, USA) with default parameters for cDNA (40 bp overlap; 90% identity). TransDecoder [29] was used to predict open reading frames (ORFs) from the isotig assembly. Predictions were improved by including the Pfam matching information. The matches were generated by comparing the isotigs to the Pfam database version 3.1b1 [30] with HMMer hmmscan version 3.1b2 ("HMMER" 2016) [31]. The nucleotide sequences of the isotigs were compared to the Uniprot Swissprot database and the plant proteins from Uniprot Trembl [32] with BLAST version 2.2.26. Hits were filtered at an e-value of 0.00001. InterProScan version 5.4–47.0 [33] was run for all protein sequences. Assemblies were assessed for completeness with BUSCO version 1.2 and the early access plant dataset [34]. Raw sequence data were uploaded to NCBI under BioProject PRJNA661039.

2.4. EST-SSR Identification and Genotyping

The assembled *H. macrophylla* transcriptome was searched for microsatellite motifs or SSRs using the program SSR Finder [35]. For the searches and comparison of microsatellites, SSRs were defined as being mononucleotide repeats (MNRs) with ≥ 10 repeats and di- (DNRs), tri- (TNRs), tetra- (TTNRs), penta-, and hexanucleotide repeats ≥ 6 repeats; criteria for composite SSRs was an interval of bases ≤ 100 bp.

Primers were designed and used to amplify SSR loci in genomic DNA from 'Veitchii' and 'Endless Summer' using a modified three-primer protocol originally described in Waldbieser et al. [36]. In summary, DNA was extracted from 1 cm² pieces of fresh leaf tissue using Qiagen Plant Mini Kit (Qiagen). Genomic DNA was quantified using a NanoDrop Spectrophotometer (Nanodrop Technologies, Wilmington, DE, USA). Forward primers were 5' tailed with the sequence 5'-CAGTTTTCCCAGTCACGAC-3' to permit product labeling, and reverse primers were tailed at the 5' end with the sequence 5'-GTTT-3' to promote non-template adenylation [37]. A primer, 5'-CAGTTTTCCCAGTCACGAC-3', was labeled with 6-carboxy-fluorescein (FAM) (Integrated DNA Technologies, Coralville, IA, USA) and added to the amplification reaction, which included Advantage2 Taq DNA Polymerase (Clontech, Mountain View, CA, USA) according to previously published proto-

cols [6]. Fluorescence-labeled PCR fragments were visualized by automated capillary gel electrophoresis on an ABI3100-Avant (Applied Biosystems, Foster City, CA, USA) using a ROX-500 size standard. GeneMapper version 4.0 (Applied Biosystems) was used to recognize and size peaks. Loci that produced high quality data, that were polymorphic between 'Veitchii' and 'Endless Summer', and that produced allele combinations compatible with the pseudo test cross strategy were selected for linkage mapping with the mapping population.

2.5. Genotyping by Sequencing and SNP Identification

GBS was performed at the University of Wisconsin-Madison Biotechnology Center (UWBC; Madison, WI, USA) following the protocols described in Elshire et al. [19]. The 4-base cutter enzyme, ApeKI (G * CWGC), was found to be efficient in producing fragments that were < 500 bp in sample DNA digestion and was selected for library preparation. The digested DNA fragments were then ligated with optimal barcodes and common adapters followed by standard PCR. Single-end sequencing (100 bp) of the library was performed on the Illumina HiSeq 2000 (Illumina Inc. San Diego, CA, USA). Raw sequence data for the total library were uploaded to NCBI under BioProject PRJNA656177.

The reference-free Java program TASSEL-UNEAK [38] was utilized for GBS data analysis given there was no reference genome available for *H. macrophylla*. Briefly, the barcodes were first removed from the raw sequence reads. The remaining sequences were analyzed by the TASSEL-UNEAK pipeline to further produce 64 bp length sequence tags and aligned with each other based on unique sequence tags. SNP discovery was performed directly within pairs of matched sequence tags and filtered through network analysis. The minimum tag count required for output was set to 5. To reduce the sequencing error, the error tolerance rate was set to 0.03. Raw SNPs were filtered to ensure high-quality genotype calling using Trait Analysis by Association, Evolution and Linkage (TASSEL) version 5.0 [39]. SNPs that had more than 10% missing data and minimum minor allele frequency (MAF) of 0.05 were excluded from the dataset, individuals that possessed more than 20% missing data were filtered out. SNPs that were polymorphic between the parents of the mapping population were retained for linkage mapping.

2.6. Linkage Map Construction

The allele data for all selected markers were tested for segregation distortion and genotypic data similarities. The linkage map was created using the cross-pollinated (CP) model in JoinMap v5.0 [40]. In the case of SSRs, five segregation types ($lm \times ll$, $nn \times np$, $hk \times hk$, $ef \times eg$, and $ab \times cd$) were used based on the software instructions, while three segregation types ($lm \times ll$, $nn \times np$, and $hk \times hk$) were used to code SNPs. Distortion of each marker from their expected frequencies was observed by a goodness-of-fit (Chi-square) test. Identical progenies, identical markers, and severely distorted loci ($p < 0.001$) were observed and excluded from mapping construction. Linkage groups (LGs) were constructed using the regression mapping method with default parameters. The independence LOD (logarithm of the odds) score was set from 2 to 15 for grouping purposes and groups were selected at the LOD score that produced group numbers equivalent to the number of chromosomes. Map distances within individual linkage groups were converted to centiMorgans (cM) using the Kosambi mapping function.

The two-step strategy was used to construct the linkage map. First, alleles segregating only in the female ($lm \times ll$) or male ($nn \times np$) parents were separated as individual datasets using the embed grouping function. Individual maps for each of the parents were constructed using the parameters mentioned above. For consensus map construction, the maternal and paternal maps were integrated by combining linkage groups sharing the same SNP alleles classified as ($hk \times hk$). The map construction, marker order, and distance for each LG in the consensus map were calculated using the same parameters as those for the parental maps. The consensus map was graphically represented using MapChart V2.2 [41].

3. Results

3.1. Transcriptome Analysis and EST-SSR Identification

The hydrangea libraries were constructed from normalized cDNA and generated a total of 1.17 million reads (444 Mb) that were de novo assembled into 42,682 isotigs, putative transcripts, comprising 24,201 isogroups, and putative unigene sets of transcripts. Open reading frames (ORFs) were found in 42,620 isotigs (>99%). Functional annotation of these data was performed using BLAST to publicly available databases. This resulted in matches for 67% of the isotigs against the SwissProt database [42] and for 85% of the isotigs against plant proteins from the TrEMBL database [32]. InterProScan [33] was used to gain further functional information in protein sequences derived from the ORFs, estimating 199,709 additional putative functions for 34,389 of the isotigs. InterProScan also yielded 171,059 gene ontology (GO) term [43] assignments with assignments of 1679 unique terms to 21,818 isotigs. To assess the completeness of the transcriptome, the software BUSCO was utilized. Based on the analysis, the *H. macrophylla* assembly includes coverage of 92% of the 956 BUSCO conserved genes (429 as complete single copy transcripts, 358 as complete but multiple transcripts, and 91 as fragmented genes).

EST-SSR development identified 30,169 new SSR loci for *H. macrophylla*. Primers could be designed for 5986 loci and 2794 loci in the contigs and singletons (non-assembled reads), respectively. The total number of new SSR loci identified was 8780 (Supplementary Table S1). The majority of these loci contained tri-nucleotide repeats (52.82%) as would be expected for coding regions. The next largest class of repeat motifs was di-nucleotide (37.15%) (Table 1). The remaining (<10%) motifs were larger than tri-nucleotides.

Table 1. The length and distribution frequency of simple sequence repeat (SSR) types in *H. macrophylla*.

Type \ Length	4	5	6	7	8	10	>10	Total	Distribution Frequency (%)
Dinucleotide	0	0	1040	692	861	395	274	3262	37.15
Trinucleotide	2675	997	434	246	202	60	24	4638	52.82
Tetranucleotide	226	57	23	15	9	2	0	332	3.78
Pentanucleotide	125	25	6	5	0	0	0	161	1.83
Hexanucleotide	241	93	29	12	6	0	0	381	4.34
Other	6	0	0	0	0	0	0	6	0.07

3.2. EST-SSR Genotyping

A selection of the identified SSR loci (1535) were evaluated with genomic DNA from ‘Veitchii’ and ‘Endless Summer’. Of these, 1226 produced high-quality data, but 35% of those loci were monomorphic and therefore not suitable for genetic mapping purposes. A total of 267 SSRs were selected for genetic mapping of the F₁ population. Among them, 115 (43.1%) showed maternal segregation (lm × ll) and 98 (36.7%) showed paternal segregation (nn × np), while 53 (19.9%) were heterozygous in both parents (44 with four distinct alleles, ab × cd type, and 9 with 3 alleles, ef × eg type), and one (0.3%) was partially informative as both parents had the same heterozygous genotype (hk × hk). Information of the 267 markers are highlighted in Supplementary Table S1.

3.3. GBS-SNP Discovery

The GBS library generated an average of 2.7 million reads per F₁ progeny and the TASSEL-UNEAK pipeline analysis resulted in 376,153 raw SNPs. By removing SNPs that showed MAF < 0.05 and more than 10% missing data, the total SNP number was reduced to 12,214. Extra criteria were also used to assure the SNP quality as follows: SNPs that were missing in either parent or homozygous in both parents were removed from further analyses. Furthermore, SNPs showing segregation patterns in the progeny that were not in agreement with the parental genotypes were discarded from the mapping process. Finally, a group of 3923 high quality informative SNPs were obtained, consisting of 1160 SNPs (29.6%) segregating in the female parent (lm × ll), 881 SNPs (22.5%) segregating in the

male parent (nn × np), and 1882 SNPs (47.9%) that were heterozygous and segregating in both parents (hk × hk). The SNP sequence information is presented in Supplementary Dataset S1.

3.4. Construction of Genetic Linkage Maps

A total of 4190 high quality markers were used for linkage mapping, including 267 SSR markers developed from transcriptome sequencing and 3923 SNP markers developed from GBS (Supplementary Table S2). Of them, 472 markers were identical to other markers and were excluded from further analyses. No identical samples were found in the mapping population.

The maternal and paternal maps were determined at LOD of 8, with each map containing 18 LGs. The maternal map consisted of 1686 markers with a total genetic length of 1396.9 cM, while the paternal map consisted of 1396 markers with a total genetic length of 1400.8 cM (Supplementary Table S3). The maternal and paternal map visualizations can be found in Supplementary Figure S1. Generally, the paternal map tended to have smaller sizes for each of the linkage groups, which resulted in an overall smaller size than the maternal and consensus maps. When comparing the markers of individual LGs between consensus map and parent maps, the maternal map contributed most of the markers on LGs 5, 8, 9, 10, 14, 15, and 17 of the consensus map, while the paternal map contributed largely to LGs 2 and 7 of the consensus map. The LGs 1, 3, 4, 6, 11, 12, 13, 16, and 18 of the consensus map had a similar number of markers derived from the corresponding LGs of each parent map.

A consensus map was generated that contained a total of 1767 markers, consisting of 1621 SNP and 146 SSR markers. The total length of the consensus map was 1383.4 cM with LG 14 (108.5 cM) being the largest group and LG 9 (39.8 cM) being the smallest group (Table 2). The number of markers per linkage group varied from 152 (LG 5) to 49 (LG 6), with an average of 98 markers per linkage group. Most LGs were made of both SNP and SSR markers, with LG 17 being an exception and only containing SNPs. Four large gaps, that were more than 10 cM, were observed on LG 8 (10.0 cM), LG 12 (11.5 cM), LG 13 (13.5 cM), and LG 17 (11.5 cM). Overall, the average distance between markers was 0.8 cM. The distribution of SNPs and SSRs on consensus map LGs is shown in Figure 2.

Table 2. Summary of the *Hydrangea* consensus map.

Linkage Group (LG)	Marker Count (#)	SNP Count (#)	SSR Count (#)	Length (cM)	Average Marker Interval (cM)	Largest Gap (cM)
1	77	70	7	71.0	0.9	5.9
2	93	83	10	75.0	0.8	6.3
3	120	111	9	74.7	0.6	6.4
4	72	65	7	72.7	1.0	6.2
5	152	138	14	84.9	0.6	3.0
6	49	49	0	45.6	0.9	4.9
7	125	109	16	98.1	0.8	4.8
8	101	98	3	76.5	0.8	10.0
9	68	66	2	39.8	0.6	3.0
10	126	114	12	97.9	0.8	6.6
11	108	98	10	80.6	0.7	6.3
12	92	82	10	99.4	1.1	11.5
13	114	101	13	83.2	0.7	13.5
14	86	77	9	108.5	1.3	7.2
15	83	76	7	75.4	0.9	6.1
16	101	97	4	61.7	0.6	5.2
17	78	78	0	77.2	1.0	11.5
18	122	109	13	61.3	0.5	6.4
Total	1767	1621	146	1383.4	0.8	13.5

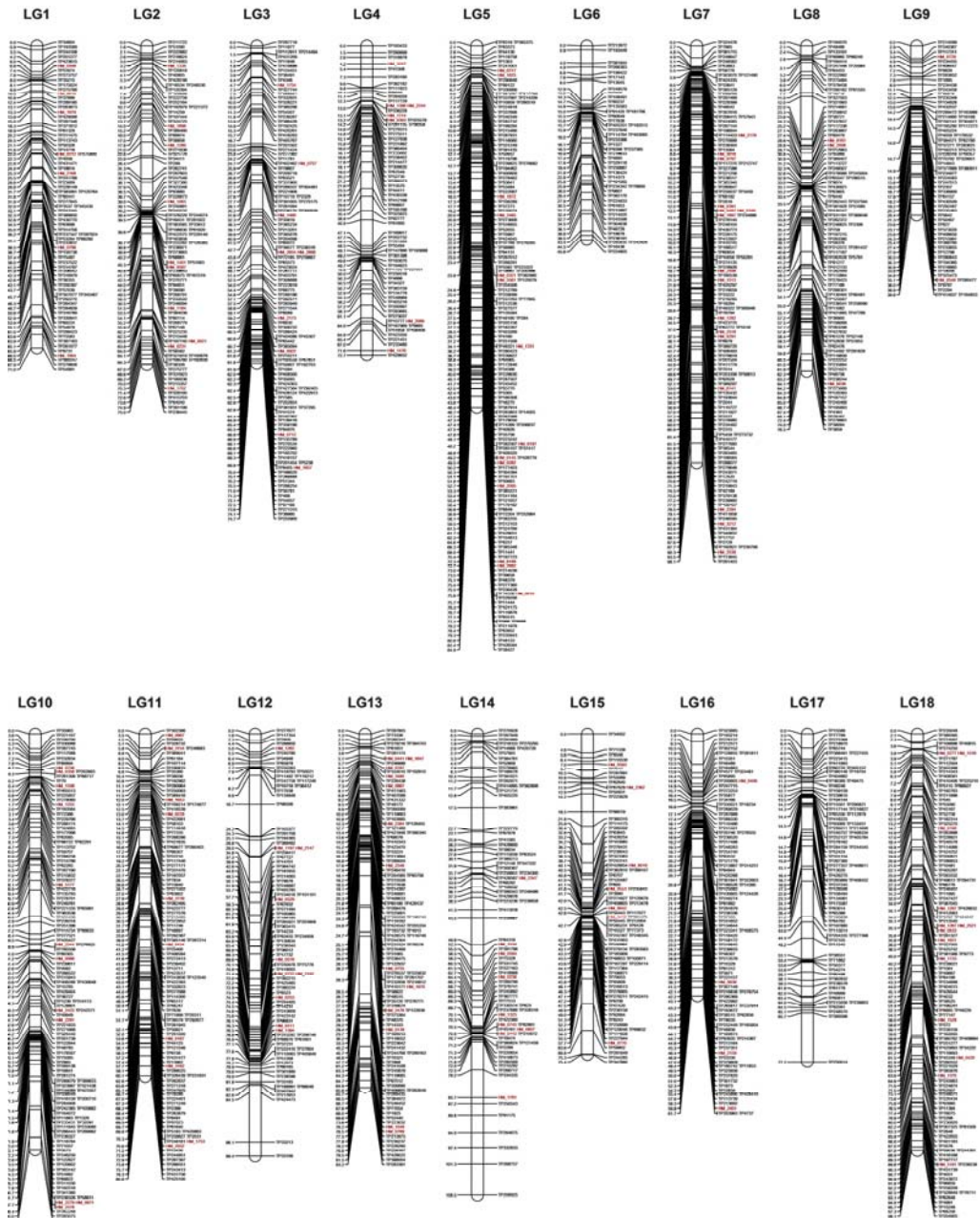


Figure 2. SSR- and single nucleotide polymorphism (SNP)-based high-density genetic consensus linkage map of *H. macrophylla*. A total of 1621 SNP markers (black) and 146 SSR markers (red) are shown in 18 linkage groups.

4. Discussion

Recently, hydrangea has been gaining popularity as an attractive plant for public and private gardens and has become an important ornamental crop for nursery growers. MAS could directly accelerate the breeding of new hydrangea cultivars to meet the consumer needs for new and novel plants [44]. Previous studies on hydrangeas mainly focused on phenotypic evaluations on a physiologic level, which have not led to an acceleration in the hydrangea breeding progress. The lack of genomic resources is a common restraint to molecular breeding in nursery crops, and *H. macrophylla* is no exception to this trend. The rapid development of sequencing technology provides opportunities of marker development not only in a fast and convenient way, but also at low cost. In order to expand the genomic resources of *H. macrophylla*, the present study implemented a transcriptomics study for SSR development, as well as a sequencing-based marker discovery method, GBS, to identify SNP markers in the population developed by crossing these two cultivars for genetic linkage mapping.

A total of 8780 SSRs were identified through the transcriptomics of important hydrangea cultivars, providing the most extensive set of genic sequences so far for this species. Among the identified SSRs, 1535 of them were tested and 267 were found to be polymorphic. SSR markers are robust tools for genetic mapping and molecular breeding applications. The polymorphic SSRs validated in this study significantly increased the availability of useful markers for genetic studies in *H. macrophylla*. In addition, high transferability of SSRs were reported between hydrangea species [10,11,45], so the discovered SSRs here should immediately enable multiple molecular applications in the numerous related species.

GBS offers an efficient way to decipher hydrangea genetics as it can discover SNPs and facilitate genotyping at the same time [19]. GBS has been widely used in popular ornamental crops, such as roses [20], for linkage mapping and subsequent quantitative trait loci (QTL) analyses. In hydrangea, valuable traits such as inflorescence shape, double flower, and recurrent blooming are thought to be quantitatively inherited and suitable for QTL studies to identify markers for MAS [13,23]. The genotyping of two hydrangea cultivars and their F₁ progeny identified 3923 SNP markers through a GBS approach, providing the possibility to facilitate construction of a high-density linkage map for future QTL studies in hydrangea.

Genetic linkage maps are powerful tools to locate genes and QTL regions. As a perennial woody plant, linkage map construction in hydrangea is more complicated than that of homozygous inbred annual plants due to its high heterozygosity and self-incompatibility. F₁ full-sibling populations have become a choice for linkage maps in woody plant species. In this study, an F₁ population was derived from the cross of two important cultivars, Veitchii and Endless Summer, and was used to build the linkage map of hydrangea with 1767 molecular markers. The genetic map contained 18 linkage groups, corresponding to the haploid number of chromosomes identified in the karyotype of diploid *H. macrophylla* (2n = 36) [7]. To date, only one linkage map was reported in hydrangea and it included only 147 SSRs [13]. The linkage map developed in this study consists of 146 SSRs and 1621 SNPs (Table 2), with an average of 98 markers per linkage group, which was far more than the markers used in the previous study [13]. The total length (1383.4 cM) and small marker interval (0.8 cM in average) indicated the high quality of the developed map when compared to the total genetic distance of 980 cM and average marker interval of 6.8 cM in the previously reported map [13]. With more total mapped markers, a larger genetic distance, and the small marker interval, the reported linkage map represents the most saturated genetic map, and will serve as a valuable tool for future genetic and breeding study in hydrangea.

All of the linkage groups identified in the current map consist of both SSR and SNP markers. However, the selected 267 SSRs alone were not sufficient to fully construct a linkage map of hydrangea with the number of linkage groups equal to the number of chromosomes. Studies in woody ornamentals, such as roses [20] and blueberry [46], have

used SSRs as the bridge for crosstalk between genetic maps, thus, more SSRs need to be validated in order to build a high-density consensus map using multiple hydrangea populations. Several regions in one linkage group showed higher density than other regions, which may indicate the uneven marker polymorphism and recombination frequency on a certain chromosome between the mapping parents. This phenomenon has also been observed in grapes [47] and Mei [48]. Though the average genetic distance was 0.8 cM, four gaps located on LG 8, LG 12, LG 13, and LG 17 were found to be larger than 10 cM (Table 2, Figure 2). Large gaps in genetic maps are usually caused by low marker detection and polymorphism in similar chromosome segments of mapping parents or centromeric regions of the chromosome [49], which could be filled by a high-density consensus map construction using different marker types [50].

Despite the substantial value of the industry, technologies available to augment the development of new and improved ornamental plants lag far behind most other agricultural crops. Paucity of genomic resources such as reference genome sequences and comprehensive transcriptome datasets are especially problematic for breeding programs focused on woody ornamentals. Challenges posed by long juvenile periods, obligate or nearly obligate out-crossing breeding systems, inbreeding depression, high heterozygosity, and poor understanding of the genetic control of traits variation are major impediments for effective application of traditional breeding approaches to improve woody ornamental cultivars. Genome-enabled research and breeding programs would greatly accelerate the development of new durable and high-value cultivars. MAS provides the opportunity to assess young plants at the genotype level for multiple traits of interest, which can greatly reduce costs associated with growing the plants to maturity. The mapping parents used in this study, 'Veitchii' and 'Endless Summer', are two important hydrangea cultivars that have contrasting phenotypes in inflorescence type, flowering habits, powdery mildew tolerance, and drought and cold stress, and the markers developed in this study will be useful for interrogation of these traits in the future. Integration of these traits in cultivars through conventional breeding methods has proved difficult but it is likely more feasible through MAS.

5. Conclusions

This study performed large-scale SSR and SNP marker discovery in a F₁ population through transcriptome and genotyping by sequencing for genetic map construct in hydrangea. The consensus linkage map contained 1767 positioned markers (146 SSRs and 1621 SNPs), spanned 1383.4 centiMorgans (cM), and was comprised of 18 linkage groups, with an average mapping interval of 0.8 cM. This study provided not only the most comprehensive marker resource currently available in hydrangea, but also an important foundation for QTL mapping, map-based gene cloning, and MAS of *H. macrophylla*. For traits where variation is readily available in cultivated germplasm, this work defined the strategies for improving hydrangea through conventional breeding. It is these traits where advanced genetic methods such as molecular markers could increase efficiency in long term, high risk projects such as germplasm improvement and new cultivar development.

Supplementary Materials: The following are available online at <https://www.mdpi.com/2311-7524/7/2/25/s1>, Supplemental Figure S1—Genetic linkage maps of maternal ('Veitchii') and paternal ('Endless Summer') *H. macrophylla* cultivars. Supplemental Table S1—Details of 8780 EST-SSR markers developed from the transcriptome of hydrangea cultivars Veitchii and Endless Summer. Supplemental Table S2—Genotype information for identified and linkage-mapped SSR and SNP markers. Supplemental Table S3—Number of markers and genetic lengths of 18 LGs in maternal, paternal, and consensus maps. Supplemental Dataset S1—Information of SNP sequence discovered by genotyping by sequencing.

Author Contributions: L.W.A. and X.W. conceived the experiment and developed and sequenced the mapping population. K.M. and Z.S. designed and performed transcriptome sequencing. K.M., Z.S., M.E.S., T.A.R., and P.A.W. performed transcriptome analysis and developed SSR markers. X.W. and A.M.H.-K. performed linkage mapping and produced the genetic map. All authors have read and agreed to the published version of the manuscript.

Funding: This research was funded in part by the U.S. Department of Agriculture (USDA) Floriculture and Nursery Research Initiative and the Agricultural Research Service including ARS project number 6066-21310-005-00D. This research used resources provided by the SCINet project of the USDA Agricultural Research Service, ARS project number 0500-00093-001-00-D. Mention of a trademark, proprietary product, or vendor does not constitute a guarantee or warranty of the product by the USDA and does not imply its approval to the exclusion of other products or vendors that also may be suitable. USDA is an equal opportunity employer and provider.

Data Availability Statement: The transcriptome sequence reads were deposited into NCBI under PRJNA661039. The Illumina sequencing data were deposited to NCBI under BioProject PRJNA656177.

Acknowledgments: The authors would like to acknowledge Carrie Witcher, Benjamin Moore, and Ram Podicheti for invaluable technical support. Two anonymous reviewers provided contributions that greatly improved the manuscript. In addition, we acknowledge Indiana University and the Biotechnology Center at University of Wisconsin-Madison for their sequencing and data process services.

Conflicts of Interest: The authors declare no conflict of interest.

References

- Wilson, E.H. The hortensias *Hydrangea macrophylla* DC. and *Hydrangea serrata* DC. *J. Arnold Arbor.* **1923**, *4*, 233–246.
- Griffiths, M. *The New Royal Horticultural Society Dictionary: Index of Garden Plants*; Macmillan Press Ltd.: London, UK, 1994.
- The 2014 Census of Horticultural Specialties*; U.S. Department of Agriculture, National Agricultural Statistics Service (USDA-NASS): Washington, DC, USA, 2015; Volume 3, Special Studies, Part 3, AC-12-SS-3.
- Rinehart, T.; Wadl, P.; Staton, M. An update on *Hydrangea macrophylla* breeding targets and genomics. In Proceedings of the III International Symposium on Woody Ornamentals of the Temperate Zone 1191, Minneapolis, MI, USA, 2–5 August 2016; pp. 217–224.
- Leus, L. *Breeding for Disease Resistance in Ornamentals in Ornamental Crops 97-125*; Springer: Cham, Switzerland, 2018.
- Mohan, M.; Nair, S.; Bhagwat, A.; Krishna, T.G.; Yano, M.; Bhatia, C.R.; Sasaki, T. Genome mapping, molecular markers and marker-assisted selection in crop plants. *Mol. Breed.* **1997**, *3*, 87–103. [[CrossRef](#)]
- Cerbah, M.; Cerbah, M.; Mortreau, E.; Brown, S.; Siljak-Yakovlev, S.; Bertrand, H.; Lambert, C. Genome size variation and species relationships in the genus *Hydrangea*. *Appl. Genet.* **2001**, *103*, 45–51. [[CrossRef](#)]
- Chen, H.; Lu, C.; Jiang, H.; Peng, J. Global transcriptome analysis reveals distinct aluminum-tolerance pathways in the Al-accumulating species *Hydrangea macrophylla* and marker identification. *PLoS ONE* **2015**, *10*, e0144927. [[CrossRef](#)]
- Negishi, T.; Oshima, K.; Hattori, M.; Kanai, M.; Mano, S.; Nishimura, M.; Yoshida, K. Tonoplast-and plasma membrane-localized aquaporin-family transporters in blue hydrangea sepals of aluminum hyperaccumulating plant. *PLoS ONE* **2012**, *7*, e43189. [[CrossRef](#)]
- Rinehart, T.A.; Scheffler, B.E.; Reed, S.M. Genetic diversity estimates for the genus *Hydrangea* and development of a molecular key based on SSR. *J. Am. Soc. Hortic. Sci.* **2006**, *131*, 787–797. [[CrossRef](#)]
- Rinehart, T.A.; Scheffler, B.E.; Reed, S.M. Ploidy variation and genetic diversity in *Dichroa*. *HortScience* **2010**, *45*, 208–213. [[CrossRef](#)]
- Reed, S.M.; Rinehart, T.A. Simple sequence repeat marker analysis of genetic relationships within *Hydrangea macrophylla*. *J. Am. Soc. Hortic. Sci.* **2007**, *132*, 341–351. [[CrossRef](#)]
- Waki, T.; Kodama, M.; Akutsu, M.; Namai, K.; Iigo, M.; Kurokura, T.; Yamamoto, T.; Nashima, K.; Nakayama, M.; Yagi, M. Development of DNA Markers Linked to Double-Flower and Hortensia Traits in *Hydrangea macrophylla* (Thunb.) Ser. *Hortic. J.* **2018**, *87*, 264–273. [[CrossRef](#)]
- Li, S.; Yang, G.; Yang, S.; Just, J.; Yan, H.; Zhou, N.; Jian, H.; Wang, Q.; Chen, M.; Qiu, X.; et al. The development of a high-density genetic map significantly improves the quality of reference genome assemblies for rose. *Sci. Rep.* **2019**, *9*, 5985. [[CrossRef](#)] [[PubMed](#)]
- Yang, Y.; Sun, M.; Li, S.; Chen, Q.; Da Silva, J.A.T.; Wang, A.; Yu, X.; Wang, L. Germplasm resources and genetic breeding of *Paeonia*: A systematic review. *Hortic. Res.* **2020**, *7*, 1–19. [[CrossRef](#)]
- Song, X.; Xu, Y.; Gao, K.; Fan, G.; Zhang, F.; Deng, C.; Dai, S.; Huang, H.; Xin, H.; Li, Y. High-density genetic map construction and identification of loci controlling flower-type traits in *Chrysanthemum* (*Chrysanthemum × morifolium* Ramat.). *Hortic. Res.* **2020**, *7*, 1–13. [[CrossRef](#)] [[PubMed](#)]
- Walve, R.; Rastas, P.; Salmela, L. Kermit: Linkage map guided long read assembly. *Algorithms Mol. Biol.* **2019**, *14*, 8. [[CrossRef](#)]
- He, J.; Zhao, X.; Laroche, A.; Lu, Z.-X.; Liu, H.; Li, Z. Genotyping-by-sequencing (GBS), an ultimate marker-assisted selection (MAS) tool to accelerate plant breeding. *Front. Plant Sci.* **2014**, *5*, 484. [[CrossRef](#)] [[PubMed](#)]

19. Elshire, R.J.; Glaubitz, J.C.; Sun, Q.; Poland, J.A.; Kawamoto, K.; Buckler, E.S.; Mitchell, S.E. A Robust, Simple Genotyping-by-Sequencing (GBS) Approach for High Diversity Species. *PLoS ONE* **2011**, *6*, e19379. [CrossRef]
20. Yan, M.; Byrne, D.H.; Klein, P.E.; Yang, J.; Dong, Q.; Anderson, N. Genotyping-by-sequencing application on diploid rose and a resulting high-density SNP-based consensus map. *Hortic. Res.* **2018**, *5*, 17. [CrossRef]
21. Di Pierro, E.A.; Gianfranceschi, L.; Di Guardo, M.; Koehorst-van Putten, H.J.; Kruisselbrink, J.W.; Longhi, S.; Troglio, M.; Bianco, L.; Muranty, H.; Pagliarini, G.; et al. A high-density, multi-parental SNP genetic map on apple validates a new mapping approach for out-crossing species. *Hortic. Res.* **2016**, *3*, 1–13. [CrossRef] [PubMed]
22. Wu, X.; Alexander, L.W. Genetic Diversity and Population Structure Analysis of Bigleaf Hydrangea Using Genotyping-by-sequencing. *J. Am. Soc. Hortic. Sci.* **2019**, *144*, 257–263. [CrossRef]
23. Wu, X.; Alexander, L.W. Genome-wide association studies for inflorescence type and remontancy in *Hydrangea macrophylla*. *Hortic. Res.* **2020**, *7*, 1–9. [CrossRef]
24. Tränkner, C.; Krüger, J.; Wanke, S.; Naumann, J.; Wenke, T.; Engel, F. Rapid identification of inflorescence type markers by genotyping-by-sequencing of diploid and triploid F1 plants of *Hydrangea macrophylla*. *BMC Genet.* **2019**, *20*, 60. [CrossRef]
25. Li, Y.; Mmbaga, M.; Zhou, B.; Joshua, J.; Rotich, E.; Parikh, L. *Diseases of Hydrangea. Handbook of Florists' Crops Diseases. Handbook of Plant Disease Management*; Springer: Cham, Germany, 2016; pp. 1–19.
26. Adkins, J.A.; Dirr, M.A. Remontant flowering potential of ten *Hydrangea macrophylla* (Thunb.) Ser. cultivars. *HortScience* **2003**, *38*, 1337–1340. [CrossRef]
27. Tae, H.; Ryu, D.; Sureshchandra, S.; Choi, J.-H. ESTclean: A cleaning tool for next-gen transcriptome shotgun sequencing. *BMC Bioinf.* **2012**, *13*, 247. [CrossRef]
28. Margulies, M.; Egholm, M.; Altman, W.E.; Attiya, S.; Bader, J.S.; Bemben, L.A.; Berka, J.; Braverman, M.S.; Chen, Y.-J.; Chen, Z.; et al. Genome sequencing in microfabricated high-density picolitre reactors. *Nat. Cell Biol.* **2005**, *437*, 376–380. [CrossRef] [PubMed]
29. Haas, B.J.; Papanicolaou, A.; Yassour, M.; Grabherr, M.; Blood, P.D.; Bowden, J.; Couger, M.B.; Eccles, D.; Li, B.; Lieber, M.; et al. De novo transcript sequence reconstruction from RNA-seq using the Trinity platform for reference generation and analysis. *Nat. Protoc.* **2013**, *8*, 1494–1512. [CrossRef]
30. Finn, R.D.; Coghill, P.; Eberhardt, R.Y.; Eddy, S.R.; Mistry, J.; Mitchell, A.L.; Potter, S.C.; Punta, M.; Qureshi, M.; Sangrador-Vegas, A.; et al. The Pfam protein families database: Towards a more sustainable future. *Nucleic Acids Res.* **2016**, *44*, D279–D285. [CrossRef]
31. Finn, R.D.; Clements, J.; Arndt, W.; Miller, B.L.; Wheeler, T.J.; Schreiber, F.; Bateman, A.; Eddy, S.R. HMMER web server: 2015 update. *Nucleic Acids Res.* **2015**, *43*, W30–W38. [CrossRef]
32. Apweiler, R. UniProt: The Universal Protein knowledgebase. *Nucleic Acids Res.* **2004**, *32*, 115D–119D. [CrossRef] [PubMed]
33. Jones, P.; Binns, D.; Chang, H.-Y.; Fraser, M.; Li, W.; McAnulla, C.; McWilliam, H.; Maslen, J.; Mitchell, A.; Nuka, G.; et al. InterProScan 5: Genome-scale protein function classification. *Bioinformatics* **2014**, *30*, 1236–1240. [CrossRef]
34. Simão, F.A.; Waterhouse, R.M.; Ioannidis, P.; Kriventseva, E.V.; Zdobnov, E.M. BUSCO: Assessing genome assembly and annotation completeness with single-copy orthologs. *Bioinformatics* **2015**, *31*, 3210–3212. [CrossRef] [PubMed]
35. Stieneke, D.; Eujayl, I. Imperfect SSR Finder, Version 1.0. Available online: <http://ssr.nwisrl.ars.usda.gov/> (accessed on 12 April 2017).
36. Waldbieser, G.C.; Quiniou, S.M.; Karsi, A. Rapid development of gene-tagged microsatellite markers from bacterial artificial chromosome clones using anchored TAA repeat primers. *Biotechniques* **2003**, *35*, 976–979. [CrossRef]
37. Brownstein, M.J.; Carpten, J.D.; Smith, J.R. Modulation of non-templated nucleotide addition by Taq DNA polymerase: Primer modifications that facilitate genotyping. *Biotechniques* **1996**, *20*, 1004–1010. [CrossRef]
38. Glaubitz, J.C.; Casstevens, T.M.; Lu, F.; Harriman, J.; Elshire, R.J.; Sun, Q.; Buckler, E.S. TASSEL-GBS: A High Capacity Genotyping by Sequencing Analysis Pipeline. *PLoS ONE* **2014**, *9*, e90346. [CrossRef]
39. Bradbury, P.J.; Zhang, Z.; Kroon, D.E.; Casstevens, T.M.; Ramdoss, Y.; Buckler, E.S. TASSEL: Software for association mapping of complex traits in diverse samples. *Bioinformatics* **2007**, *23*, 2633–2635. [CrossRef]
40. Van Ooijen, J. *JoinMap 4. Software for the Calculation of Genetic Linkage Maps in Experimental Populations*; Kyazma BV: Wageningen, The Netherlands, 2006; p. 33.
41. Voorrips, R. MapChart: Software for the graphical presentation of linkage maps and QTLs. *J. Hered.* **2002**, *93*, 77–78. [CrossRef]
42. Consortium, U. UniProt: A hub for protein information. *Nucleic Acids Res.* **2015**, *43*, D204–D212. [CrossRef]
43. Ashburner, M.; Ball, C.A.; Blake, J.A.; Botstein, D.; Butler, H.; Cherry, J.M.; Davis, A.P.; Dolinski, K.; Dwight, S.S.; Eppig, J.T.; et al. Gene Ontology: Tool for the unification of biology. *Nat. Genet.* **2000**, *25*, 25–29. [CrossRef]
44. Bailey, D.A. *Hydrangea Production*; Timber Press, Inc.: Portland, OR, USA, 1989.
45. Reed, S.M.; Jones, K.D.; Rinehart, T.A. Production and characterization of intergeneric hybrids between *Dichroa febrifuga* and *Hydrangea macrophylla*. *J. Am. Soc. Hortic. Sci.* **2008**, *133*, 84–91. [CrossRef]
46. McCallum, S.; Graham, J.; Jorgensen, L.; Rowland, L.J.; Bassil, N.V.; Hancock, J.F.; Wheeler, E.J.; Vining, K.J.; Poland, J.; Olmstead, J.W.; et al. Construction of a SNP and SSR linkage map in autotetraploid blueberry using genotyping by sequencing. *Mol. Breed.* **2016**, *36*, 41. [CrossRef]
47. Wang, N.; Fang, L.; Xin, H.; Wang, L.; Li, S. Construction of a high-density genetic map for grape using next generation restriction-site associated DNA sequencing. *BMC Plant Biol.* **2012**, *12*, 148. [CrossRef]

48. Sun, L.; Yang, W.; Zhang, Q.; Cheng, T.; Pan, H.; Xu, Z.; Zhang, J.; Chen, C. Genome-Wide Characterization and Linkage Mapping of Simple Sequence Repeats in Mei (*Prunus mume* Sieb. et Zucc.). *PLoS ONE* **2013**, *8*, e59562. [[CrossRef](#)]
49. Guajardo, V.; Solís, S.; Sagredo, B.; Gainza-Cortés, F.; Muñoz, C.; Gasic, K.; Hinrichsen, P. Construction of High Density Sweet Cherry (*Prunus avium* L.) Linkage Maps Using Microsatellite Markers and SNPs Detected by Genotyping-by-Sequencing (GBS). *PLoS ONE* **2015**, *10*, e0127750. [[CrossRef](#)] [[PubMed](#)]
50. Kirov, I.; Van Laere, K.; De Riek, J.; De Keyser, E.; Van Roy, N.; Khrustaleva, L. Anchoring Linkage Groups of the Rosa Genetic Map to Physical Chromosomes with Tyramide-FISH and EST-SNP Markers. *PLoS ONE* **2014**, *9*, e95793. [[CrossRef](#)]



Article

Developing Triploid Maples

Ryan N. Contreras * and Tyler C. Hoskins

Department of Horticulture, Oregon State University, 4017 Agricultural and Life Sciences, Corvallis, OR 97331, USA; tyler.hoskins@oregonstate.edu

* Correspondence: ryan.contreras@oregonstate.edu; Tel.: +541-737-5462

Received: 5 September 2020; Accepted: 19 October 2020; Published: 21 October 2020

Abstract: Maples are common street and shade trees throughout the temperate zone. They are widely used for their wide range of ornamental traits and adaptability, particularly to urban settings. Unfortunately, some species such as *Acer tataricum* ssp. *ginnala* (Amur maple) and *A. platanoides* (Norway maple) have escaped cultivation to become pests or in some cases threaten native flora. However, these species remain economically important and are still asked for by name. To ameliorate potential future ecological damage from additional escapes, we have been breeding for sterile forms using ploidy manipulation and backcrossing to develop triploids. We began with a series of experiments to develop tetraploids of Amur, Norway, and trident (*A. buergerianum*) maples. Treatment of seedlings at the cotyledon or first true leaf stage was successful in inducing tetraploids of each species. Mortality, cytochimeras, and tetraploids varied among species. After identifying tetraploids, they were field planted alongside diploid cultivars and seedlings, which served as pollinizers in open-pollination. Seedlings derived from open-pollinated tetraploids were generally found to be a high percentage triploids. Thus far, no Norway or trident maple triploids have flowered but after three years we observed five, 22, and 22 Amur maple triploids flowering over three respective years with no seedlings recovered to date. Further evaluation is required but our findings are encouraging that the triploids we have developed thus far will be sterile and provide new cultivars for nursery growers and land managers.

Keywords: *Acer buergerianum*; *Acer ginnala*; *Acer platanoides*; *Acer tataricum* ssp. *ginnala*; ploidy manipulation; sterility

1. Introduction

Maples (*Acer* sp.) are popular landscape trees often identified by commonly having palmately lobed leaves and characteristic schizocarps (joined samaras). However, many species differ from the archetype palmately lobed leaves and most species are not particularly desired for their flowers or fruit, though few exceptions exist (e.g., ‘Flame’ amur maple grown for its red schizocarps). In 2014, overall U.S. sales of maples exceeded \$173 million, which accounted for 31% of the nearly \$562 million of deciduous shade trees sold nationally [1]. Much of the nursery stock produced around the country is marketed to population centers in the upper Midwest and New England regions. In fact, Oregon, the leading shade tree production state in the U.S., ships approximately 80% of its nursery plant material out of state and historically has relied on regions in the eastern part of the U.S. as principle markets.

With the nearly complete loss of elms and ash from the market due to Dutch elm disease [2] and emerald ash borer [3], respectively, the nursery and landscape industries are more reliant on maples to fill the urban canopy. However, many maples have the significant drawback of being weedy. Several species have escaped cultivation and become invasive to the point of being banned in some states, which has resulted in a significant decline of staple species in historically key markets such as New England.

Among the most widely used maples, Norway maple (*A. platanoides*) became popular in the U.S. in the mid- to late-1800s and continues to be widely used as a street and shade tree. Following previous devastating losses of elm trees from Dutch elm disease, large numbers of Norway maples were planted. Desirable forms include columnar growth habit, red leaves, and cultivars with improved fall color. Norway maples grow well under a wide range of conditions including sand to clay and acid to calcareous soils. It is hardy from USDA Zone 4 to 7 and tolerates hot, dry conditions better than sugar maple. Furthermore, Norway maple is tolerant of air pollution, including ozone and sulfur dioxide, making it ideal for use as a street tree. However, a major problem with Norway maple is that it has become naturalized to the point of invasiveness in forests of New England. Between 2009 and 2014, sales of Norway maple fell by more than 5% from \$14.4 million to \$13.6 million but many growers have seen much more dramatic declines in sales. Based on conversations with leading shade tree growers, this downward trend continues. Robinson Nursery, an Oregon shade tree grower, estimates their market is down 90% from a decade ago. Their data indicates they sold approximately 25,000 Norway maples annually between 2000 and 2006, but today they sell closer to 3000. It is likely that a continued downward trend will be observed unless alternative cultivars are introduced.

Other street trees that previously were dominant in the market have seen precipitous declines in sales due to emerging pests. Ash (*Fraxinus* spp.) was a leading street tree until recently; however, with the emergence of emerald ash borer as a major pest, the viability of ash as a commercial crop has been reduced. Sales declined from nearly \$15 million in 2009 to less than \$10 million in 2014 [1] and the pest continues to devastate the Midwestern urban tree canopy, thus one would expect ash sales to continue to fall. Since currently there is not a viable source of resistance in the U.S., it is imperative we have alternatives in the nursery and landscape industry to replace street trees in American cities.

Ecological and economic harm occurs when ornamental plants escape cultivation and displace native flora, which requires costly action on the part of land managers [4]. Furthermore, legislation preventing nurseries from producing and selling these species causes economic harm to growers. The fruit (winged samaras or schizocarps) that are so well recognized in the landscape are also notorious for introducing unwanted maple seedlings into both the urban and natural landscapes. Currently, there are three maple species [*Acer tataricum* ssp. *ginnala* (Amur maple), *A. platanoides*, *A. pseudoplatanus* (sycamore maple)] listed as noxious weeds in Connecticut and Massachusetts. Of these three species, two are banned from the state of Massachusetts and one is banned in Connecticut [5]. While not yet listed in other regions of the country, these species are widely distributed and have naturalized over large areas (Figure 1). Norway maple is extremely shade tolerant and its phenology is such that it releases its seeds at an appropriate time for survival (early fall) and natural cold stratification. This is in contrast to red maple (*A. rubrum*), for example, that has mature schizocarps during summer when summer drought often prevents recalcitrant seeds from surviving.

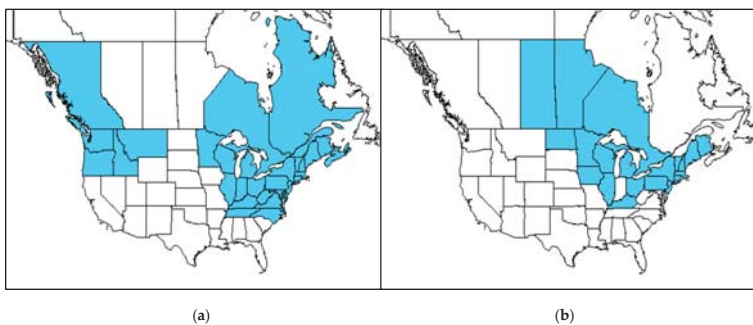


Figure 1. Distribution (filled regions) of naturalized (a) Norway maple and Amur maple (b) from the USDA PLANTS database <https://plants.sc.gov.usda.gov/java/>.

Species listed as “maple, other” accounted for more than \$32 million in sales during 2014 [1]. This is important to note because many of these other species produce copious amounts of viable seed that have the potential to escape cultivation and create similar ecological issues as Norway and Amur maple. It is worth noting that Norway maple was introduced into the U.S. around 1756 [6] and there was a lag phase before populations reached levels sufficient to cause ecological harm. It is reasonable to predict that with time; other species of maples have the potential to spread from cultivation. They, too, could become noxious weeds and eventually be banned from production or sale. As such, the methods and results described herein have application in other maple species.

Fertility of weedy species can be reduced using a number of techniques including ploidy manipulation. Other more technical methods such as gene editing and transgenics are far more expensive, require intimate knowledge of genomes of interest, and regeneration systems to recover whole plants from in vitro transgenic cell lines [7], all of which are generally lacking for maples. Furthermore, negative public perception and the cost of navigating regulatory approval is estimated to be in the tens of millions of dollars [8]. Ploidy manipulation to develop sterile triploids is relatively inexpensive and proven effective in many plant taxa. Inducing polyploids using chemical means, particularly the dinitroaniline herbicide, oryzalin, has become commonplace in woody plants including *Acer* [9–11]. Ploidy is the number of chromosome sets found in an organism and most organisms have two sets (diploids = $2x$) but plants are capable of existing with more than two sets of chromosomes. Plants can be rendered sterile, or at least have their fertility reduced, by producing cultivars with an odd number of chromosome sets—most commonly three sets (i.e., triploids = $3x$) [12]. Sterility resulting from triploidy occurs because plants with an odd ploidy number cannot be equally divided during meiosis such that daughter cells contain between n and $2n$ chromosomes [13]. In most cases where rare seedlings do arise from triploids, they often are aneuploids with reduced fitness and pose little or no ecological threat to escape cultivation [14]. This is a longstanding and common technique that resulted in seedless food crops such as bananas [15], watermelons [16], and some cultivars of grapes [17]. In nature, triploids can occur through production of unreduced ($2n$) gametes [14]. However, plant breeders can double the chromosomes of a diploid plant using various chemicals and the resulting tetraploid ($4x$) plant is then crossed with the diploid plant to create triploids. Induced polyploidy has been used in a wide variety of woody plants [7]. However, fewer examples are found for woody ornamentals. Lehrer et al. (2008) developed tetraploids of Japanese barberry (*Berberis thunbergii*), a weedy species in New England [18]. Their use of ploidy manipulation resulted in plants later released as ‘UCONNBTC4N’ USPP 30,095 Crimson Cutie® and ‘UCONNBTC048’ USPP 30,127 Lemon Glow® barberry. These examples are interesting, as they were found to be nearly sterile at the autotetraploid level, presumably due to multivalent formation, which avoided the need to proceed to the next generation. Rounsaville et al. (2011) compared fertility of diploid to triploid cytotypes of maidengrass (*Miscanthus sinensis*) and found the latter to have as low as 0.7% fertility relative to the wild type [19]. Phillips et al. (2016) developed triploid flowering pears (*Pyrus* sp.) that ranged from 0% to 34% relative fertility compared to diploid controls—a study that highlights the need for extensive and thorough testing of resulting triploids [20]. *Campsis* × *tagliabuana* ‘Chastity’ is a triploid cultivar of trumpet creeper that was developed by crossing a diploid cultivar with an oryzalin-induced tetraploid that is reported to have >99% reduction in fertility compared to diploid *C. radicans* [21].

Maples generally are diploids with two copies of 13 base chromosomes ($2n = 2x = 26$). To address the issue of weediness among maples, we developed triploids ($3x = 39$) that we hoped would exhibit reduced fertility and thus lessen the potential negative impacts of weedy and potentially invasive maple species. Introducing cultivars of maple with reduced fertility would allow land managers to maintain ecologically well-adapted species that thrive in difficult urban environments. Cultivars with reduced fertility would support the urban forests where they are planted and also protect the surrounding natural environments by preventing escape from cultivation. Furthermore, such cultivars support the sustainability of nursery producers who have relied heavily on these economically important species but have suffered due to the decline in demand as a result of their weediness. To address the

need for sterile maple cultivars, the objectives of the current research were to (1) develop tetraploids (2) backcross to diploids to produce triploids and (3) evaluate fertility as plants began flowering to determine if triploid maples exhibit reduced fertility. While we discuss the methods used to generate tetraploids, we do not consider these necessarily to be optimized methods.

2. Materials and Methods

2.1. Inducing Polyploidy Using Expanding Norway Maple Buds

Dormant plants of ‘Crimson King’, ‘Emerald Queen’, and ‘Royal Red’ were received bareroot from J. Frank Schmidt & Sons Co (Boring, OR, USA) during January 2010. Roots were trimmed to encourage new growth and all trees were topped to 1.8 m before potting into 60 L containers filled with 70% unaged douglas-fir bark, 15% peat, and 15% pumice and topped with label rate of control-release fertilizer (19-2.63-9.96, Apex®, J.R. Simplot, Boise, ID, USA). Trees were maintained in a glasshouse with day/night set temperatures of 22/18 °C and 16 h supplemental lighting provided by high-intensity discharge lamps.

In 2010, shoot tips were exposed by removing leaves as buds were emerging from dormancy and treatments were applied to two plants per cultivar. A 5-day treatment was applied to between 12 and 23 meristems per tree from March 11 to March 15 and a 3-day treatment was applied to between 3 and 13 previously untreated meristems from April 2 and 5 (Table 1). All treatments were 150 µM oryzalin supplied as Surflan AS (United Phosphorous, King of Prussia, PA, USA) solidified with 0.8% agar. Following this, 1.5 mL of the melted agar-oryzalin solution was distributed into microcentrifuge tubes that were carefully placed over meristems. Ploidy analysis was conducted on surviving branches during July.

Table 1. Meristems of *Acer platanoides* (Norway maple) cultivars after treating with 150 µM oryzalin supplied as Surflan and solidified with 0.8% agar during 2010. Meristems were exposed by removing bud scales and submerging in agar-solidified oryzalin solution for 3 or 5 d.

Cultivar	Rep ¹	Trt (d) ²	No. Meristems ³	Bud ⁴	Dead (%)	2x (%)	2x + 4x (%)	4x (%) ⁵
Emerald Queen	1	5	23	0	21 (91)	2 (9)	0	0
Emerald Queen	2	5	14	0	9 (64)	5 (36)	0	0
Royal Red	1	5	15	0	11 (73)	2 (13)	1 (7)	1 (7)
Royal Red	2	5	12	0	7 (58)	3 (25)	0	2 (17)
Crimson King	1	5	17	1 (6)	14 (82)	2 (12)	0	0
Crimson King	2	5	16	0	13 (81)	3 (19)	0	0
Emerald Queen	1	3	16	1 (6)	10 (63)	5 (31)	0	0
Emerald Queen	2	3	7	1 (14)	1 (14)	4 (57)	0	1 (14)
Royal Red	1	3	2	0	1 (50)	1 (50)	0	0
Royal Red	2	3	3	0	0	2 (67)	1 (33)	0
Crimson King	1	3	4	0	3 (75)	0	1 (25)	0
Crimson King	2	3	2	0	1 (50)	1 (50)	0	0

¹ Rep = replicate, ² Trt (d) = treatment (days), ³ No. meristems = number of meristems, ⁴ Meristem did not expand/elongate following treatment but did not appear dead., ⁵ All meristems later reverted to 2x.

In 2011, trees were moved into a glasshouse on Jan 7 under conditions described above. On Feb 21, bud scales were removed from swollen, unbroken buds to expose meristems. Meristems treated for 5 or 6 d, each with 100µM oryzalin supplied as Surflan solidified with 0.8% using plastic caps filled with 2mL of solution (Figure 2). Ploidy analysis was conducted on surviving branches during July.



Figure 2. The 2011 application of 100 μM oryzalin to meristems of *Acer platanoides* ‘Emerald Queen’. (a) a representative tree that was cut back and treated as meristems emerged from dormancy and (b) closeup of meristem exposed by removing bud scales as emerged after dormancy.

2.2. Inducing Polyploidy of Using Germinated Seedlings

Norway maple seed was collected during July 2010 from three sources in Corvallis, OR including 223 seed of a green cultivar on Bridgeway St., 1200 seed of a green cultivar on Jefferson St. on Oregon State University campus, and 316 seed of ‘Crimson King’ at the Lewis-Brown Horticulture Research Farm. Cultivar identity was not confirmed using molecular or other tools but phenotype of both Jefferson St. and Bridgeway St. collections were similar to ‘Emerald Queen’. Seeds were stratified for 90 d at 3 °C and then sown in 10 × 20 cm flats filled with a 1 bagged potting mix Sunshine LA4 P (Sun Gro Horticulture, Agawam, MA, USA): 1 douglas-fir-based media. Flats were maintained under glasshouse conditions described above with the modification of no supplemental lighting.

After the first pair of true leaves emerged, the meristem was treated for five consecutive days with 25 μL of 150 μM oryzalin solution supplied as Surf lan solidified with 0.55% agar (Figure 3). There were 155 seedlings of Bridgeway St. selection, 231 seedlings of Jefferson St. selection, and 154 seedlings of ‘Crimson King’ treated. Surviving seedlings were transplanted into 237 cm^3 pots and allowed to grow under glasshouse conditions. All seedlings were fertilized every 7 to 10 d with liquid fertilizer with micronutrients (20-8.74-16.6, Jack’s Professional, J.R. Peters Inc., Allentown, PA). During August 2011, fully expanded and mature leaves of each surviving seedling were run on the flow cytometer to determine change in ploidy.



Figure 3. A droplet of 150 μM oryzalin semi-solidified using 0.2% agar was applied to the meristem of a Norway maple seedling.

Amur and trident maple seed were collected from a single source each from an unidentified selection on Oregon State University, Corvallis, OR campus during 2011. Seed were stratified for treatment in 2012. Treatment and handling were all conducted as described for Norway maple.

2.3. Assessing Ploidy Level

Flow cytometry analysis of extracted nuclei stained with DAPI (4',6-diamidino-2-phenylindole) was carried out according to Contreras and Shearer [10] with the modification that only one sample was used for parent and seedlings.

2.4. Interploidy Crossing

During 2014 and 2015, a subset of Amur maple trees flowered and were used in controlled crosses between tetraploids, diploids, and mixoploids for which the LII was confirmed as tetraploid by measuring pollen. During 2014, we conducted reciprocal interploidy crosses that yielded 56 seed from 165 pollinated flowers, resulting in few triploids (data not shown). During 2015, we made 828 reciprocal crosses and collected 78 seeds (data not shown). Based on observations of relatively low yield from a substantial investment of time, we opted to field plant diploids and tetraploids of Amur and trident maples during 2015 to facilitate interploidy crossing (Figure 4). Additionally, we planted several diploids of *Acer tataricum* that were collected from as seed from a single source on the Oregon State University campus, Corvallis, OR. These new plantings added to Norway maples that were field planted during March 2014. Additionally, 54 trees (V01.01 through V01.54) were planted at the Smith Horticultural Research Farm in a single row including six diploids, 12 cytochimeras, and 36 tetraploids. Of the 54 trees, 34 were derived from the Jefferson St. seed source, 16 were derived from ‘Crimson King’, and four were derived from the Bridgeway St. seed source.

			74.23 2x AT	
71.22 4x AP	72.22 4x AB		74.22 4x AG	
71.21 4x AP	72.21 2x AB		74.21 2x AG	
71.20 4x AP	72.20 2x/4x AB		74.20 2x AT	
71.19 4x AP	72.19 4x AB	73.19 4x AB	74.19 4x AG	
71.18 4x AP	72.18 2x/4x AB	73.18 2x/4x AB		75.18 4x AG
71.17 4x AP	72.17 3x AB	73.17 4x AB		75.17 2x AT
71.16 4x AP	72.16 2x AB	OPEN		75.16 2x AG
71.15 4x AP	72.15 4x AB			75.15 4x AG
71.14 4x AP	72.14 2x/4x AB			75.14 2x AT
71.13 4x AP	72.13 2x/4x AB			75.13 2x/4x AG
71.12 4x AP				75.12 4x AG
71.11 4x AP				75.11 4x AG
71.10 4x AP				75.10 2x AG
71.09 4x AP				75.09 4x AG
71.08 4x AP				75.08 2x AT
71.07 4x AP				75.07 4x AP
71.06 4x AP				75.06 AP Royal Red
71.05 4x AP				75.05 4x AP
71.04 4x AP				75.04 AP Deborah
71.03 4x AP				75.03 4x AP
71.02 4x AP				75.02 4x AP
71.01 4x AP				75.01 4x AP
Row 71	Row 72	Row 73	Row 74	Row 75

Figure 4. Field map for *Acer buergerianum* (AB), *Acer tataricum* ssp. *ginnala* (AG), *A. platanooides* (AP), and *A. tataricum* (AT) at the Lewis Brown Horticulture Research Farm, Corvallis, OR including diploids (2x), triploids (3x), mixoploids (2x/4x) and tetraploids (4x). For Row 71, all tetraploids were derived from Jefferson St. seed source except 71.02, 71.10, 71.12, and 71.22, which were derived from ‘Crimson King’. Trees 75.01, 75.03, and 75.07 were derived from the Jefferson St. seed source and trees 75.02 and 75.05 were derived from ‘Crimson King’. For Row 76, all tetraploids were derived from Jefferson St. seed source except 76.05, which was derived from ‘Crimson King’.

3. Results

3.1. Inducing Polyploidy Using Expanding Norway Maple Buds

Survival was low in all treatments of buds during 2010 and 2011 (Tables 1 and 2). Ploidy analysis of the 2010 treatments identified five tetraploid meristems of ‘Royal Red’—four from the 5 d treatment and one from the 3 d treatment. During August 2010, 51 buds were sent for propagation and field testing with a commercial nursery. During March and April 2011, we assessed ploidy from these plants and found all were diploid, indicating complete reversion of these meristems even in those that previously appeared to be homogeneous (non-chimeric) tetraploids. Thus, no tetraploids were obtained from this treatment. No polyploids were identified from the 2011 treatments (Table 2).

Table 2. Meristems of *Acer platanoides* cultivars after treating with 100 μ M oryzalin supplied as Surflan and solidified with 0.8% agar during 2011. Meristems were exposed by removing bud scales and submerging in agar-solidified oryzalin solution for 5 or 6 d.

Cultivar	Rep	Trt (d)	No. Meristems	Dead (%)	2x
Crimson King	1	5	23	20 (87)	3 (13)
Crimson King	2	5	11	7 (64)	4 (36)
Emerald Queen	1	5	11	9 (82)	2 (18)
Emerald Queen	2	5	12	10 (83)	2 (17)
Royal Red	1	5	14	9 (64)	5 (36)
Royal Red	2	5	13	11 (85)	2 (15)
Crimson King	1	6	2	2 (100)	0
Crimson King	2	6	4	3 (75)	1 (25)
Emerald Queen	1	6	6	6 (100)	0
Emerald Queen	2	6	3	3 (100)	0
Royal Red	1	6	1	0	1 (100)
Royal Red	2	6	1	1 (100)	0

3.2. Inducing Polyploidy of Using Germinated Seedlings

3.2.1. Norway Maple

Stable tetraploids of Norway maple were obtained in 2011 by treating meristems of germinated seedlings at the cotyledon or first true leaf stage (Table 3). Percent tetraploids ranged from 5% to 35% of treated seedlings. Mortality ranged from 23% to 60% of treated seedlings. During 2012, 11 tetraploid genotypes were propagated by a commercial nursery. Nine of these genotypes were confirmed to be stable, homogeneous (non-chimeric) tetraploids during spring 2013, after leaves emerged. These nine were transplanted to the Lewis Brown Horticulture (LBH) farm in Corvallis, OR during fall 2013.

Table 3. Seedlings of *Acer platanoides* (Norway maple) collected and treated during 2010, for 5 d with 25 μ L of 150 μ M oryzalin supplied as Surflan + 0.55% agar for 5 d. Ploidy analysis conducted during 2011.

Cultivar/Collection	Seedlings Treated	Dead (%)	2x (%) ¹	2x + 4x (%) ¹	4x (%) ¹
Bridgeway St. ²	155	61 (39)	75 (48)	12 (8)	7 (5)
Crimson King	154	92 (60)	30 (19)	8 (5)	24 (16)
Jefferson St. ²	231	52 (23)	67 (29)	30 (13)	82 (35)

¹ Percent of treated seedlings at each ploidy level. ² Seed collected in Corvallis, OR from trees on Bridgeway St. and Jefferson St., respectively. Both trees were green foliage types that resembled ‘Emerald Queen’ but were not confirmed by molecular or other means.

3.2.2. Amur Maple

There was a low percentage of both mixoploids and tetraploids that resulted from meristem treatment of Amur maple (Table 4). Six homogenous tetraploids were recovered along with six mixoploids, of which three reverted to diploids, two stabilized as tetraploids, and one remained a cytochimera. There was no mortality following seedling treatment, in contrast to the relatively high percentage of dead seedlings among cultivars of Norway maple. Leaves of Amur maple tetraploids were darker green and thicker than diploids (Figure 5).

Table 4. Ploidy of seedlings of *Acer buergerianum* (trident maple) and *A. tataricum* ssp. *ginnala* (Amur maple) treated during 2012, for 5 d with 25 μ L of 150 μ M oryzalin supplied as Surflan + 0.55% agar applied to meristems at the first true leaf stage.

Species	Treated (No.)	2x (%)	3x (%)	2x + 4x (%)	4x (%)
<i>A. buergerianum</i>	244	220 (91)	1 (0.004)	15 (6)	8 (3)
<i>A. tataricum</i> ssp. <i>ginnala</i>	198	186 (94)	0	6 ¹ (3)	6 (3)

¹ Three later reverted to diploids and two stabilized at tetraploids.



Figure 5. Two leaves of tetraploid (a) and two leaves of diploid (b) forms of *Acer tataricum* ssp. *ginnala*.

3.2.3. Trident Maple

There was a low percentage of tetraploids (3%) and mixoploids (6%) recovered following treatment of trident maple (Table 4). Of particular interest, a single triploid was found following treatment but it is unclear if this was due to treatment or unreduced gamete(s). There was no mortality following seedling treatment.

3.3. Interploidy Crossing

3.3.1. Norway Maple

In 2014, one Norway maple tetraploid plant flowered, indicating that precocious flowering is possible, albeit at a low percentage. This tree did not set fruit and has not flowered since. In 2015, several more trees flowered but none set fruit. In 2016, one tetraploid set fruit, all of which were collected, cold-stratified, and sown (Table 5). Fifty-four of 416 seeds germinated (13%) and yielded 47 triploids (89%), 5 tetraploids (9%), and 1 pentaploid (2%). During 2017, no tetraploids of Norway maple flowered—only Amur maple tetraploids flowered and produced seed (Table 6). During the 2018 flowering season, four plants previously identified as tetraploids flowered, two of which produced 43 and 19 seeds, respectively (Table 7). No flowering was observed from diploid or mixoploid plants. All 43 seeds from V01.34 were direct seeded in field raised beds but none germinated. Across all taxa and ploidy levels we had no germination in field beds. V01.45 produced 19 seeds, 17 of which germinated in containers. However, ploidy was retested and it was confirmed that V01.34 and V01.45 had reverted to diploid, therefore neither tetraploid that flowered set seed during 2018. In 2019, flowering was observed in 5 diploids (44%), no mixoploids, and 4 tetraploids (16%). During the 2019 flowering season, V01.34 flowered again and produced 404 seeds, nine of which germinated (Table 7). Ploidy analysis has not been conducted on seedlings from 2018 and 2019 flowering seasons due to time constraints and efforts to create efficiencies in the breeding process. We have opted to delay ploidy analysis on these and future populations based on the high percentage of triploids from 2016 flowering season (89%), which indicated it is likely that most seedlings will be triploid when collected from tetraploids. In 2020, flowering was observed in 3 diploids (33%), 2 mixoploids (18%) and 2 tetraploids (6%) with seed collection ongoing. None of the triploids have flowered at this time.

Table 5. Ploidy analysis using flow cytometry of seedlings resulting from open-pollination of field grown *Acer platanoides* (Norway maple) tetraploids. Seed were collected from 2016 flowering season and evaluated in 2017.

Field Location	Seed (No.)	Seedlings (No.)	2x (%)	3x (%)	4x (%)	5x (%)
71.03	416	54	0	48 (89)	5 (9)	1 (2)

Table 6. Ploidy analysis using flow cytometry of seedlings resulting from open-pollination of field grown *Acer tataricum* ssp. *ginnala* (Amur maple) tetraploids. Seed were collected from 2016 and 2017 flowering seasons, respectively, and evaluated the following spring.

Field Location	Seed (No.)	Seedlings (No.) ¹	No. Plants at Each Ploidy Level (% of Tested)			
			2x	3x	4x	5x
2016						
74.19	1277	176	1 (1)	106 (81)	17 (13)	7 (5)
74.22	562	29	1 (3)	25 (86)	3 (10)	0
75.11	869	94	0	18 (95)	1 (5)	0
75.15	247	9	0	3 (33)	6 (67)	0
75.18	619	64	0	59 (94)	3 (5)	1 (2)
2017						
74.19	1884	530	6 (1)	445 (97)	8 (2)	0
75.11	7	0	-	-	-	0
75.15	297	28	0	22 (79)	6 (21)	0

¹ Seedling number does not correspond to plants analyzed for ploidy level in all cases, as plants died or did not produce sufficient leaf material for analysis, presumably due to verticillium wilt.

Table 7. Number of seeds and seedlings resulting from open-pollination of field grown *Acer buergerianum*, *A. tataricum* ssp. *ginnala*, and *A. platanoides* including seeds collected from diploid, cytochimera (2x + 4x) and tetraploid branches. Seed were collected from 2018 and 2019 flowering season.

Species	Location	Ploidy ¹	Seed (No.)	Sowing Method ²	Germinated (%)
2018					
<i>A. buergerianum</i>	72.16	2x	76	Field	0
<i>A. buergerianum</i>	72.16	2x	38	Containers	3 (8)
<i>A. buergerianum</i>	72.18	2x	312	Field	0
<i>A. buergerianum</i>	72.18	2x	156	Containers	11 (7)
<i>A. buergerianum</i>	72.21	2x	374	Field	0
<i>A. buergerianum</i>	72.21	2x	187	Containers	9 (5)
<i>A. buergerianum</i>	72.18	2x + 4x	19	Field	0
<i>A. buergerianum</i>	72.18	2x + 4x	19	Containers	3 (16)
<i>A. buergerianum</i>	72.18	4x	29	Field	0
<i>A. buergerianum</i>	72.18	4x	29	Containers	3 (10)
<i>A.f. ssp. ginnala</i>	74.22	4x	1694	Field	0
<i>A.f. ssp. ginnala</i>	74.22	4x	847	Containers	150 (18)
<i>A.f. ssp. ginnala</i>	75.11	4x	174	Field	0
<i>A.f. ssp. ginnala</i>	75.11	4x	87	Containers	0
<i>A.f. ssp. ginnala</i>	75.12	4x	30	Field	0
<i>A.f. ssp. ginnala</i>	75.12	4x	29	Containers	0
<i>A.f. ssp. ginnala</i>	75.15	4x	162	Containers	10 (6)
<i>A. platanoides</i>	71.16	4x	68	Field	0
<i>A. platanoides</i>	V01.34 ³	4x	43	Field	0
<i>A. platanoides</i>	V01.45 ³	4x	19	Containers	17 (89)
2019					
<i>A. buergerianum</i>	72.13	2x	142	Containers	2 (1)
<i>A. buergerianum</i>	72.18	2x	377	Containers	1 (0.3)
<i>A. buergerianum</i>	72.20	2x	113	Containers	4 (4)
<i>A. buergerianum</i>	73.18	2x	66	Containers	9 (3)
<i>A. buergerianum</i>	72.13	2x + 4x	133	Containers	0
<i>A. buergerianum</i>	72.18	2x + 4x	1136	Containers	11 (1)
<i>A. buergerianum</i>	72.20	2x + 4x	423	Containers	9 (2)
<i>A. buergerianum</i>	73.19	2x + 4x	160	Containers	2 (1)
<i>A.f. ssp. ginnala</i>	75.15	4x	775	Containers	72 (9)
<i>A.f. ssp. ginnala</i>	107.07	4x	152	Containers	0
<i>A.f. ssp. ginnala</i>	109.05	3x	5	Containers	0
<i>A.f. ssp. ginnala</i>	112.06	3x	79	Containers	0
<i>A.f. ssp. ginnala</i>	114.02	3x	16	Containers	0
<i>A.f. ssp. ginnala</i>	107.12	5x	27	Containers	0
<i>A. platanoides</i>	V01.34 ³	2x	404	Containers	9 (2)

¹ When seeds were collected from respective branches they were tested for ploidy level and some trees were found to be cytochimeras including some trees with 2x, 2x + 4x, and 4x branches. Different ploidy levels were kept separate for analysis. ² During 2018 seed sowing, direct field seeding was attempted to increase efficiency of production but resulted in no germination. ³ Trees were tested during 2018 and determined to have reverted to 2x. For 2019 flowering V01.34 was labeled as 2x, however additional sampling is required to confirm if the entire tree has reverted or specific branches.

3.3.2. Amur Maple

During 2016, seven tetraploid Amur maples flowered and five set seed. These resulted in two diploids, 211 triploids, 30 tetraploids, and eight pentaploids (Table 5). Plant 74.19 was the most prolific in terms of production with 1277 seeds, 176 seedlings, and 106 triploids. However, the highest percentage of triploids were recovered from plant 75.11, which yielded 95% triploids. Overall, the percentage of triploids recovered from 2016 flowering ranged from 33% to 95%. It is unclear why plant 75.15 had such a low percentage of triploids recovered since it had diploids on either side within its row, thus diploid pollen was presumably not limiting.

During 2017, three tetraploids flowered and resulted in a high percentage of triploids (Table 6). Percentage triploids included 79% from plant 75.15, up from 33% in 2016. Plant 74.19 yielded 97% triploids and again was the most prolific producer of seed and seedlings.

During 2018, eight tetraploids flowered and produced 3347 seeds and 160 seedlings (Table 7). As with the Norway maples, seed lots were split between field beds and containers and none of the 2222 seeds that were field planted germinated. Of the 1125 seeds sown in containers, 160 (14%)

germinated. The mean percent of triploids from previous years' flowering was 81%, thus we expect similar results from 2018, 2019, and future flowering seasons. By the end of the 2018 season, all Amur maples from the original tetraploid population except 75.15 experienced severe verticillium wilt (*Verticillium dahliae*) infestation, were killed to the ground and removed from the field.

During 2019, the remaining tetraploid (accession 75.15) from the original population flowered and produced 775 seeds, of which 72 (9%) germinated. A seedling tetraploid (accession 107.07) from a 2016 tetraploid parent (74.19) flowered, produced 152 seed, but none germinated (Table 7). Plant 75.15 is the only tree that has flowered each of the four years included in these data.

Amur maple in our plots have been relatively precocious and there were five, 22, and 22 triploids that flowered during 2018, 2019, and 2020, respectively. Most of these dropped undeveloped samaras prior to maturation but some did hold until the end of the season. Upon close observation, most appeared empty but all were stratified and sown. None have germinated to date.

3.3.3. Trident Maple

One trident maple flowered during 2016, from which we collected 793 seeds (Table 5). However, no seeds germinated. Neither the single triploid, nor any tetraploids flowered during 2017. During 2018, we collected seed from three diploids, one mixoploid, and one tetraploid. No germination occurred in field beds and germination in containers across ploidy levels was low and ranged from 5% to 8% for diploids, was 16% for the mixoploid, and was 10% for the tetraploid (Table 7). Seedlings from diploid branches were 85% diploid, 10% triploid and 5% tetraploid. Seedlings from mixoploid branches were all diploid, indicating these are likely chimeras with diploid LII histogenic layers. Surprisingly, the three seedlings from the tetraploid branch were all diploid, indicating that perhaps within this branch there are some nodes giving rise to tetraploid leaves and some remaining as chimeras with diploid LII histogenic layers (Table 8). During 2019, we collected seeds from four diploids and four mixoploids. Germination ranged from 0% to 4% for diploids and 0% to 2% for mixoploids (Table 7). Seedlings from diploid branches were 63% diploid, 13% triploid, 6% tetraploid and 19% pentaploid (Table 8). Seedlings from mixoploid branches were 59% diploid, 23% triploid and 18% tetraploid (Table 8).

Table 8. Ploidy analysis using flow cytometry of seedlings resulting from open-pollination of field grown *Acer buergerianum* (trident maple). Seed were collected from 2016, 2018, and 2019 flowering season, respectively.

Parent Location	Branch Ploidy	Plants at each Ploidy Level (% of Tested)			
		2x	3x	4x	5x
2016					
72.15 ¹	4x	-	-	-	-
2018					
72.18	2x	9 (82)	2 (18)	0	0
72.21	2x	8 (89)	0	1 (11)	0
72.16	2x + 4x	3 (100)	0	0	0
72.18	2x + 4x	3 (100)	0	0	0
72.18	4x	3 (100)	0	0	0
2019					
72.13	2x	2 (100)	0	0	0
72.18	2x	1 (100)	0	0	0
72.20	2x	0	1 (25)	1 (25)	2 (50)
73.18	2x	8 (89)	1 (11)	0	0
72.18	2x + 4x	11 (100)	0	0	0
72.20	2x + 4x	2 (22)	4 (44)	3 (33)	0
73.19	2x + 4x	0	1 (50)	1 (50)	0

¹ 793 seeds were collected and none germinated.

4. Discussion

Norway and Amur maples are important nursery and landscape species that have declined in sales due to their invasiveness. Previous research has attempted to address this by identifying existing cultivars of Norway maple that have reduced fertility [22]. Conklin and Sellmer [22] observed low to moderate germination during their study even though many of the cultivars studied are known to be relatively weedy but conceded that even though recommended methods for overcoming dormancy were followed, there may have been confounding factors. We have observed delayed germination of some Norway maple genotypes that required longer cold stratification than commonly recommended for the species. Additional observations related to flowering and seed set resulted in the conclusion that some cultivars such as Crimson King, Globosum, Faasen's Black, and Rubrum had relatively low seed set and were safe alternatives for landscapes [23]. Our observations of several of these cultivars in Western Oregon, particularly for Crimson King, have found that they are not reduced in fertility. Conflicting observations from different climatic regions points toward an environmental factor in fertility. This idea of safety among existing Norway maple cultivars has been propagated by others through citation of the Conklin and Sellmer research and also refers to newer cultivars that were developed for use in eastern North America such as 'Medzam' (Medallion™) as "virtually-seedless" [24] but it is unclear on what basis that claim was made other than that of the nursery that introduced the cultivar. These assertions of reduced fertility without sufficient evidence may have an impact on future releases of sterile cultivars. Touting plants as sterile that have either not been properly evaluated or have not flowered may prevent any future exceptions to be made following bans and/or could jeopardize acceptance among the public, who may rightly view such cultivars with skepticism. Indeed, even when there is a scientific basis for a plant that "should" have reduced fertility (e.g., triploidy), testing is still required. For instance, among 13 populations of triploid pears, Phillips et al. [20] observed 0% to 33% fertility compared to a fertile diploid control, which illustrated a genetic factor related to fertility.

To provide sterile cultivars for growers and land managers that will not escape cultivation we first successfully induced tetraploids by treating the meristem of newly germinated seedlings. This technique has been widely used across diverse taxa including *Hibiscus acetosella* [25] and *Rhododendron* [26], whereas other research used in vitro treatment to develop tetraploids to maintain the phenotype of 'Crimson Sentry' [27]. We were not successful in developing tetraploids by treating vegetative meristems in situ and thus if future researchers wish to use cultivars to maintain superior phenotypes, it is recommended to follow a similar protocol to Lattier et al. [27], which focused on in vitro treatment. Similar to previous research, we observed varying percentage of tetraploids and cytochimeras both within and among species. We did not further investigate the resulting mixoploids to determine LI and LIII histogenic layers through stomatal measurements (LI) or observations related to adventitious roots (LIII) as performed on *Hibiscus acetosella* [25]; however, we did retain all mixoploids due to the potential that they may be more precocious to flower and would breed as tetraploids based on the ploidy of LII. Additionally, we confirmed one cytochimera of Amur maple to be an LII tetraploid based on pollen size. Utility of cytochimeras to breed as tetraploids has been illustrated in other taxa such as the bigeneric hybrid *xChitalpa* [28]. However, due to the relative number of tetraploids in the current study and the precocity of flowering among them, we have not relied heavily on them for breeding. Cytochimeras in our program continue to exhibit variable ploidy levels including some stabilizing as diploids, others as tetraploids, and some maintaining as chimeras. Among chimeras we have confirmed individual branches varying in ploidy level, which requires testing ploidy level each year during flowering. Annual confirmation of ploidy of plants from which we collect seed has become our standard practice to ensure efficiency through sowing only populations of seed that will yield high percentage of triploids.

Other researchers have used non-targeted mutagenesis to develop sterile forms of Amur maple and observed that several selections had not flowered or produced seed for several years [29]. While sterility or reduced fertility is a common result following mutagenesis using radiation (e.g., 'Meiguicheng'

orange [30]), the authors conceded that the treatment may simply have resulted in the non-flowering plants having a longer than typical juvenility period. In order to have the greatest assurance that plants will not set seed is to observe flowering in many environments in the presence of fertile pollinizers over many years. We chose to use ploidy manipulation, as developing triploid cytotypes has been demonstrated to be a reliable means to achieve greatly reduced fertility in woody landscape plants such as *Campsis* [21], *Hypericum* [31], and *Pyrus* [20].

To our knowledge, these are the first confirmed reports of triploid forms of Amur, Norway, or trident maples developed to date. After attempting interploidy crosses using hand pollination we found that the process was inefficient and resulted in relatively few seedlings. We opted to interplant diploids and tetraploids to allow open-pollination. Prior to planting we were not certain of the pollination syndromes of any of the three species. There are five breeding systems in the genus *Acer*, several of which are highly complex and variably expressed temporally but can be summarized to range from including perfect flowers to dioecy during a single season [32]. Norway maple has been referred to as having perfect flowers [33] but this is a miscategorization, and even making careful observations can result in erroneous conclusions if based on a single period of time, as flowers can shift from perfect to male or female. We have made seasonal observations over the past several years but have not conducted observations on the frequency required to resolve sex expression these three species. However, we have confirmed the presence of perfect and male flowers in both Amur and Norway maples. Regardless of sex expression and/or pollination syndrome, the relatively high percentage of triploids derived from tetraploid plants suggests that there is a high rate of outcrossing among the maples studied.

Thus far we have observed triploids of Amur maple flowering for three seasons and have not recovered any seedlings, even though there are fertile pollinizers interplanted. All plants that flowered initially set samaras but all desiccated prior to maturation. Nevertheless, we collected, stratified, and sowed these seeds and observed no germination. It is premature to refer to these plants as sterile, but the findings suggest these plants may have reduced fertility to remove the ecological threat presented by the species-type. Triploids of Amur, Norway, and trident maples all have been propagated by stem cuttings for evaluation in multiple locations over multiple years.

5. Conclusions

Treating germinated seedlings of Amur, Norway, and trident maples with oryzalin was effective in developing tetraploids. Early flowering tetraploids were hand pollinated but this was found to be inefficient at developing large seed lots. Alternatively, interplanting diploids and tetraploids that were allowed to open-pollinate resulting in thousands of seeds and many triploids. Triploids have now been interplanted with fertile diploids as well as tetraploids for evaluation. We have recovered no seedlings from five, 22, and 22 trees that flowered during these respective years, suggesting triploids may be sterile but further evaluation over multiple years and environments is required. Furthermore, our methods described for inducing polyploids were not necessarily optimized and improvements could be made to more efficiently induce polyploids of these and additional species of maple.

Author Contributions: Conceptualization, R.N.C.; methodology, R.N.C. and T.C.H.; formal analysis, R.N.C.; investigation, R.N.C. and T.C.H.; data curation, R.N.C. and T.C.H.; writing—original draft preparation, R.N.C.; writing—review and editing, R.N.C. and T.C.H.; supervision, R.N.C. and T.C.H.; project administration, R.N.C.; funding acquisition, R.N.C. All authors have read and agreed to the published version of the manuscript.

Funding: This research was funded Oregon Department of Agriculture for partial funding of this research provided in cooperation between the Oregon Department of Agriculture (ODA) Nursery Research and Regulatory Advisory Committee and the Oregon Association of Nurseries (OAN) Research Committee. Financial support for this program is provided through a research assessment included as part of ODA's annual nursery license fee. Additional funding provided from the J. Frank Schmidt Family Charitable Foundation, Hatch Act funds, and the USDA Northwest Center for Nursery Crops Research.

Acknowledgments: We wish to thank Mara Friddle, Gwyn Alanko, Adigun McLeod, Andrew Baker, Jason Lattier, and Kim Shearer for their technical support.

Conflicts of Interest: The authors declare no conflict of interest.

References

1. Census of Horticultural Specialties for 2014. Available online: https://www.agcensus.usda.gov/Publications/2012/Online_Resources/Census_of_Horticulture_Specialties/ (accessed on 1 April 2020).
2. Karnosky, D.F. Dutch elm disease: A review of the history, environmental implications, control, and research needs. *Environ. Conserv.* **1979**, *6*, 311–322. [CrossRef]
3. Herms, D.A.; McCullough, D.G. Emerald ash borer invasion of North America: History, biology, ecology, impacts, and management. *Annu. Rev. Entomol.* **2014**, *59*, 13–30. [CrossRef] [PubMed]
4. Pimentel, D.; Zuniga, R.; Morrison, D. Update on the environmental and economic costs associated with alien-invasive species in the United States. *Ecol. Econ.* **2005**, *52*, 273–288. [CrossRef]
5. The PLANTS Database. Available online: <http://plants.usda.gov> (accessed on 1 April 2020).
6. Nowak, D.J.; Rowntree, R.A. History and range of Norway maple. *J. Arboric.* **1990**, *16*, 291–296.
7. Vining, K.J.; Contreras, R.N.; Ranik, M.; Strauss, S.H. Genetic methods for mitigating invasiveness of woody ornamental plants: Research needs and opportunities. *HortScience* **2012**, *47*, 1210–1216. [CrossRef]
8. Miller, J.; Bradford, K. The regulatory bottleneck for biotech specialty crops. *Nat. Biotechnol.* **2010**, *28*, 1012–1014. [CrossRef]
9. Contreras, R.N. The struggle is real (but fun!): Long term plant breeding at a public university. *Acta Hort.* **2017**, *1212*, 223–224. [CrossRef]
10. Contreras, R.N.; Shearer, K. Genome size, ploidy, and base composition of wild and cultivated. *Acer. J. Amer. Soc. Hort. Sci.* **2018**, *143*, 470–485. [CrossRef]
11. Lattier, J.D.; Chen, H.; Contreras, R.N. Improved method for enzyme digestion of root tips for cytology. *HortScience* **2017**, *52*, 1029–1032. [CrossRef]
12. Kumar, A.; Gupta, N. Applications of triploids in agriculture. In *Plant Biology and Biotechnology*; Bahadur, B., Venkat Rajam, M., Sahijram, L., Krishnamurthy, K., Eds.; Springer: New Delhi, India, 2015; pp. 385–396.
13. Wilson, J.Y. Cytological investigation of triploid sterility. *Nature* **1962**, *195*, 1329–1330. [CrossRef]
14. Ramsey, J.; Schemske, D.W. Pathways, mechanisms, and rates of polyploid formation in flowering plants. *Annu. Rev. Ecol. Syst.* **1998**, *29*, 467–501. [CrossRef]
15. Simmonds, N.W. Megasporogenesis and female fertility in three edible triploid bananas. *J. Genet.* **1960**, *57*, 269–278. [CrossRef]
16. Kihara, H. Triploid watermelons. *Proc. Amer. Soc. Hort. Sci.* **1951**, *58*, 217–230.
17. Ji, W.; Li, Z.Q.; Zhou, Q.; Yao, W.K.; Wang, Y.J. Breeding new seedless grape by means of in vitro embryo rescue. *Genet. Mol. Res.* **2013**, *12*, 859–869. [CrossRef] [PubMed]
18. Lehrer, J.M.; Brand, M.H.; Lubell, J.D. Induction of tetraploidy in meristematically active seeds of Japanese barberry (*Berberis thunbergii* var. *atropurpurea*) through exposure to colchicine and oryzalin. *Sci. Hort.* **2008**, *119*, 67–71.
19. Rounsaville, T.J.; Touchell, D.H.; Ranney, T.G. Fertility and reproductive pathways in diploid and triploid *Miscanthus sinensis*. *HortScience* **2011**, *46*, 1353–1357. [CrossRef]
20. Phillips, W.D.; Ranney, T.G.; Touchell, D.H.; Eaker, T.A. Fertility and reproductive pathways of triploid flowering pears (*Pyrus* sp.). *HortScience* **2016**, *51*, 968–971. [CrossRef]
21. Oates, K.M.; Ranney, T.G.; Touchell, D.H.; Vilorio, Z. *Campsis* × *tagliabuana* ‘Chastity’: A highly infertile triploid trumpet vine. *HortScience* **2014**, *49*, 343–345. [CrossRef]
22. Conklin, J.R.; Sellmer, J.C. Germination and seed viability of Norway maple cultivars, hybrids, and species. *HortTechnology* **2009**, *19*, 120–126. [CrossRef]
23. Conklin, J.R.; Selmer, J.C. Flower and seed production of Norway maple cultivars. *HortTechnology* **2009**, *19*, 91–95. [CrossRef]
24. Llewellyn, J. ONnursery crops Blog. Research Shows: Some Norway Maple Cultivars are Not Invasive. Available online: <https://onnurserycrops.com/2016/07/07/research-shows-some-norway-maple-cultivars-are-not-invasive/> (accessed on 3 September 2020).
25. Contreras, R.N.; Ruter, J.M.; Hanna, W.W. An oryzalin-induced autoallootetraploid of *Hibiscus acetosella* Welw. ex Hiern. ‘Panama Red’ (*Malvaceae*). *J. Am. Soc. Hort. Sci.* **2009**, *134*, 553–559. [CrossRef]

26. Jones, J.R.; Ranney, T.G.; Eaker, T.A. A novel method for inducing polyploidy in *Rhododendron* seedlings. *J. Am. Rhododendr. Soc.* **2008**, *62*, 130–135.
27. Lattier, J.D.; Touchell, D.H.; Ranney, T.G.; Smith, J. In Vitro regeneration and polyploid induction of *Acer platanoides* L. 'Crimson Sentry'. *J. Environ. Hort.* **2013**, *31*, 246–252.
28. Olsen, R.T.; Ranney, T.G.; Vilorio, Z. Reproductive behavior of induced allotetraploid x*Chitalpa* and in vitro embryo culture of polyploid progeny. *J. Am. Soc. Hort. Sci.* **2006**, *131*, 716–724. [[CrossRef](#)]
29. Smith, A.G.; Noyszewski, A.K. Mutagenesis breeding for seedless varieties of popular landscape plants. *ActaHort.* **2018**, *1191*, 43–51. [[CrossRef](#)]
30. Huang, J.H.; Wen, S.X.; Zhang, Y.F.; Zhong, Q.Z.; Yang, L.; Chen, L.S. Abnormal megagametogenesis results in seedlessness of a polyembryonic 'Meiguicheng' orange (*Citrus sinensis*) mutant created with gamma-rays. *Sci. Hortic.* **2017**, *217*, 73–83. [[CrossRef](#)]
31. Trueblood, C.; Ranney, T.G.; Lynch, N.; Neal, J.; Olsen, R. Evaluating fertility of triploid clones of *Hypericum androsaemum* L. for use as non-invasive landscape plants. *HortScience* **2010**, *45*, 1026–1028. [[CrossRef](#)]
32. Gleiser, G.; Verdú, M. Repeated evolution of dioecy from androdioecy in *Acer*. *New Phytol.* **2004**, *165*, 633–640. [[CrossRef](#)]
33. Dirr, M.A. *Manual of Woody Landscape Plants: Their Identification, Ornamental Characteristics, Culture, Propagation, and Uses*; Stipes: Champaign, IL, USA, 2009.

Publisher's Note: MDPI stays neutral with regard to jurisdictional claims in published maps and institutional affiliations.



© 2020 by the authors. Licensee MDPI, Basel, Switzerland. This article is an open access article distributed under the terms and conditions of the Creative Commons Attribution (CC BY) license (<http://creativecommons.org/licenses/by/4.0/>).

MDPI
St. Alban-Anlage 66
4052 Basel
Switzerland
Tel. +41 61 683 77 34
Fax +41 61 302 89 18
www.mdpi.com

Horticulturae Editorial Office
E-mail: horticulturae@mdpi.com
www.mdpi.com/journal/horticulturae



MDPI
St. Alban-Anlage 66
4052 Basel
Switzerland

Tel: +41 61 683 77 34
Fax: +41 61 302 89 18

www.mdpi.com



ISBN 978-3-0365-3794-8